REPORT NO. GDC-DDB67-006
CONTRACT NAS 8-20146
DCN 1-6-52-01144

CRYOGENIC ZERO-GRAVITY PROTOTYPE VENT SYSTEM

GENERAL DYNAMICS
Convair Division

REPORT NO. GDC-DDB67-006

CRYOGENIC ZERO-GRAVITY PROTOTYPE VENT SYSTEM

J. A. Stark and M. H. Blatt

October 1967

Prepared Under
Contract NAS8-20146
DCN 1-6-52-01144

Prepared by
CONVAIR DIVISION OF GENERAL DYNAMICS
San Diego, California

Security Classification Approved
per Requirements of Paragraph 10, DOD 5220.22-M

D. J. Hallman

D. J. Hallman,
Supervisor, Technical Reports

FOREWORD

This report was prepared by Convair division of General Dynamics under Contract NAS8-20146, "Study of Zero Gravity, Vapor-Liquid Separators," for the George C. Marshall Space Flight Center of the National Aeronautics and Space Administration. The work was administered under the technical direction of the Propulsion and Vehicle Engineering Laboratory, George C. Marshall Space Flight Center with Mr. R. Stonemetz and Mr. C. D. Arnett acting as project managers. The current project manager is Mr. R. Stonemetz.

In addition to the project leader, Mr. J. A. Stark, the following Convair personnel contributed to the program: Messrs. M. H. Blatt, R. D. Bradshaw, C. F. McLean, W. G. Michael, J. N. Sharmahd, R. E. Tatro, and G. B. Wood.

TABLE OF CONTENTS

TABLE OF CONTENTS, Contd

LIST OF FIGURES

LIST OF FIGURES, Contd

LIST OF FIGURES, Contd

LIST OF FIGURES, Contd

LIST OF TABLES

LIST OF SYMBOLS

A	heat transfer area
A_o	orifice flow area
AG	system actuation (pump on and vent open) with a gas vent inlet
AL	system actuation (pump on and vent open) with a liquid vent inlet
Bo	Bond number, $\frac{\rho g L^2}{\sigma}$
C_D	orifice discharge coefficient
C_f	flow coefficient
C_p	specific heat at constant pressure
D	diameter
DG	system deactuation (pump off and vent closed) with a gas vent inlet
DL	system deactuation (pump off and vent closed) with a liquid vent inlet
e	vapor desntiy to liquid density ratio in the tank
GL	cycled vent inlet from gas to liquid using three-way valve
g	local acceleration of gravity, $\frac{ft}{sec^2}$
H	head loss, liquid height
h	specific enthalpy
h_f	heat transfer film coefficient
k	fluid thermal conductivity
L	length

LG	cycled vent inlet from liquid to gas using three-way valve
M	correction to orifice flow equation for velocity of approach
m	mass, lb_m
$\dot{m}$	mass flow rate
N	rate of rotation of impeller, rpm
P	power
Pr	Prandtl number, $\frac{C_p \mu}{k}$
p	pressure
Q	volume flow rate
$\dot{Q}$	rate of heat flow, Btu/hr
Re	Reynolds number, $\frac{VD\rho}{\mu}$
T	absolute temperature
TF	time fraction
t	time
U	overall heat transfer coefficient
V	velocity
We	Weber number, $\frac{\rho L V^2}{\sigma}$
Δ	finite difference
θ	time to mixed condition
λ	heat of vaporization, $\frac{Btu}{lb_m}$
λ	energy transfer parameter

LIST OF SYMBOLS, Contd

μ	viscosity
η	heat exchange effectiveness, $\frac{T_{co} - T_{ci}}{T_{Hi} - T_{ci}}$
ρ	density
σ	surface tension

Subscripts

c	cold side
E	external
e	exit
ex	exchanger
g	gas, saturated vapor
h	hydraulic
H	hot side
i	inlet
j	jet
L	liquid
o	outlet
p	pump
T	total
t	tank
v	vent
W	wall

SUMMARY

The information contained in this report is the result of the Phase II study under Contract NAS8-20146.

Previous work under this contract (Phase I) compared various methods of venting vapor from a cryogenic propellant tank under zero-gravity conditions where the orientation of liquid and vapor is unknown. These studies showed that a heat exchange-type vent system has the best potential for existing and future cryogenic vehicles. Study results are reported in Reference 1-1.

This report covers the follow-on Phase II work to define, design, fabricate, and test a prototype of this heat exchanger vent system. The major requirement is for the system to control hydrogen tank pressure to 17 ± 1 psia when the external heating rate is 20-30 Btu/hr. The design application is for a fourteen day mission in an orbital experiment.

In the system definition phase, trade-offs were made to determine the type of heat exchanger (bulk versus wall), type of pump drive (electric motor versus turbine), optimum vent flow rates, vent cycle, and fluid mixing criteria. The availability, state-of-the-art, and costs of components were taken into account in selecting final system operating requirements.

The above trade-offs resulted in a near optimum system for the present application. The system operates intermittently with an on-off vent cycle. Actuation of a shut-off valve and heat exchanger pump initiates venting, causing tank pressure decay. Deactuation terminates venting allowing the pressure to rise. Deactuation and actuation of the system are controlled by a pressure-switch sensing tank pressure. The unit was designed for actuation at 18 psia maximum and 16 psia minimum, with a minimum deadband of 0.5 psi.

The optimum vent flow rate was determined to be 3 lb/hr, resulting in actual venting during approximately one-thirtieth of the total mission time.

The pump for circulating bulk or hot-side fluid through the exchanger is an axial-flow type with an electric motor drive. The electric drive is more economical and practical for the low vent rates considered. The input power to the pump is approximately 7 watts with a flow of 4.5 cfm and a static head rise of 2.5 ft of hydrogen.

Based on results of initial studies (Reference 1-1) the throttling regulator is required to control downstream or heat exchanger pressure to 5 ± 0.5 psia, and the heat exchanger must provide a vent exit temperature of 36°R with an inlet of 31°R saturated LH_2. The hot side flow rate at the design condition is 1200 lb/hr of 37.5°R LH_2 with

a maximum pressure drop of 1.25 ft of LH_2. The system is, however, capable of operating with both liquid and gaseous hydrogen.

The above requirements were given to hardware vendors, bids received, and selections made on the basis of technical ability, minimum costs and the ability to deliver on schedule. The following items were procured and assembled into a complete test package:

a. A throttling regulator of aluminum construction with an evacuated bellows sensing downstream pressure (Wallace O. Leonard P/N 187250-2). Weight of the unit is 0.62 lb. This unit was originally qualified for hot gas service on the Dynasoar Program.

b. Shut-off valve with an aluminum body and a 28-v latching solenoid (Wallace O. Leonard P/N 201200-2). For both opening and closing, power is applied for one to five seconds, and the unit remains in its last selected position upon removal of power. The weight of this unit is 1.31 lb, and is used on the SIVB vent valve control in a similar configuration.

c. The heat exchanger is of all aluminum construction and weighs 2.75 lb (Geoscience P/N 02B1-1). The cold or vent side flow is through a single coil of 3/8 inch tubing, and the hot side flow is vortexed over the outside of this tubing. This design allows for highly efficient heat transfer of a boiling fluid and minimizes the possibility of liquid "carry-over."

d. The axial flow pump is basically of aluminum construction and weighs 0.6 lb (Pesco P/N 189019-030). The unit was modified from an existing pump used for air-flow. The motor was modified from a 400-cps unit to minimize the required power by lowering its speed to approximately 3300 rpm with 60 cycles single phase and 17.3-v input. The speed and flow of the unit can be reduced to approximately one-third of design by proportionately reducing the frequency and voltage.

e. The pressure switch is of stainless steel construction and weighs 0.75 lb. (Freebank P/N 8394-1). It is located external to the propellant tank in a near ambient environment.

The entire test package, including instrumentation bosses, a filter, mounting bracketry, and a safety relief valve, weighs 11 lb (Figure 3-7). In this system, heavy wall stainless tubing and instrumentation bosses were used in order to be compatible with existing CRES temperature probe fixtures. A flight weight system of this same design, only using aluminum tubing and bracketry, is estimated at 8.25 lb.

The system shown in Figure 3-7 was tested with hydrogen in a 40-in. diameter, 84-in. long container, simulating the Project THERMO propellant storage tank. This tank

was superinsulated with 25 layers of NRC-2 type insulation, and installed in a large vacuum chamber at Convair. The test package was located approximately 22 in. from the bottom of the tank (Figure 5-6).

Testing was accomplished with liquid levels at 13 in. (system in GH_2), 43 in. (system in LH_2) and 70 in. A three-way valve was located at the vent inlet with one side leading to the gaseous ullage and the other side in liquid near the bottom of the tank. This allowed switching the vent inlet from gas to liquid, and vice-versa, to determine transient operation of the system.

Testing was accomplished with vent flow rates up to four lb/hr and pump speeds from 1100 to 3300 rpm.

Operation during venting down from 30 psia was also determined.

The unit was operated with both the pump flow down and with the pump flow up to determine any heat transfer effects which might be sensitive to gravity.

During the testing, temperatures throughout the tank were measured to determine stratification and destratification characteristics of the system. This portion of the testing was part of the Convair 1967 IRAD program and not part of, or a requirement of, the NAS8-20146 contract; however, data taken during system operation are being analyzed and will be made available to MSFC. Some of these data are presented in this report.

Temperatures and pressures of the test package were recorded upstream of the throttling regulator, downstream of the regulator (inlet to heat exchanger), at the outlet of the heat exchanger cold side, and at the inlet and outlet of the exchanger hot side. Vent gas-flow rate was measured at the exchanger outlet and at a point downstream in the facility where any liquid present at the exchanger outlet would certainly be vaporized. Use of this dual orifice system gives a quantitative indication of the quality of the fluid leaving the heat exchanger.

An optical, discontinuity liquid detector was also located at the exchanger outlet to determine qualitatively if any liquid were being vented.

The testing demonstrated the ability and efficiency of the system in controlling tank pressure and venting only vapor when operating in both gaseous and liquid hydrogen with either gas or liquid at the system vent inlet.

During initial testing, some discrepancies, which were later corrected, were noted in the operation of the system. During the first series of tests, with the pump flow down and the exchanger outlet directed radially towards the tank walls, system operation was satisfactory until, after approximately 22 hours of testing, the throttling regulator appeared to be stuck open and the exchanger pressure remained

high. Subsequent testing was performed at ambient conditions and, at Convair's Sycamore Canyon facility, in LH_2; the regulator operated satisfactorily in each case. The failure was apparently caused by contamination or, possibly, the formation of solid hydrogen in the regulator due to expansion of LH_2 to a vacuum.

The regulator unit was re-installed in the test package and a second series of testing performed; this time with the pump flow up and the heat exchanger outlet flow directed up the center of the tank. In this series of tests the system, after 35 hours, also regulated high as in the previous test. Again, after purging and detanking operations, the system regulated satisfactorily at ambient conditions. The regulator was removed and checked for leakage which could be forming solid hydrogen in the regulator and interfering with its operation. The unit leaked approximately 1.98 SCC/hr He (2×10^{-5} lb/hr LH_2) at ambient conditions, and it was determined that this could have caused the problem.

One likely fix was to provide for shut-off of the vent system downstream of the heat exchanger such that any leakage through the regulator, heat exchanger, and fittings would not be to a vacuum (below the triple point); thus precluding the possibility of solid hydrogen formation. A third series of tests was run with the shut-off located downstream of the heat exchanger and external to the test tank to prove this concept and to obtain additional data on heat exchanger performance and system pressure control functions. During this series of tests, the pump flow was down with the heat exchanger outlet flow directed downward rather than radially as in the first series of tests. Forty two hours of testing was accomplished with satisfactory throttling regulation and system performance throughout.

The following conclusions and recommendations are made as a result of this program;

a. The feasibility and efficiency of the system to control tank pressure while venting only vapor when operating in an environment at least as severe as that of the orbital experiment has been demonstrated. The next logical step in preparing for operational use of the system would be to perform complete qualification testing of the system. Such a program is outlined in Section 6.0.

b. Tank fluid mixing and liquid/ullage coupling are extremely important for efficient pressure control. Tank pressure decay with the system and the vent inlet in liquid and with the heat exchanger outlet directed downward was very slow. This is attributed to the fact that liquid mixing and subsequent liquid/ullage coupling were not sufficient enough to reduce the tank pressure. This was verified by temperature measurements which showed the liquid in the tank was progressively subcooled, with the respect to the ullage, as energy was removed via the heat exchanger.

c. The best location for the shut-off valve appears to be downstream of the heat exchanger and external to the propellant tank, in order to minimize the possibility of the formation of solid hydrogen by LH_2 leakage to a vacuum.

d. Results showed that flow directly up the center of the tank was best in promoting fluid mixing. In this case, pressure control was very efficient for both gas and liquid inlets. Radial flow at the exchanger outlet was second best, and flow directly down was significantly worse than either radial or upward flow.

e. It is recommended that for orbital testing the system be located near one end of the tank with the heat exchanger outlet flow directed toward the other end.

f. Since it was verified that tank mixing is an essential criteria for efficient operation of this system and is integral with it, it is recommended that further analyses and testing be accomplished with this system to determine its mixing characteristics in LH_2 at various liquid levels, pump speeds, and power levels.

SECTION 1

INTRODUCTION

This is the Phase II study under Contract NAS8-20146. Phase I work under this contract compared various methods of venting vapor from a cryogenic propellant tank under zero-gravity conditions where the orientation of liquid and vapor is unknown. These studies showed the use of a heat exchange-type vent system to have the best potential for existing and future cryogenic vehicles. Results are reported in Reference 1-1.

This report covers follow-on work performed under DCN 1-6-52-01144 of Contract NAS8-20146 in defining, designing, fabricating, and testing a prototype of such a heat exchanger vent system. The system is designed to operate with an external hydrogen tank heating rate of 20-30 Btu/hr and control tank pressure to 17 ± 1 psia. The mission duration is 14 days.

Details of the system definition task, performed to determine system requirements and specifications, are contained in Section 2.0. The various trade-offs which were made and are discussed in this section are;

a. Bulk heat exchanger versus wall type.

b. Pump turbine drive versus electric motor.

c. Determination of optimum vent-flow rates and vent cycle.

d. Determination of tank mixing requirements.

e. Optimum location and packaging of system components.

Design details which cover delivered hardware and package design are presented in Section 3.0.

An analysis to determine system vent down characteristics at tank pressures up to 50 psia is presented in Section 4.0. This analysis was performed to provide information useful to Project THERMO in determining possibilities for reducing required vent down times following orbital stratification tests.

The test system configuration, testing performed, test results, and data are presented in Section 5.0. The purpose of the test program was to prove the feasibility of the heat exchanger vent system and to determine its operating characteristics under both transient and steady-state conditions.

A test pr gram required to flight qualify the system is outlined in Section 6.0.

Overall study conclusions and recommendations are presented in Section 7.0.

SECTION 2

SYSTEM DEFINITION

During this phase of the program, trade-off and sizing analyses were performed to define the type of heat exchanger (bulk versus wall), type of pump drive (electric motor versus turbine), optimum vent flow and vent cycle, mixing requirements, and system configuration.

Overall performance requirements are based on using the system in a LH_2 orbital experiment. These requirements are presented in Paragraph 2.1.

Trade-off studies are discussed in Paragraph 2.2 and resulting system requirements and component specifications are presented in Paragraph 2.3.

2.1 DESIGN REQUIREMENTS

The basic design requirements of the vent system are presented in Table 2-1.

Table 2-1. Vent System Requirements

Propellant	LH_2
Pressure Range	0-50 psia
Pressure Control Range	17 [illegible]
Operational Temperature	35-39°R
Total Temperature Range	35-400°R
Ground Vent Flowrate	200 lb/hr
Ground Vent Pressure Drop	1 psi
Operational Boil-off Rate	0.105 to 0.156 lb/hr
Operational External Heat Leak	20-30 Btu/hr
Minimum Lifetime	14 days
Vibration Levels	20 g's nonoperational 5 g's operational

The system designed and tested under this contract is not capable of flowing the ground-hold vent rates. Designing a heat exchanger vent system to allow approximately 2,000 times the steady state low-g vent flow requirement would impose intolerable requirements on sizing the heat exchanger flow passages. The schematic, Figure 2-1, shows the additional components necessary to handle the ground-hold vent rates. These additional components were not designed, procured, or tested in this program.

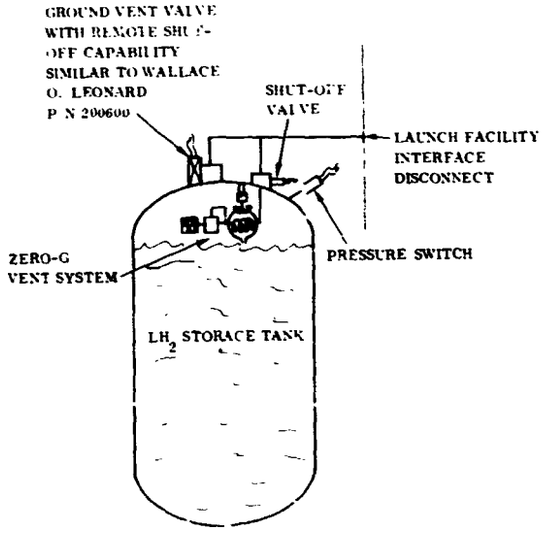

Figure 2-1. Diagram Showing Both Ground and Space Vent Systems

Also, since the initial application for this system is in an orbital experiment where long term storage is to be studied and only hydrogen is present in the tank, the analyses assumed only the existance of liquid and gaseous hydrogen. For a specific application where helium pressurant was to be used, the operation of the system would be the same, except for the sizing of the heat exchanger to allow for reduced heat transfer coefficients on the hot (tank) side.

For the helium case, further testing of the heat exchanger under controlled conditions would be required. In the present testing, control of the percentage of helium flowing through the heat exchanger was not practical and testing, therefore, was accomplished using hydrogen.

The scope of the present program was such that sufficient testing could not be performed to flight qualify or man rate the hardware. The philosophy, however, was that the hardware designs be capable of being flight qualified at a later date. A program to flight qualify the system is outlined in Section 6.0.

2.2 SYSTEM TRADE-OFFS AND OPTIMIZATIONS

System trade-offs and optimizations performed to define the most efficient, reliable, and low cost system are described in the following paragraphs.

2.2.1 BULK VERSUS WALL EXCHANGER. One of the initial decisions made in the system definition phase was whether or not the heat exchanger should be designed to, 1) absorb heat from the bulk propellant by forced convection provided by a mixer as shown in Figure 2-1, or 2) intercept external heat leakage at the tank wall, a typical

example is shown in Figure 2-2. The advantages and disadvantages of each method are presented below.

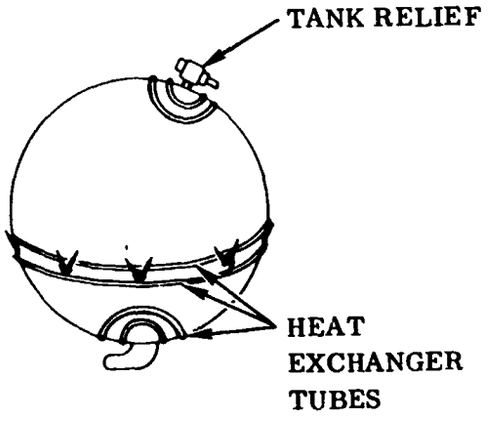

Figure 2-2. Wall Type Heat Exchanger System

Wall Exchanger

a. In general, has greater weight than the bulk type units. This can be significant in large vehicles.

b. Has the possibility of doing without a fluid mixer, thus increasing overall system reliability. However, realistic analysis of this system is presently limited to the case where venting is continuous such that stratification does not occur between vent cycles. Continuous operation at the extremely low flow rates involved in the present application may result in significant control problems. Based on an external heat leak of 20 Btu/hr, the vent flow would be as low as 0.105 lb/hr for a continuous vent system. This would result in a requirement for very small throttling regulator seating, with equivalent orifice sizes on the order of 0.004-in. diameter. The regulator would be very sensitive to contamination and seat damage tending to reduce system reliability. This is further discussed in Paragraph 2.2.3.

c. System design would be a strong function of the type of insulation to be used, the actual penetrations through the insulation, and the operating gravity level. Testing would be limited in its application. Vehicle tank design would also be effected, and possibly compromised, by the requirement to incorporate such a venting system.

Bulk Exchanger

a. Low weight.

b. Can be packaged into a single compact envelope; the same general configuration can be used for a variety of vehicle applications and heat rates.

c. Venting can be either continuous or intermittent.

d. Assuming the use of a mixer or pump such that heat transfer is forced-convection dominated, the operation of the unit can be more easily demonstrated at one g.

The main disadvantage to the bulk-type unit operating with a mixer is the added complexity associated with such a mixer. However, since it could not be demonstrated

that the wall unit will operate satisfactorily without a mixer under all conditions, and in light of the many other advantages of the bulk type unit, especially its universal application, it was chosen as the system to be tested in a prototype configuration.

2.2.2 PUMP TURBINE DRIVE VERSUS ELECTRIC MOTOR. For the small flow rates involved in the present application, the use of a turbine driven unit would require extensive development in order to be practical. Circulating pumps driven by an electric motor and capable of operating in LH_2 are presently state-of-the-art.

The main advantage of the turbine drive is that addition of external power to the propellant is minimized; however, by operating the electric motor on an intermittent vent cycle, this power input from the electric motor driven system can be very low (Paragraph 2.2.3).

Also, with the turbine driven system, a rotating seal between the vent fluid and the tank fluid would be required, thus requiring additional development for use with LH_2. Leakage of LH_2 during venting would reduce system efficiency.

It is conceivable that, for certain applications, it will be desirable to mix the tank fluid and destroy temperature stratification prior to actual venting. This could not be done with a turbine driven system.

For the above reasons, and since reliability of the two methods is judged about equal, an electric motor-driven pump was chosen for circulating the hot side fluid.

2.2.3 VENT FLOW AND VENT CYCLE OPTIMIZATION. The external heating rates (20-30 Btu/hr) for which the vent system must be designed are extremely low, and a major consideration is the limitation on practical hardware sizes. In order to minimize the heat input to the tank from the mixer or pump, this unit should be as small and as efficient as practical to provide for heat transfer and fluid circulation. One problem, however, is that for very small power requirements the unit efficiency decreases rapidly as shown in Figure 2-3. The efficiencies presented in Figure 2-3 represent the ratio of pump fluid output power (ρQH) to electrical input power to the pump motor. The data are for pump operation in LH_2 at a density of 4.32 lb/ft^3. A reasonable minimum practical pump power, using existing technology, would be about 5 to 7 watts. Units having smaller input power would have significantly smaller output power which, estimates (Paragraph 2.2.4) indicate, could be marginal in providing required mixing. Also, any contamination in the fluids entering the small bearings, or between rotor and stator to interfere with free rotation, would constitute a reliability problem with extremely low power motors. A 7-watt unit operating continuously adds 24 Btu/hr to the tank fluid. This is approximately equal to that added from external sources and essentially doubles the amount of vented fluid. There is, then, a weight trade-off between increasing the vent flow and heat exchanger size and reducing the time during which the pump must operate.

Curves of heat exchanger plus vented propellant weight as a function of vent rate are plotted in Figure 2-4 through 2-6 for various types of heat exchanger configurations where the external heating rate is 21 Btu/hr. A 14-day mission is assumed. Curves are also presented in Figure 2-7 for the Cryogenic Service Module case described in Reference 1-1, where the external heating rate is 94.5 Btu/hr and exchange ratios between fixed hardware weight and vented propellant and actual payload loss are used.

Heat transfer calculations and heat exchanger sizing are based on the methods described in References 1-1 and 2-2. The exchanger is divided into three heat transfer sections based on the vent or cold side fluid condition.

I Boiling up to 90-percent quality.

II Constant temperature vapor, 90-percent to 100-percent quality.

III Variable temperature, superheated gas.

Cold side heat transfer coefficients in Section I are based on the Kutateladze data (Reference 1-1). In Sections II and III, cold side coefficients for the tubular exchangers are obtained from the Dittus-Boelter Equation;

$$\frac{h_f D}{k} = 0.023\,(Re)^{0.8}\,(Pr)^{0.4} \qquad (2\text{-}1)$$

Hot side heat transfer coefficients and cold side coefficients in Sections II and III for the plate-fin unit are obtained from data of Kays and London as used in Reference 1-1.

Hot side heat transfer coefficients for the shrouded tubular exchangers are based on the following equation from McAdams (Reference 2-3).

$$\frac{h_f D}{k} = \left[\, 0.35 + 0.56\,(Re)^{0.52} \,\right](Pr)^{0.3} \qquad (2\text{-}2)$$

Hot side coefficients for the unshrouded tubular exchangers are obtained from

$$\frac{h_f D}{k} = 1.01\,(Re)^{0.62}\,(Pr)^{1/3} \qquad (2\text{-}3)$$

taken from Strek (Reference 2-4). In this case, Re and Pr numbers are based on the mixer characteristics.

Heat transfer sizing for each section is based on the following heat balance:

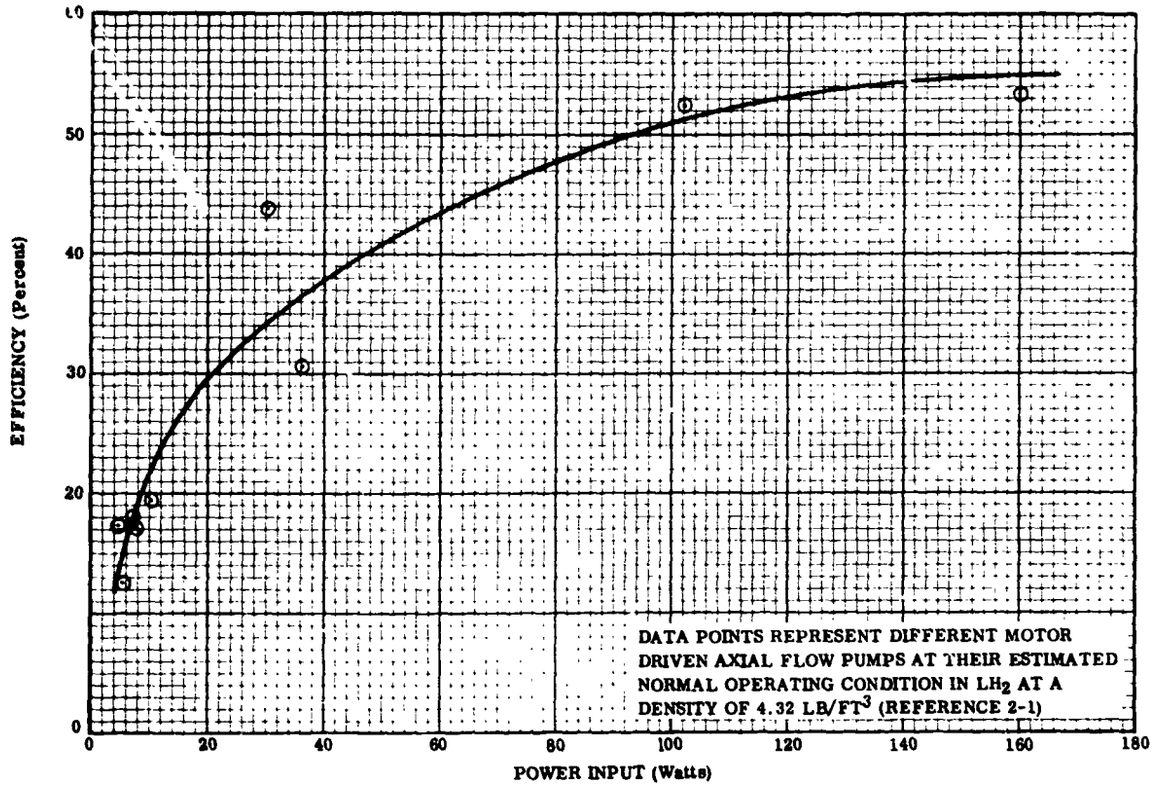

Figure 2-3. Pump Efficiency Vs. Power Input

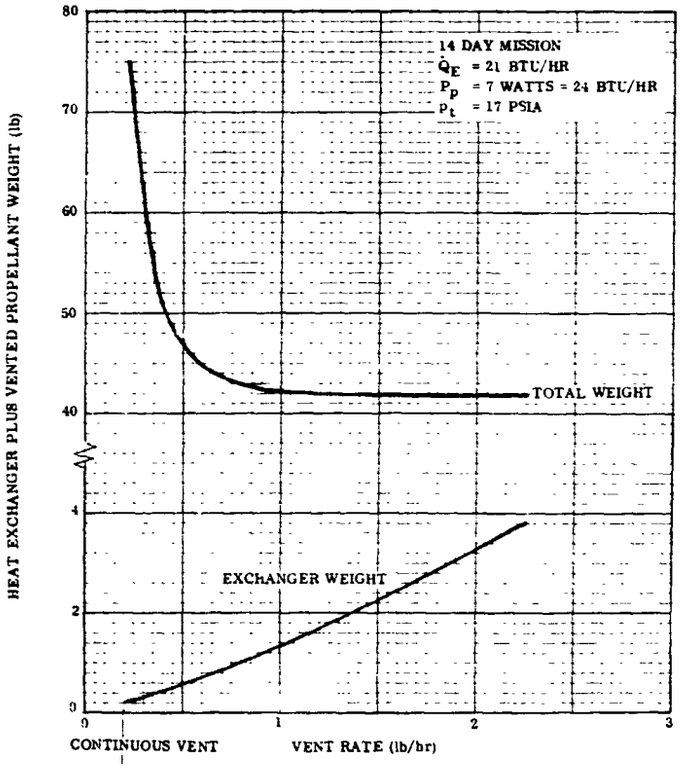

Figure 2-4. Weight Vs. Vent Rate (Unshrouded Coiled Tube Heat Exchanger)

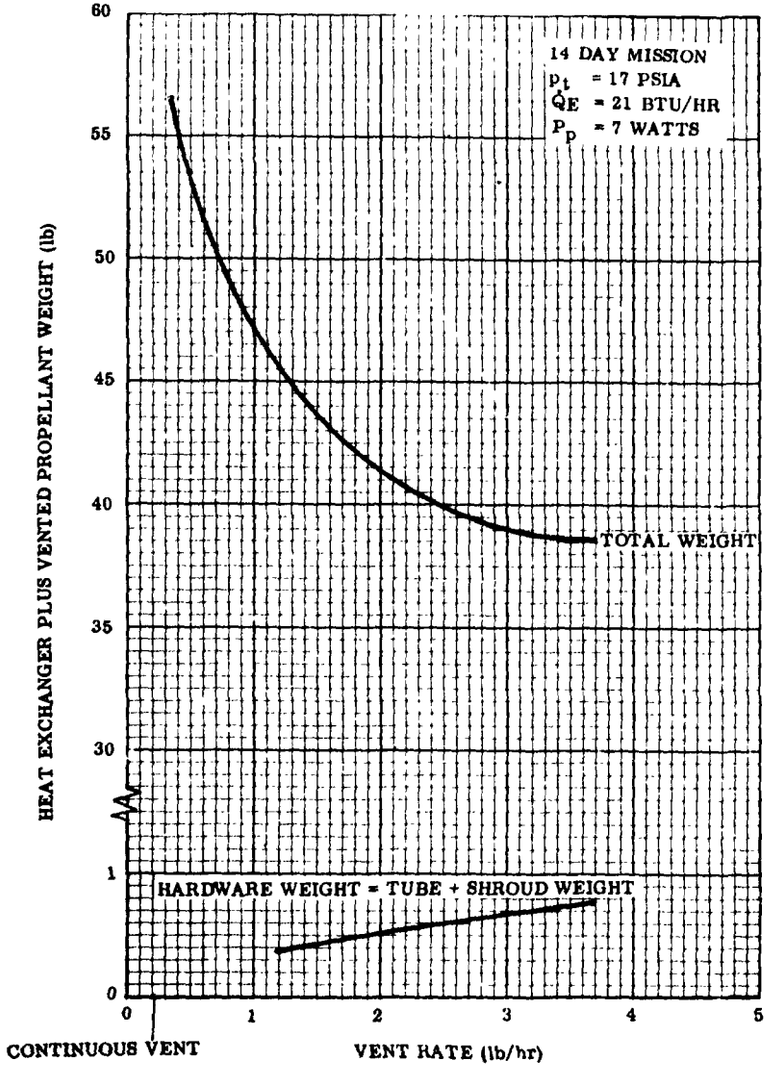

Figure 2-5. Weight Vs. Vent Rate (Shrouded Coiled Tube Heat Exchanger)

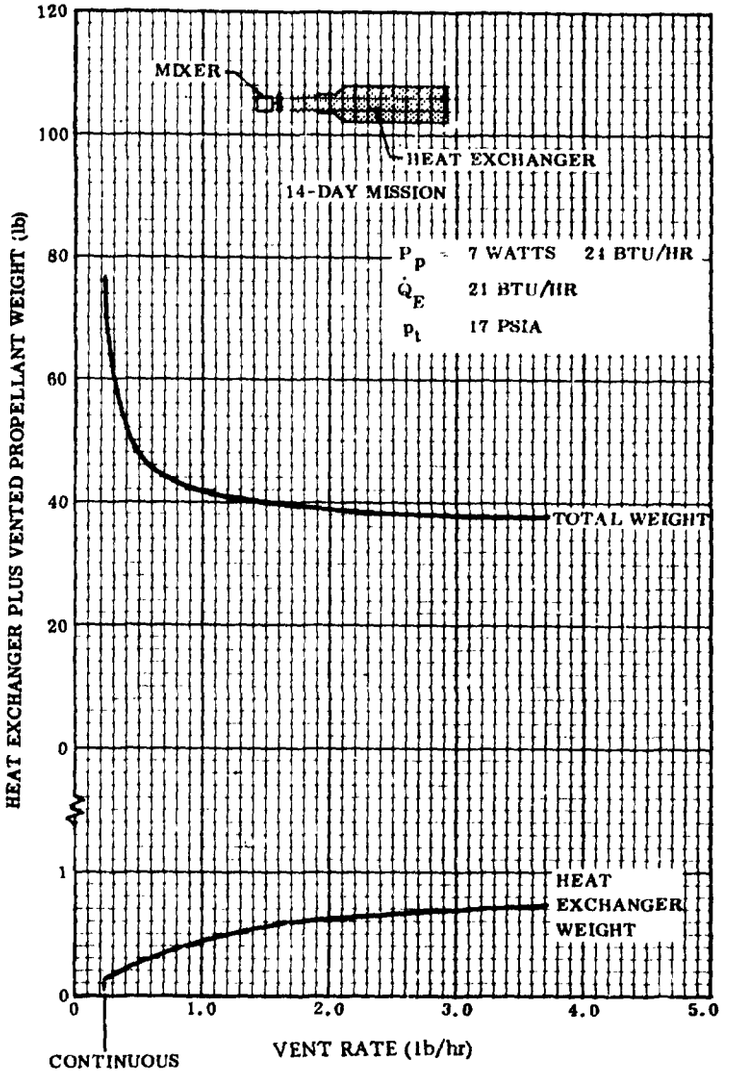

Figure 2-6. Weight Vs. Vent Rate (Plate-Fin Heat Exchanger)

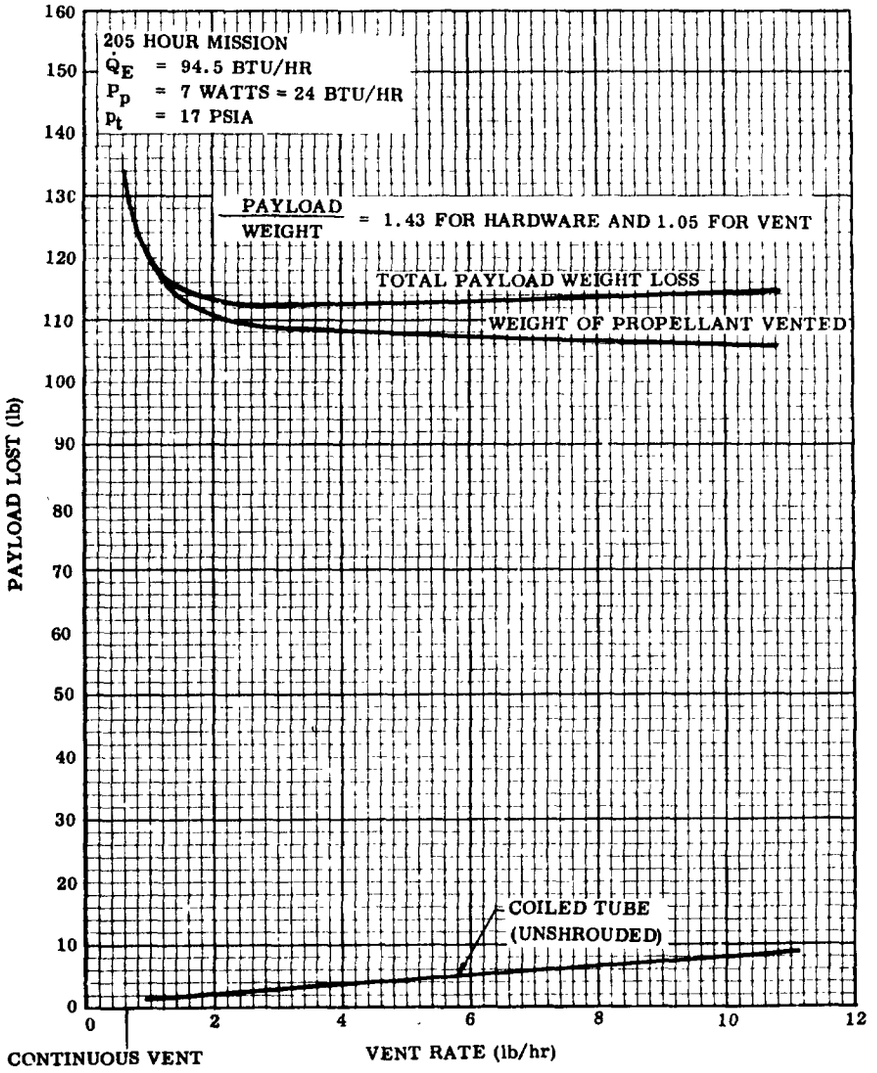

Figure 2-7. Payload Loss as a Function of Vent Rate (Cryogenic Service Module)

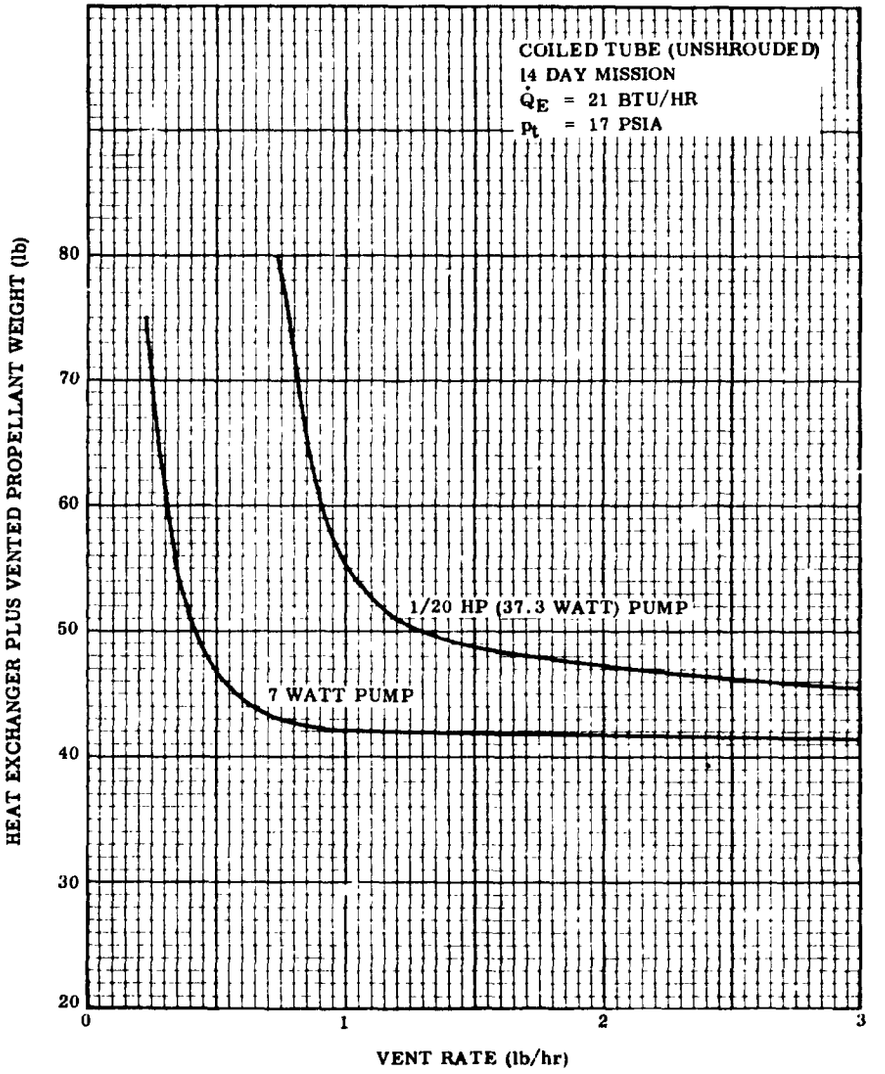

Figure 2-8. Effect of Pump Power on System Weight

$$\dot{Q} = h_{f_H} A_H (T_H - T_W) = h_{fc} A_c (T_W - T_c) \tag{2-4}$$

where

$$(T_H - T_W) + (T_W - T_c) = (T_H - T_c) \tag{2-5}$$

and

$\dot{Q} = \dot{m}_v \Delta h$ (enthalpy change in the exchanger section)

Heat transfer calculations are based on 17-psia saturated LH_2 on the hot side and 5-psia saturated LH_2 on the cold side inlet. Hot side flow rate is 1260 lb/hr. In addition to the heat transfer requirement, the exchanger is designed to operate with a maximum cold side pressure drop of 0.4 psi with GH_2 at the vent inlet. The hot side pressure drop is 2.60 ft of LH_2.

Iterations are made to determine the minimum unit size (tubing length and diameter or plate-fin surface) meeting both heat transfer and pressure drop requirements. Weight is then determined assuming the use of aluminum tubing and construction.

The weight of vented propellant is determined from

$$m_{vT} = (\text{total mission time}) \left[\frac{\dot{Q}_E}{\dot{m}_v \left(\frac{e\lambda}{1-e} + h_v - h_L \right) - P_p} \right] \dot{m}_v \tag{2-6}$$

This equation for intermittent venting follows from the basic relation between energy input to the fluid and vent requirement, as derived in Appendix E of Reference 1-1.

From Figures 2-4 through 2-7, the optimum flow rate in all cases is close to 3 lb/hr. In any case, higher flow rates would result in a larger system package without a significant decrease in weight.

The use of a 37-watt mixer as compared to the 7-watt unit is shown in Figure 2-8. This illustrates that the use of the higher-power mixer will not become competitive, if at all, until quite high flow rates. This would result in a relatively short on-time, thus increasing system response requirements. Even though the system weight would still be fairly low, the heat exchanger and resulting overall system package would be larger. Using the 7-watt mixer with a vent flow of 3 lb/hr was, therefore, chosen for further consideration.

The fraction of the total mission time which the vent system must operate is a function of the vent flow rate and is illustrated in Figure 2-9. The amount of time

it takes the system to vent down to a given pressure depends on the pressure rise rate in the tank during non-vent conditions, as well as the actual vent rate, because when the system actuates it is assumed that any temperature stratification will be initially destroyed. The pressure rise rate of a closed tank is illustrated in Figure 2-10 for a mixed model, for a "surface evaporation" model, and for an average of these. Test data obtained by NASA Lewis Research Center (Reference 2-5) show that the average case is a reasonable approximation of actual orbital conditions. For the case where the vent flow is 3 lb/hr or 0.036 vent fraction, the actual time to vent from 17.5 psia to 16.5 psia is approximately 13 minutes. This is estimated to be more than sufficient to obtain complete mixing in the reference tank using the 7-watt pump. This is discussed further in Paragraph 2.2.4.

Another reason for going to vent-flow rates higher than those required for continuous operation is to increase allowable control valve sizes. This results in increased reliability and less stringent design requirements as to contamination and valve control. The equivalent required throttling valve orifice size is plotted as a function of flow rate in Figure 2-11. For a flow rate of 3 lb/hr, the equivalent minimum orifice is a reasonable 0.023-inches. For continuous flow, the equivalent orifice would be approximately 0.004-inches.

2.2.4 TANK FLUID MIXING. With respect to the heat exchanger vent system, the purpose of mixing the fluid in the tank is to obtain high efficiency in removing energy from the tank. The higher the energy at the heat exchanger during venting, the more efficient the system (lower vent mass for given heat input). In both low-g and one-g environments, a certain amount of temperature stratification will exist between heat entering the tank (heat source) and the energy leaving the tank through the heat exchanger (heat sink). Mixing the tank fluid is then accomplished to minimize these temperature differences.

Several criteria have been developed to determine pumping requirements to minimize stratification and promote mixing the tank fluid. These are discussed below.

2.2.4.1 Complete Mixing of Gas and Liquid at Low-G. Work has been accomplished in this regard at the Lewis Research Center using drop tower facilities (Reference 2-6). Mixing tests were performed using a fluid jet directed along the wall of a spherical tank.

The Weber number was the measure of complete mixing when g levels were very low (Bond number below 25). At higher Bond numbers it was found that the Froude number is the controlling parameter. These tests are presently continuing, and the results presented here are unconfirmed and preliminary. Also, it is realized that the extension of this work to cylindrical tanks will only be approximate. The terms in the Froude and Weber numbers are evaluated using the fluid jet velocity and the tank diameter as the characteristic dimensions. For the spherical tank used in the testing, it was found that a Weber number of 50 was required to completely circulate the tank fluid.

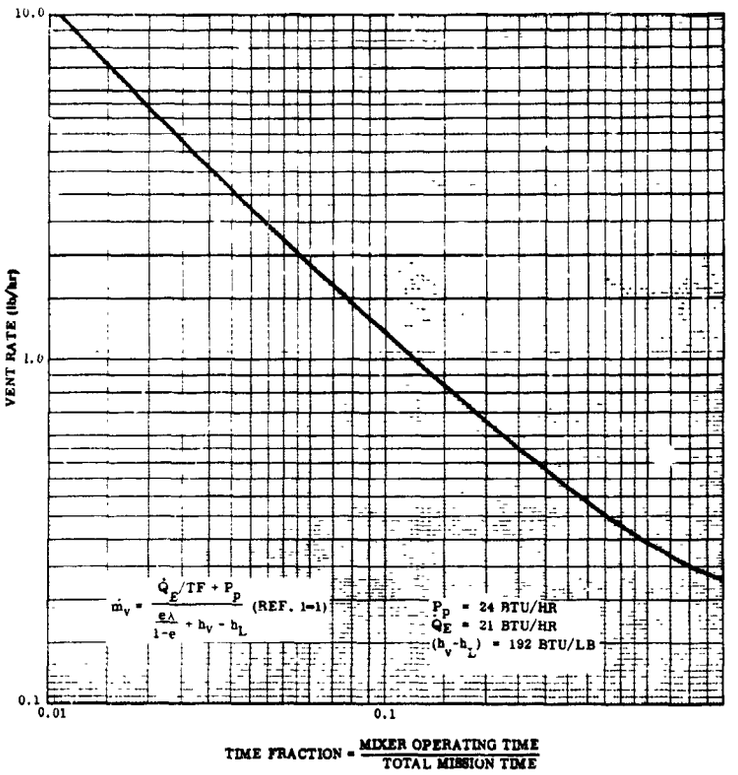

Figure 2-9. System Operating Time as a Function of Vent Rate

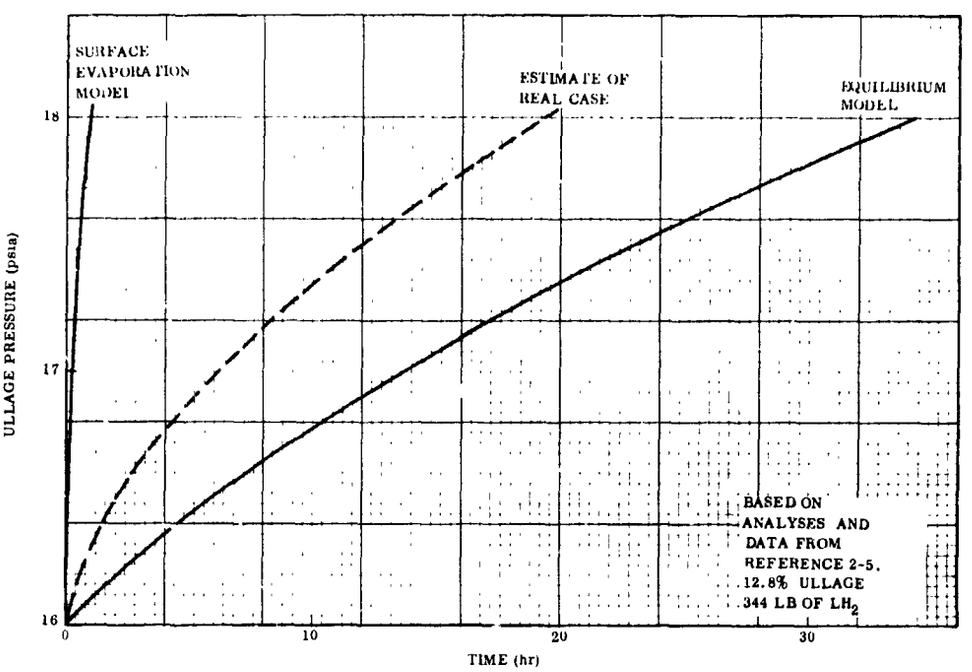

Figure 2-10. Orbital Tank Pressure Time History (Non-Venting)

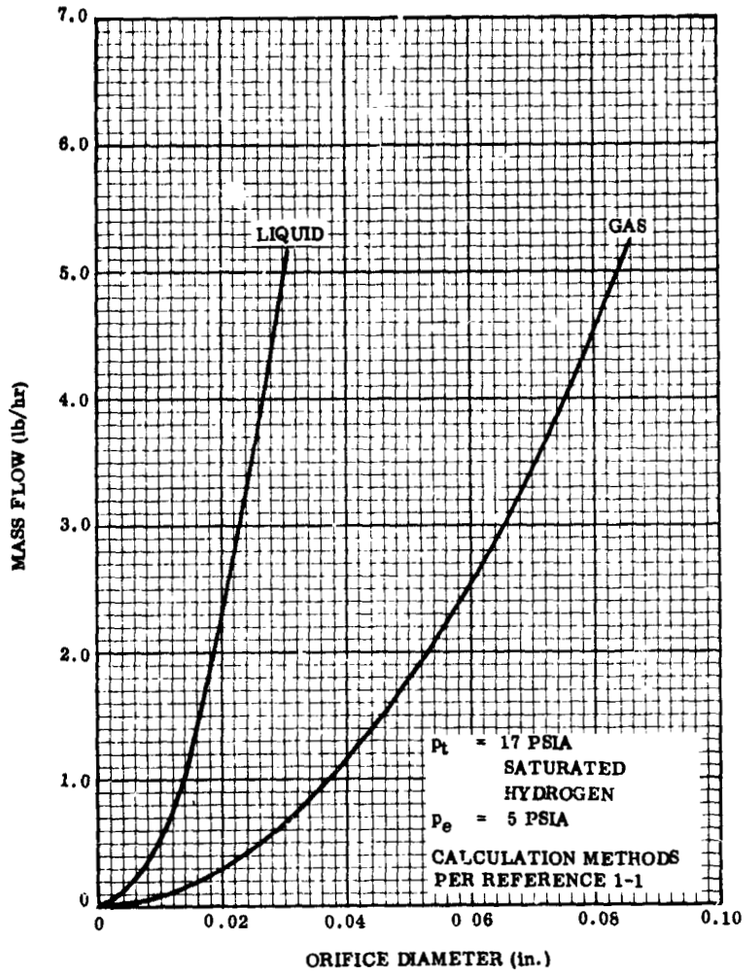

Figure 2-11. Throttling Valve Equivalent Orifice Diameter

Assuming the use of a hydrogen pump capable of pumping 1200 lb/hr of LH_2, the Weber number for the project THERMO test tank is plotted in Figure 2-12 as a function of jet diameter and velocity. A very low jet velocity, on the order of 0.1 ft/sec, is required to give a Weber number of 50.

2.2.4.2 Thermal Mixing or Stratification Reduction. An estimate of the degree of stratification reduction which can be accomplished with the heat exchanger pump system was made using data developed in Reference 2-7.

An energy transfer parameter (λ) is defined by

$$\lambda = \frac{\dot{Q}}{\dot{m}_L \, C_P \, \Delta T_R} \tag{2-7}$$

where

$\dot{m}_L$ = required liquid flow rate for destratification

$\dot{Q}$ = heat input rate to the propellant

C_P = specific heat of the liquid

ΔT_R = difference between the maximum fluid temperature and the bulk fluid temperature. The lower this value the less the stratification and the more uniform the mixture.

Values of λ have been calculated using several flow models and jet flow configurations (Reference 2-7). Calculated values range all the way from 0.25 to 4.0.

Based on the present heating requirements for the test tank (30 Btu/hr maximum) and including the heat input to the mixer (24 Btu/hr), the total heating rate to the tank fluid is 54 Btu/hr. Using a conservative value of λ equal to 0.1 and

$$C_P = 2.4 \text{ Btu/lb } ^\circ\text{F}$$

$$\dot{m}_L = 1200 \text{ lb/hr}$$

From Equation 2-7

$$\Delta T_R = \underline{\underline{0.1875^\circ\text{F}}}$$

This shows the amount of stratification to be small under the foregoing conditions.

2.2.4.3 Time to Attain Complete Mixing. The above analyses assume a steady-state condition has been reached; however, the operation of the proposed system is

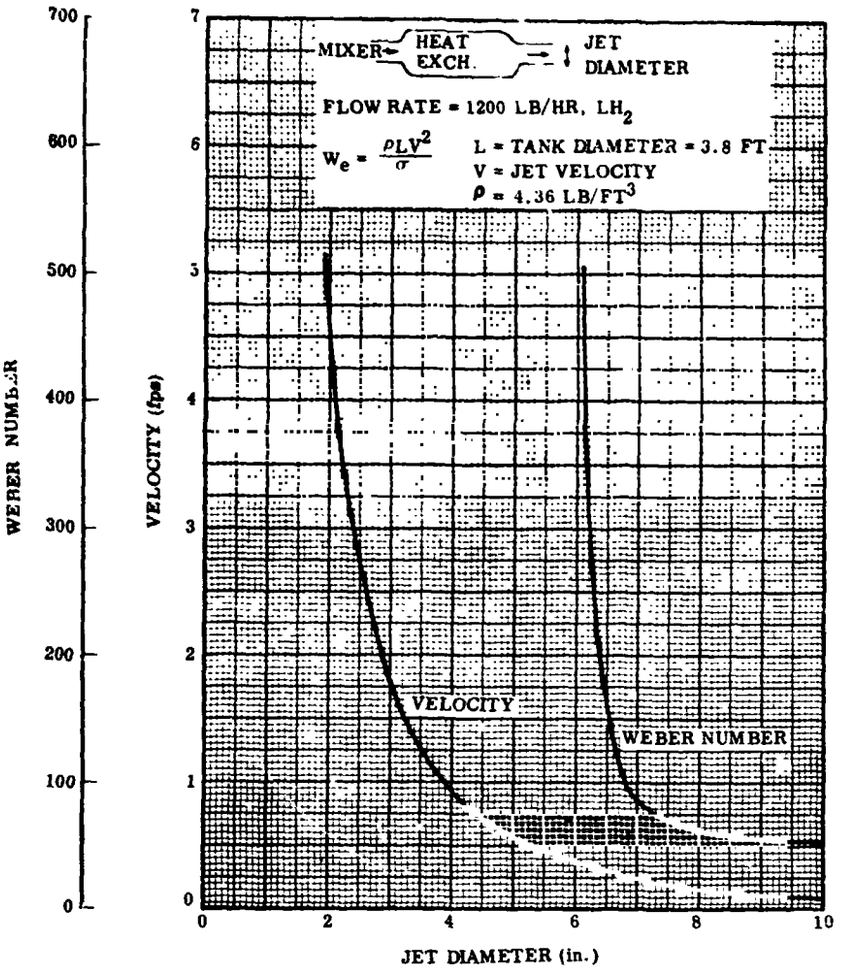

Figure 2-12. Weber Number Criteria for Tank Mixing

intermittent, and the pump mixer will be operating for a fairly short time during each cycle. Therefore, the time to attain complete tank mixing is an important consideration. The pump operating time during one cycle is estimated from Figures 2-9 and 2-10. Assuming system actuation at $17.6\ ^{+0.4}_{-0.3}$ and deactuation at $16.4\ ^{+0.4}_{-0.4}$, operating time during each cycle is calculated to range between 10 and 32 minutes.

Jet fluid momentum is of primary importance in developing complete mixing. Estimation of operating time is accomplished using the following equation taken from Reference 2-8.

$$\theta = K_2 \frac{H^{1/2} D_t}{(D_j V_j)^{4/6} g^{1/6}} \left(\frac{D_j V_j \rho}{\mu} \right)^{a_2} \qquad (2\text{-}8)$$

where the constants have the values

Reynolds No.	K_2	a_2
Greater than 2,000	118	-1/6
Between 200 and 2,000	8×10^5	-8/6

θ = time to attain complete mixing

H = liquid depth

D_t = tank diameter

V_j = velocity of jet discharge

D_j = diameter of jet discharge

The above equation is developed from test data for jet mixing of a dye in a single-phase fluid. This should give an approximation, however, of mixing times required for a two-phase fluid at low-g.

Using the project THERMO tank requirements where

$H = 7$ ft

$D_t = 3.8$ ft

$\rho = 4.36$ lb/ft^3

$\mu = 8.5 \times 10^{-6}$ lb/ft-sec

Then from Equation 2-8, where the jet fluid is turbulent;

$$\theta, \text{ sec} = \frac{74}{\left[(D_j, \text{ ft}) (V_j, \text{ ft/sec}) \right]^{5/6}} \tag{2-9}$$

This mixing time is plotted as a function of the product of the jet diameter and velocity in Figure 2-13. For values of $D_j V_j$ greater than approximately 1.0, the mixing time is fairly insensitive to further increases in jet momentum. For values of $D_j V_j$ less than 0.4, the mixing time is sensitive to changes in the jet momentum.

The total output head available from the pump must be equal to the sum of frictional flow losses through the heat exchanger and expansion flow losses at the exit of the exchanger. The fluid velocity at the exit of the exchanger causes mixing of the bulk fluid. The head requirement for mixing alone is assumed to be equal to the total dynamic head of the jet issuing from the exchanger. This assumes that the heat exchanger exit jet expands to zero velocity in order to mix the bulk fluid. This is a reasonably conservative assumption.

For the range of pump flow rates considered in the present study, the higher the head loss or velocity in the exchanger the smaller the required exchanger. The relationship of head loss to exchanger length for a three-eighth inch diameter tubular unit is shown in Figure 2-14. The pressure drop on the vent side, with only gas flowing, is also shown in this figure.

A study was made of the optimum relation between heat exchanger head loss and jet mixing head loss for various pump sizes. The total pump output power was assumed constant at 3,000 ft-lb/hr.

The total head loss through the pumping system is;

$$H_T = H_{ex} + H_j \tag{2-10}$$

where H_j, the head loss due to jet mixing is

$$H_j = \frac{V_j^2}{2g} \tag{2-11}$$

and H_{ex} is the frictional head loss through the heat exchanger system.

Fixing the heat exchanger size or head loss will result in the definition of an optimum pump flow and total head for a given total fluid power available. This is illustrated in Figure 2-15, where values of $D_j V_j$ versus the pump flow rate are plotted for various

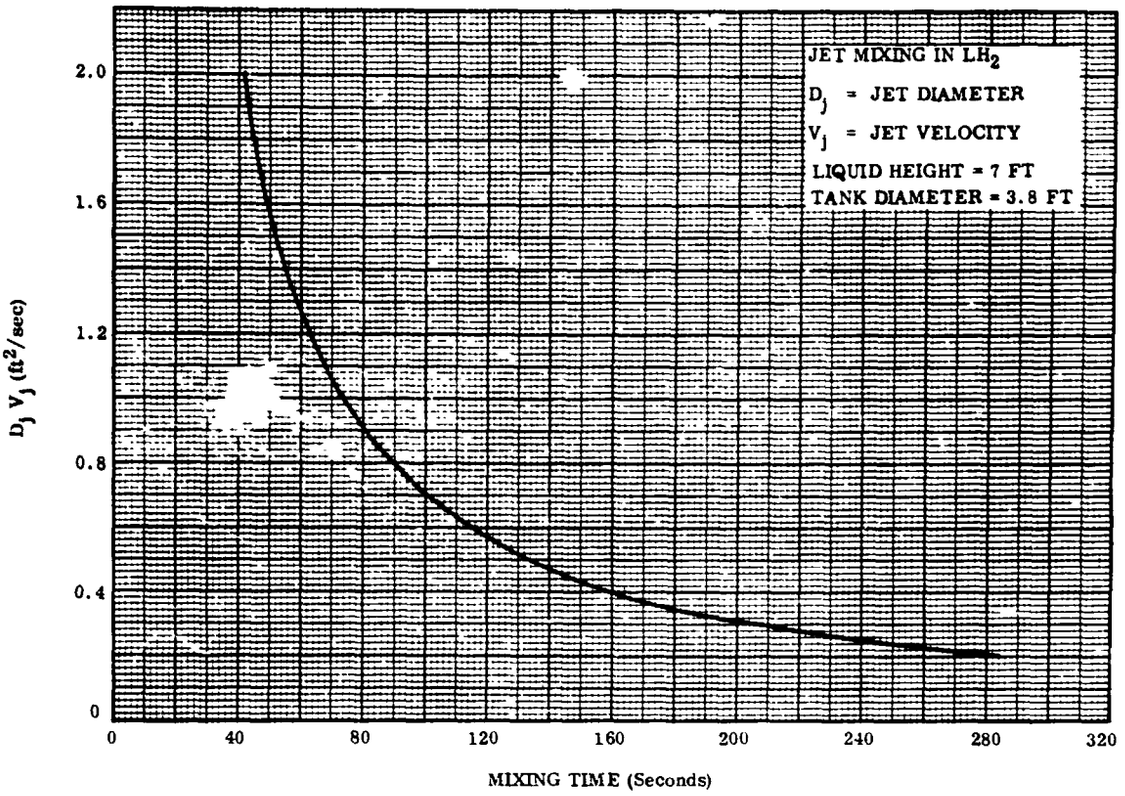

Figure 2-13. Time to Accomplish Fluid Mixing

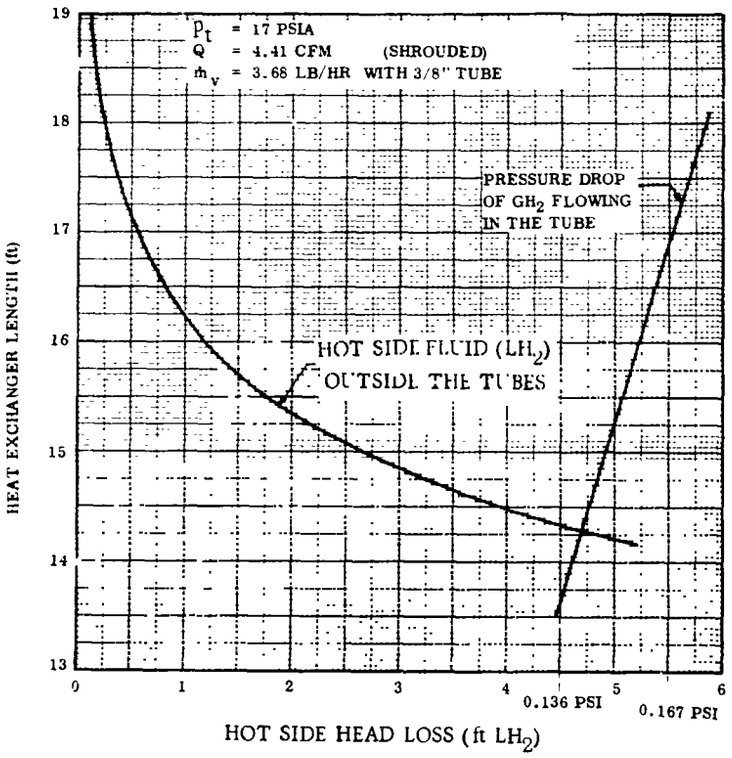

Figure 2-14. Exchanger Size Vs. Head Loss

values of head loss through the heat exchanger. It is seen that for a heat exchanger head loss of 1.25 ft the optimum pump flow rate is 1200 lb/hr.

The curves of Figure 2-15 are obtained by assuming a total pump flow rate and calculating the total fluid head available from the total fluid power

$$\dot{m}_p H_T = \text{Constant} = 3,000 \frac{\text{ft-lb}}{\text{hr}}$$

The jet head loss (H_j) is calculated from Equation 2-10 for a particular value of the heat exchanger frictional head loss (H_{ex}). The exchanger exit mixing jet velocity (V_j) is calculated from Equation 2-11 and the jet diameter (D_j) is calculated from the continuity equation.

Values of $D_j V_j$ versus exchanger head loss are plotted for various values of total pump flow rate and corresponding total head in Figure 2-16. These data illustrate the effect of heat exchanger head loss on fluid mixing times for the various pump sizes.

From the above analyses the use of the 1200 lb/hr, 7-watt pump, as described in Paragraph 2.2.3 appears reasonably optimum for the present application where good heat exchanger performance and fluid mixing are required. Therefore, a pump operating with a minimum flow of 1200 lb/hr LH_2 and a minimum static head of 2.5 ft LH_2 is recommended. The total head loss through the heat exchanger hot side is 1.25 ft LH_2.

The system defined above results in a small heat exchanger size (16 ft of three-eighths inch tubing for the tubular exchanger), from Figure 2-14. The mixing time, from Figures 2-13 and 2-15, is then approximately 78 sec, representing only slightly over 10 percent of the minimum system "on" time.

2.2.5 PLATE-FIN VERSUS COILED TUBE EXCHANGER. A number of preliminary envelope drawings were made for estimation of system installation requirements and to aid in selecting the type of exchanger. Typical drawings are shown in Figure 2-17 and 2-18. The dimensions given can be considered only nominal for an operational, integrated system without instrumentation. Following selection of vendors and components, detail installation drawings were prepared, including instrumentation, as described in Section 3.0.

A choice had to be made between the use of a plate-fin heat exchanger and the tube type. There are a number of advantages to the use of the tubular type; however, the final decision was not made until receipt of quotes on the plate-fin units. The major advantages and disadvantages of each are listed below.

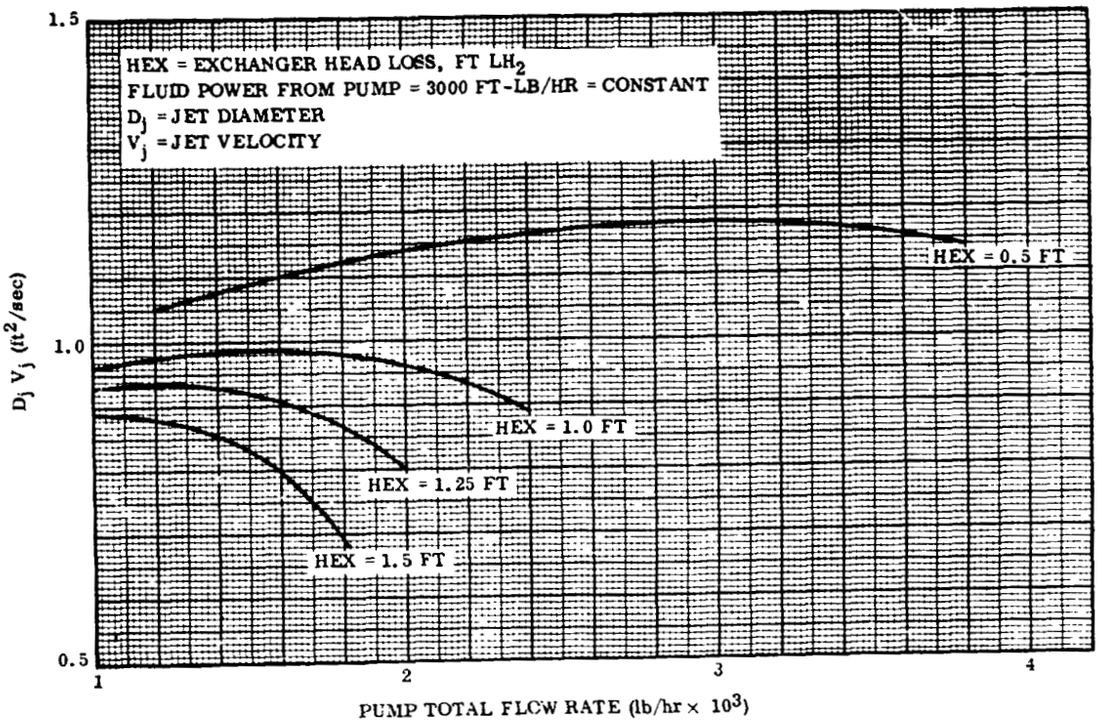

Figure 2-15. Effect of Hot Side Flow and Exchanger Head Loss on Tank Mixing

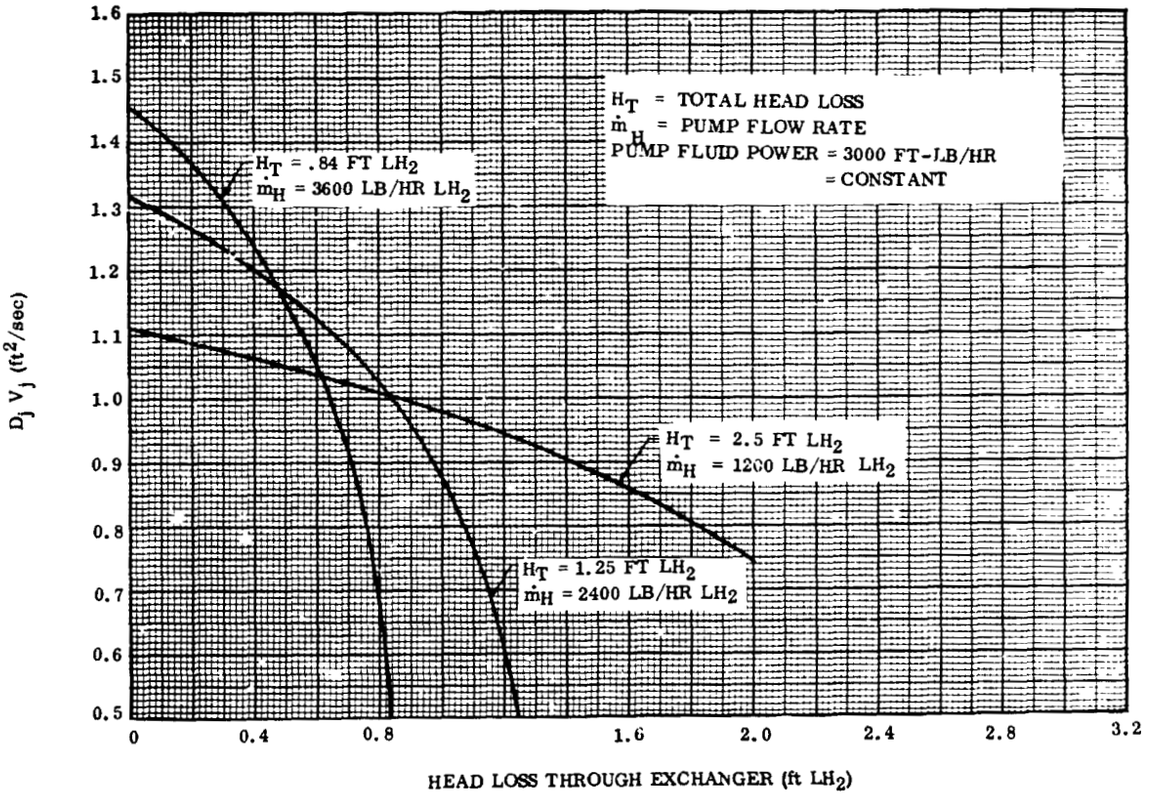

Figure 2-16. Effect of Exchanger Hot Side Head Loss on Tank Mixing

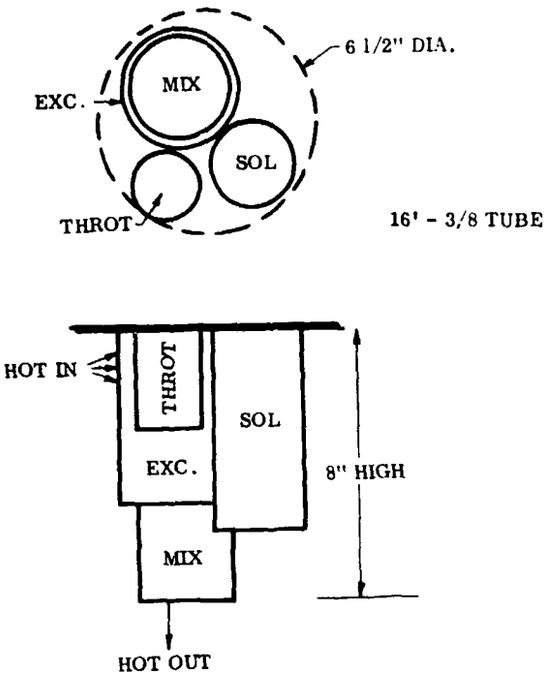

Figure 2-17. Typical Exchanger System Package (Coiled Tube)

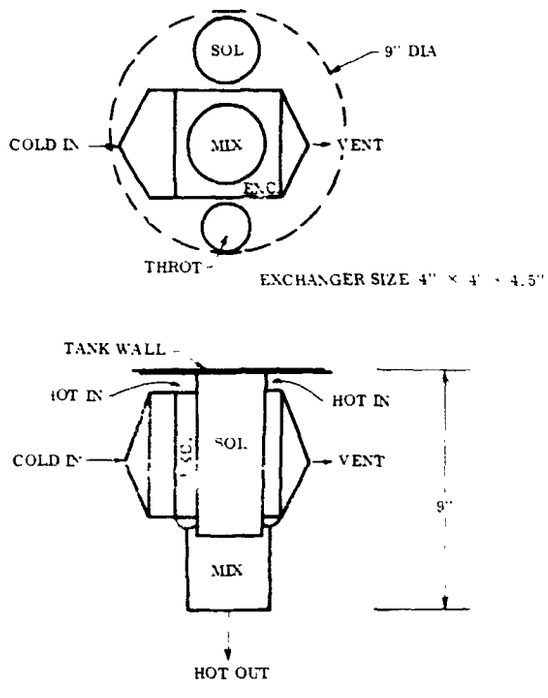

Figure 2-18. Typical Exchanger Package (Plate-Fin)

Coiled Tube Heat Exchanger

Advantages:

Liquid/vapor distribution on the vent side is not a problem.

The flow dynamics of the coiled tube configuration tends to cause liquid at the tube wall, thus reducing the probability of liquid "carry-over" at low-g. "Liquid carry-over," with respect to evaporator heat exchanger performance is the entrainment of liquid in the gas exiting from the exchanger. Such entrained liquid would not be vaporized and thus would be vented overboard, reducing the efficiency of the vent system.

Low cost and ease of fabrication.

Minimum leakage between tank and vent during system shut-down.

Disadvantages:

The surface efficiency is lower than for the plate-fin; i.e. pump power or pressure drop required to produce a given heat transfer coefficient is slightly higher.

Plate-Fin Heat Exchanger

Advantages:

Small package.

High surface efficiency.

Disadvantages:

Distribution of two-phase fluid within the core is a significant problem and is compounded at low-flow rates due to small flow passages required for individual paths.

Cost is high, especially in small quantities.

It may be difficult to prevent liquid "carry-over" at low-g.

In the final analysis, after receiving vendor quotes on the heat exchanger, it was determined that the cost of a plate-fin unit was approximately five times that of a tubular type, of special design, having both hot side and cold side vortexing flow such that heat transfer efficiency was very high in both the boiling and superheat sections of the unit. Also, the weight is approximately half that of a plate-fin unit, which must be significantly overdesigned to prevent liquid "carry-over" at low-gravity conditions. For these reasons, the tubular unit was chosen for prototype testing.

2.2.6 LOCATION OF COMPONENTS (SYSTEM CONFIGURATION). The major system configurations which were considered, along with major advantages and disadvantages and relative reliability estimates, are shown in Figure 2-19. The basic configuration chosen for initial testing was the one shown in drawing b, Figure 2-19. For the present testing, it was planned to vary the vent-flow rate by adjusting a hand valve downstream of the system and external to the vacuum chamber. The use of a pressure switch external to the tank, such that any adjustments or repairs could be easily made without having to enter the propellant tank, was selected. This component performs the basic control of the tank pressure, and the band may be critical for a given mission. Also, putting this unit outside the tank allows for maintaining a reasonably warm unit temperature, thus increasing the reliability and reducing costs. Furthermore, the switch is an absolute pressure referencing device, and, in space, a failure of the evacuated cavity to seal externally would not be serious if the unit were located in the

	ADVANTAGES	DISADVANTAGES	RELATIVE RELIABILITY (failures/10^5 flight hours)
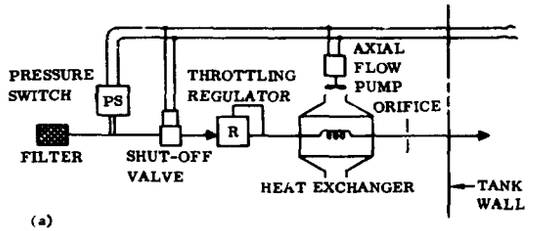 (a)	NEAT PACKAGE, SELF CONTAINED. PRESSURE SWITCH IS AT CONSTANT TEMPERATURE DURING OPERATION.	PRESSURE SWITCH AND SOLENOID ARE SUBMERGED IN LH_2 MAKING DEVELOPMENT MORE DIFFICULT. COMPONENTS ARE NOT ACCESSIBLE FOR MAINTENANCE CHECKOUT. POSSIBLE FIRST CYCLE PROBLEMS WITH PS.	285
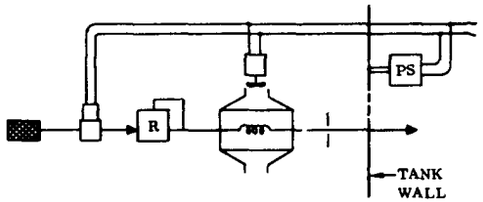 (b)	PRESSURE SWITCH NOT SUBMERGED SO IS EASIER TO DEVELOP. FIRST CYCLE PROBLEM ON PS IS MINIMIZED. NO LIQUID LOSS AT START-UP. REGULATOR IS SIMPLE DESIGN WITH NO INTERNAL LEAKAGE REQUIREMENTS.	EXTERNAL LEAKAGE SOURCES GREATER THAN (c) OR (d). POSSIBLE EXPANSION OF LH_2 TO VACUUM AT SHUT-OFF AND DURING COAST.	283
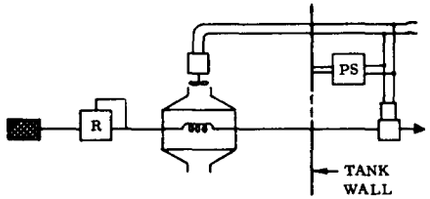 (c)	SOLENOID AND PS NOT SUBMERGED IN LH_2 SO DEVELOPMENT IS EASIER. MINIMUM OF EXTERNAL LEAKAGE SOURCES. NO EXPANSION OF LH_2 TO VACUUM THROUGH REGULATOR.	MAY OVERBOARD 0.10 LB LIQUID AT FIRST OF EACH CYCLE. REGULATOR DOWNSTREAM BELLOWS NEEDS TO BE DESIGNED FOR TANK PRESSURE. SHUT-OFF VALVE MUST BE LARGER IF NOT USED AS DOWNSTREAM ORIFICE.	260
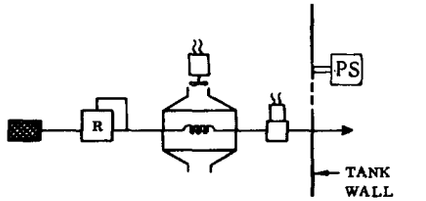 (d)	POSSIBLE SLIGHTLY SMALLER HEAT LEAK THAN (c) DUE TO VACUUM IN VENT LINE PENETRATION. OTHERWISE SAME AS (c).	DEVELOPMENT AND CHECKOUT OF SOLENOID NOT AS EASY DUE TO SUBMERGENCE IN LH_2. IF USED AS DOWNSTREAM ORFICIE NOT EASILY ACCESSIBLE FOR ADJUSTMENT OF FLOW; OTHERWISE SAME AS (c).	283

Figure 2-19. System Configurations Considered

vacuum environment rather than in the tank.

The other main choice was whether to locate the shut-off valve upstream or downstream of the heat exchanger system. Initially, location of the shut-off upstream of the exchanger was chosen since a fairly large valve would be required if located downstream, unless the valve itself were to be used as the downstream flow restriction. This might be desirable in an operational system, but, in the present case, the ability to vary the vent flow rate was desired.

The main objection to installing the shut-off valve upstream is that LH_2 leakage, if it were present through the heat exchanger fittings, regulator seals, and instrumentation bosses, could form solid hydrogen when expanding to the vacuum at pressures below the triple point. However, the major source of leakage would be through the shut-off valve and would be essentially independent of its location, since it was not proposed in the present case to require a regulator with a very low internal leakage. Such a requirement would tend to reduce reliability and increase cost. Subsequent testing of the system, however, showed that there was a significant amount of leakage through the regulator static seals and also, possibly, through the temperature instrumentation bosses. As a result, solid hydrogen could be forming and causing failure of the system regulation, as reported in Paragraph 5.2. Also, when the system is deactuated (shut-off valve closed), the liquid trapped in the system downstream of the shut-off valve tends to expand and boil-off quite rapidly and could possibly freeze.

In order to provide a high reliability system with shut-off upstream, the system leakage would need to be reduced and the pump allowed to operate for a sufficient time after vent shut-off to allow liquid trapped in the exchanger to be vaporized at a temperature above the triple point.

Locating the shut-off external to the tank for ease of access is also desirable. The practicality of such a location in an operational vehicle would be dependent upon the penetration of the vent line which would now contain a fluid rather than a vacuum. This heat leak, however, could be minimized to the same order of magnitude as with the valve in the tank by insulating completely over the shut-off valve external to the tank.

During the final series of testing, the heat exchanger vent shut-off valve was located downstream of the heat exchanger and external to the test tank and vacuum chamber. This testing demonstrated the desirability of locating the valve downstream. Design of the system is thus simpler with respect to external leakage of components and prevention of solid hydrogen formation. The recommended location for this shut-off valve in a flight system would be downstream of the heat exchanger and external to the propellant tank.

2.3 SYSTEM SPECIFICATIONS

Based on the design requirements of Paragraph 2.1 and the results of trade-offs and optimizations discussed in Paragraph 2.2, the component specifications presented in

Tables 2-2 through 2-7 were developed.

In all cases, the components are designed for operating vibration of 5 g and non-operating vibration of 20 g, with a duty cycle of 10 minutes on and 300 minutes off for a total of 2500 cycles. The vent flow rate is nominally 3 lb/hr. The vent exit is 100 percent gaseous hydrogen at 36°R and 4.5 $^{+1.0}_{-0.4}$ psia for flows up to 3.5 lb/hr.

Table 2-2. Regulator Specification

Type:	Internal Pressure Sensing Reducing Valve
Inlet Pressure:	17 ± 1 psia Operating. 50 psia Maximum Design
Inlet Fluid:	Saturated LH_2 or GH_2
Flow Rate During Operation:	Maximum 4 lb/hr LH_2 or GH_2. Minimum 2 lb/hr LH_2 or GH_2
Environment:	Same as Inlet Conditions.
Outlet Pressure:	5 ± 0.5 psia While Operating. 0 psia Non-Operating
Internal Leakage Allowable:	750 scim of H_2 or He With Valve at Operating Temperature and Pressure

Table 2-3. Shut-Off Valve Specification

Type:	On/Off Solenoid. Latches Closed or Open Depending on Last Command Received
Operating Pressure:	50 psia Maximum
Operating Temperature:	30° to 580°R
Outlet Pressure:	0 psia Minimum
Pressure Drop:	0.4 psia max. at 4 lb/hr GH_2, 16 psia Inlet, Temperature 36°R.
Internal Leakage:	0.001 lb/hr max. H_2 or He at operating pressure and temperature.
Electrical Requirements:	Voltage, 18 to 30 volts. Maximum duration of Operating Pulse 5 sec.
Current:	Max. 2.0 amps, 28 VDC 70°F Max. 5.7 amps, 28 VDC -422°F

Table 2-4. Pump Specification

Type:	Axial Flow
Flow:	1200 lb/hr minimum, when operating in LH_2 at $\rho = 4.36$ lb/ft^3
Static Head Rise:	2.5 ft LH_2 minimum, when operating in LH_2 at $\rho = 4.36$ lb/ft^3
Service:	Saturated LH_2 and GH_2, separate or mixed.
External Pressure at Operating Conditions:	16 to 50 psia
External Temperature at Operating Conditions:	35 to 45°R
Input Power to the Motor:	7 watts, maximum
Drive.	Electric Motor

Table 2-5. Heat Exchanger Specification

Type:	Cross-Flow
Service:	LH_2 and/or GH_2 on both hot and cold side
Flows:	Cold Side, 3.5 lb/hr; Hot Side, 1200 lb/hr, $LH_2 \rho = 4.35$ lb/ft^3
Design:	To operate in any orientation without liquid "carry-over" on cold side.
Pressures:	Cold Side Inlet, 5 psia $\pm$ 0.5 psia, Δp_{max} = 0.40 psi with GH_2. Hot Side Inlet, 17 psia $\pm$ 1 psia, Δp_{max} = 1.25 ft LH_2. For Structural Purposes, $p_{HOT\ Max}$ = 50 psia, p_{COLD} = 0 psi.
Temperatures:	Cold Side Inlet, 31°R, Exit 36°R; Hot Side Inlet 37.5°R.
Enthalpy:	Cold Side Inlet h = -110 Btu/lb$_M$, Exit = 86 Btu/lb$_M$
Connections:	Cold Side - Flanged or Threaded 3/8 tube; Hot Side - Flanged Ends
Size:	Smallest envelope possible; max. size, approximately 6" × 6" × 12"
Leakage Rates:	0.0001 lb/hr LH_2 at Operating Pressure and Temperature

Table 2-6. Pressure Switch Specification

Setting:	Actuation, 18.0 psia maximum Deactivation, 16.0 psia minimum Minimum Deadband Δp, 0.5 psi
Ambient Operating Temperature:	70° F ± 50° F
Electrical Requirements:	Circuit 1 - Single Pole Double Throw Max. 2.0 amp 28 vdc, 70° F Max. 5.7 amp 28 vdc, -422° F (Operates Solenoids on Solenoid Valve) Circuit 2 - Single Pole Single Throw 17.3 volts, 60 cps ac (Operates 7-watt mixer motor)
Maximum Pressure at Sensing Port:	50 psia

Table 2-7. Filter Specification

Type:	10 Micron Nominal Rating
Operating Medium:	Saturated GH_2 and LH_2 at 16 to 50 psia.
Pressure Drop:	0.5 psi Maximum at 4 lb/hr flow and 17 psia GH_2 at inlet with density of 0.075 lb/ft^3
Environment:	Submerged in Hydrogen at operating conditions

SECTION 3

DETAIL DESIGN

Following system definition and preparation of component specifications, as presented in Section 2.0, requirements were provided to hardware vendors, bids were received, and selections were made on the basis of technical ability and economy.

Within the scope of the present program, sufficient testing could not be performed to flight qualify or man-rate the hardware. However, the design philosophy was that the hardware be capable of being flight qualified at a later date. Also, components used in other flight programs, or components similar to flight-qualified units, were procured wherever possible.

Design details of the hardware and the test package used in this program, incorporating provisions for temperature and pressure sensing, are presented in the following paragraphs.

3.1 DELIVERED HARDWARE

Envelope drawings of the delivered hardware are presented in Figures 3-1 through 3-5, giving important dimensions for mating with the overall test package. A description of

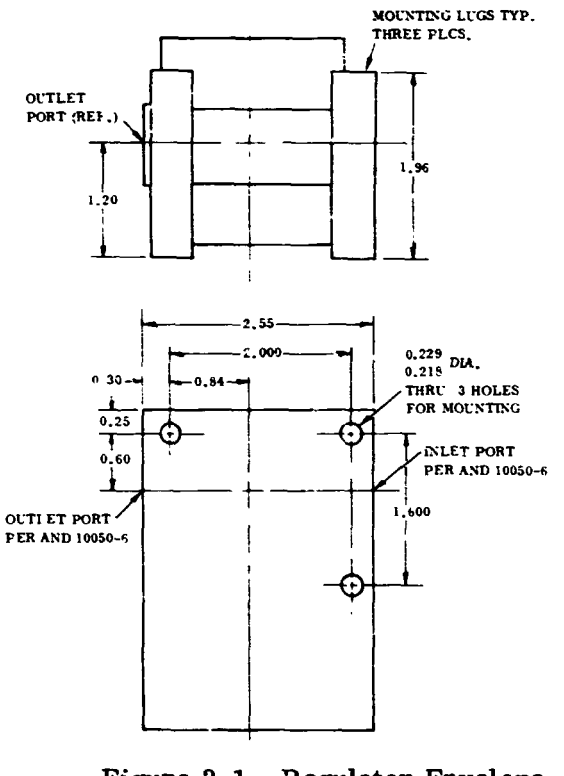

Figure 3-1. Regulator Envelope

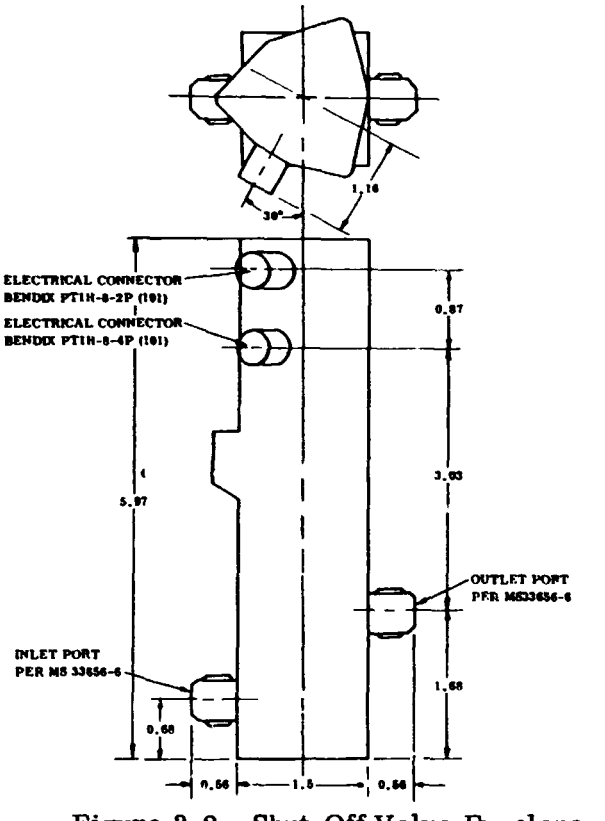

Figure 3-2. Shut-Off Valve Envelope

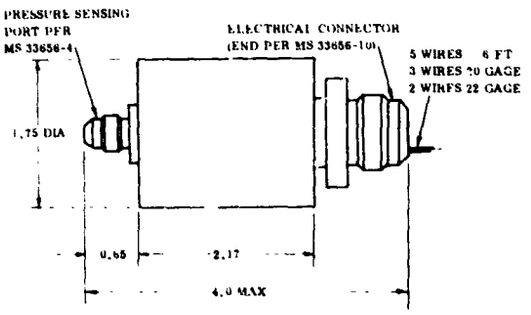

Figure 3-3. Pressure Switch Envelope

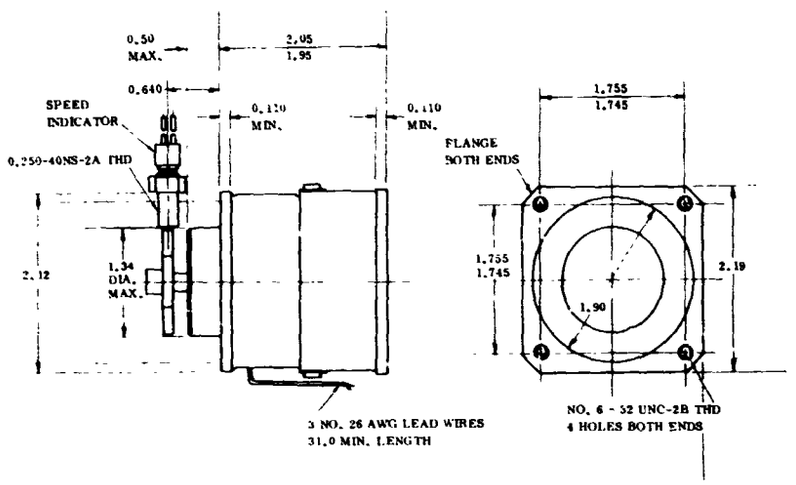

Figure 3-4. Pump Envelope

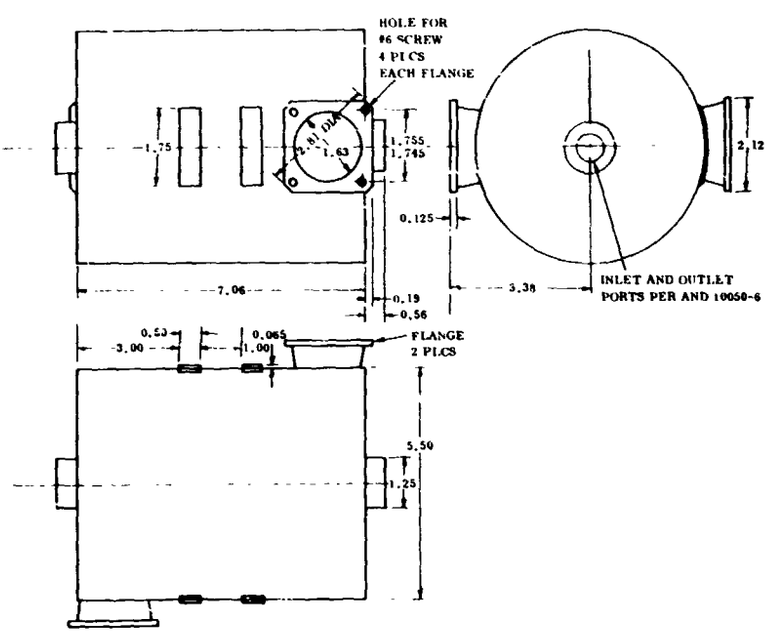

Figure 3-5. Heat Exchanger Envelope

these components and results of testing at the vendor's facility is presented below.

REGULATOR (Wallace O. Leonard P/N 187250-2)

The throttling regulator has an aluminum body, and the total unit weight is 0.62 pounds. Downstream pressure is sensed with an evacuated bellows, with an internal spring which actuates a positive ball-shut-off to meter the flow. This regulator is essentially the same as one qualified for hot gas service on the DYNASOAR program.

Testing performed at Wallace O. Leonard consisted of flowing helium gas through the unit at LN_2 temperature with the regulator immersed in LN_2 (Reference 3-1). Results are presented below.

Inlet Pressure (psia)	He Flow (scfm)	Controlled Outlet Pressure (psia)
18	1.5 to 3	5
16	1.5 to 3	4.8

SHUT-OFF VALVE (Wallace O. Leonard P/N 201200-2).

This unit has an aluminum body and a 28-v latching solenoid and weighs 1.31 pounds. For both opening and closing, power is applied for one to five seconds, and the unit remains in its last selected position upon removal of power. The solenoid and latching mechanism are presently used on the pilot control portion of the SIVB vent valve manufactured for Douglas.

Vendor testing was accomplished using helium gas at LN_2 temperatures (-300/-320° F) and with the unit submerged in LN_2 (Reference 3-2). No leakage was detected in the shut-off mode, and the pressure drop across the valve with three scfm (1.89 lb/hr) of helium flow was 0.15 psi. This converts to 0.4 psi at 4 lb/hr of GH_2 at a density of 0.075 lb/ft^3.

HEAT EXCHANGER (Geoscience P/N 02B101).

This unit is of all aluminum welded construction and weighs 2.75 lb. The cold or vent side flow is through a single coil of three-eights inch tubing, and the hot side flow is vortexed over the outside of this tubing. This design allows for highly efficient heat transfer of a boiling fluid and minimizes the possibility of liquid "carry-over."

Vendor testing was accomplished using Freon and water (Reference 3-3). Conversion of these test data to predictions for hydrogen performance gives:

Cold Side Δp_{GH_2} = 0.23 psi at 3.5 lb/hr flow.

Hot Side Δp_{LH_2} = 1.5 ft of LH_2 at 1200 lb/hr flow.

Overall UA = 190 Btu/hr ° F in the evaporation region.

With the design temperature difference between hot and cold side of 6.5° F, it is calculated that some superheat will exist at the exchanger outlet for vent-flow rates up to 6.4 lb/hr.

PUMP (Pesco P/N 189019-030).

The axial flow pump is basically of aluminum construction and weighs 0.6 pounds. The unit was modified from an existing pump used for air-flow. The motor was modified from a 400 cps unit and the required power minimized by lowering its speed to approximately 3300 rpm, 60 cycles single phase, and 17.3-v input. The speed and flow of the unit can be reduced to approximately one-third of design by proportionately reducing the frequency and voltage to the unit.

The delivered configuration incorporates a speed pickup wheel mounted on the motor shaft. Testing was performed at Pesco in both saturated GH_2 and LH_2 (Reference 3-4) with the following results:

Operation in -421° F GH_2:	Speed = 3470 rpm
	Input Power = 3.6 watts
Operation in LH_2:	Speed = 3200 to 3210 rpm
	Input Power = 7.0 to 7.2 watts
	Head Rise = 2.23 to 2.2 ft of LH_2
	Flow Rate = 4.5 cfm LH_2 (1190 lb/hr)

PRESSURE SWITCH (Frebank P/N 8394-1).

This unit is of stainless steel construction, weighs 0.75 pounds and uses a toggle type action. Vendor testing was accomplished using air at temperatures of 0° F to 145° F (Reference 3-5). Results are summarized below.

Actuation Pressure, psia	Deactuation Pressure, psia	Δp, psi	Ambient Temperature
17.8	16.2	1.6	0° F
17.7	16.2	1.5	0° F
17.2	16.2	1.0	145° F
17.1	16.2	0.9	145° F
17.6	16.2	1.4	55° F
17.5	16.2	1.3	55° F
17.4	16.1	1.3	75° F
17.3	16.1	1.2	75° F

In addition, the following vibration testing was accomplished.

Phase I: With the switch mounted at the sensing port, vibration testing was performed from 20-2,000 cps at 5-g peak while pressure cycling at 8 ± 2 cpm.

Phase II: With the switch sensing port vented to atmosphere, vibration testing was performed from 20-2,000 cps at 20 g peak.

The switch remained within print setting tolerance and NO chatter, contact resistance variation, or discrepancies of any nature were observed during both Phase I and Phase II of the vibration test.

3.2 TEST PACKAGE DESIGN

Design of the overall test package incorporated provisions for temperature and pressure sensing, system mounting, and heat exchanger inlet and outlet flow transition. A photograph of the assembled package is presented in Figure 3-6. The pressure switch, which is located externally to the test tank, is shown in Figure 3-7. The layout shown in Figure 3-8 was made after receipt of vendor and component drawings.

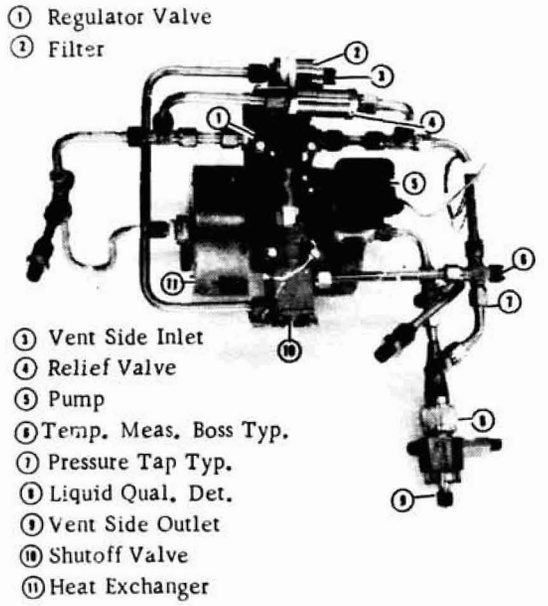

Figure 3-6. Heat Exchanger Vent System

Figure 3-7. Pressure Switch

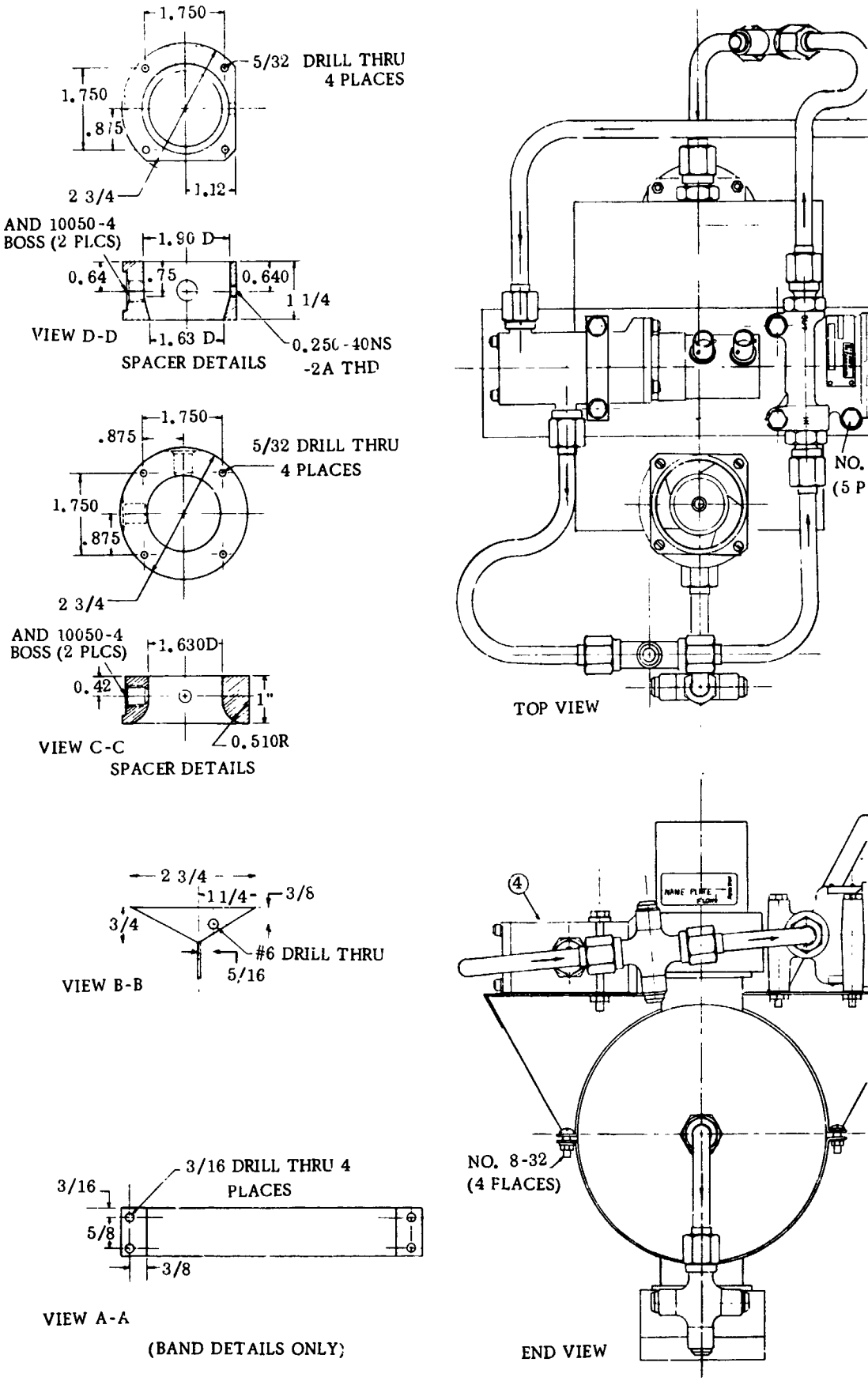

Figure 3-8. Heat Exchanger Test Package Layout

Fold out Frame 2

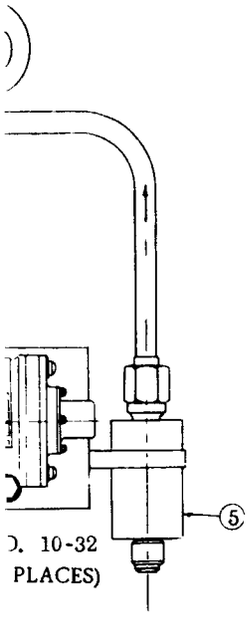

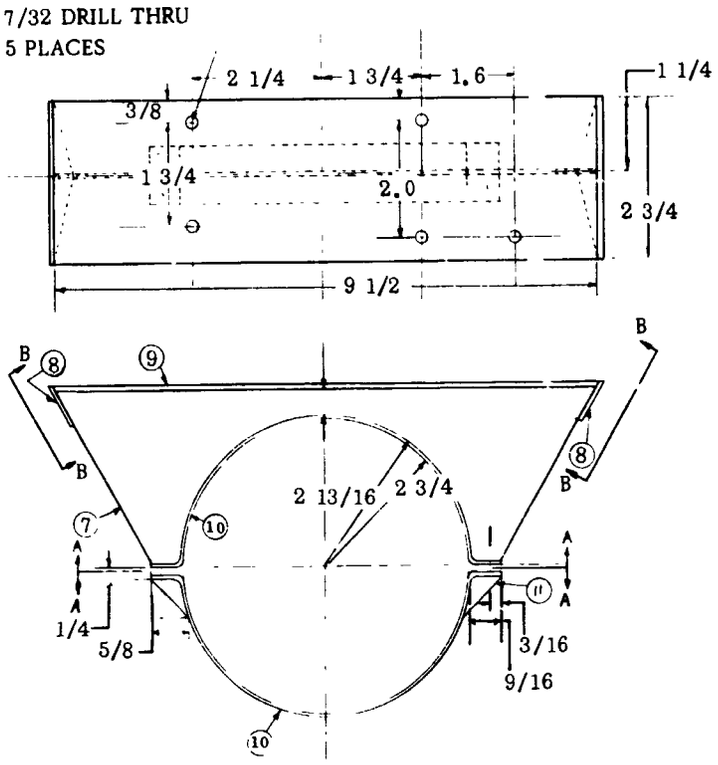

MOUNTING BRACKET DETAIL

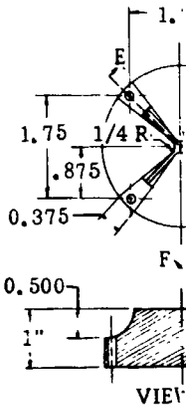

⑥ FLOW D

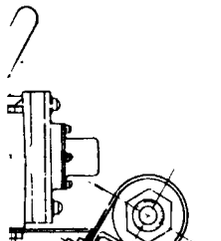

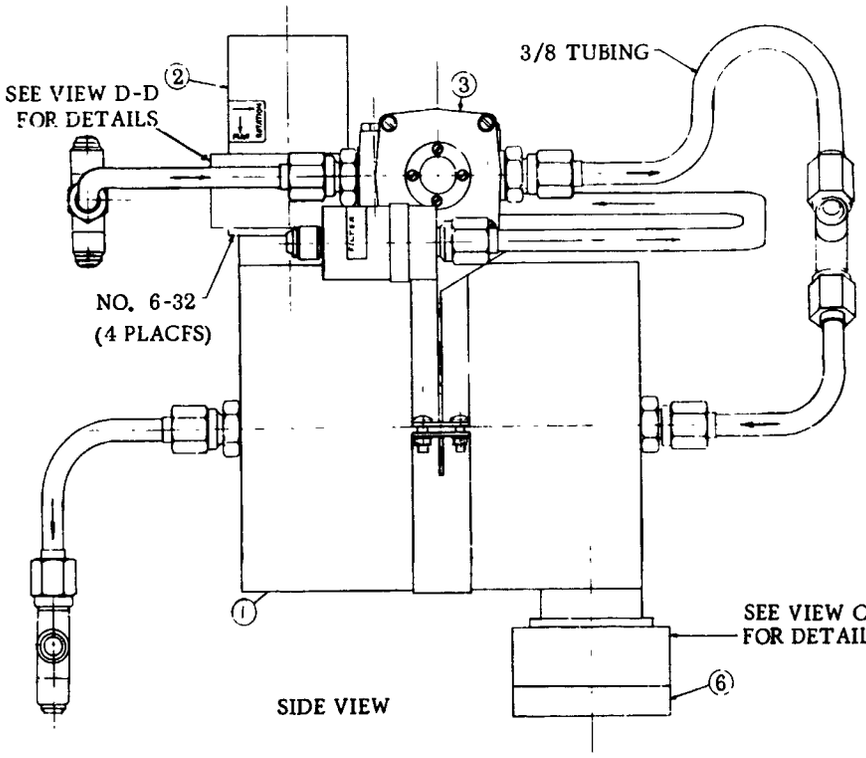

FIND NO.	NO. REQ.	DESCRIP
1	1	HEAT EXCHANGER, GE
2	1	MIXER, PESCO PROD. DI
3	1	REGULATOR, W. O. LE
4	1	SOLENOID VALVE, W.
5	1	FILTER, WINTEC, INGL
6	1	FLOW DEFLECTOR
7	1	MOUNTING BRACKET E
8	2	MOUNTING BRACKET E
9	1	MOUNTING BRACKET T
10	2	MOUNTING BRACKET S
11	2	MOUNTING BRACKET S

Solenoid Frame 3

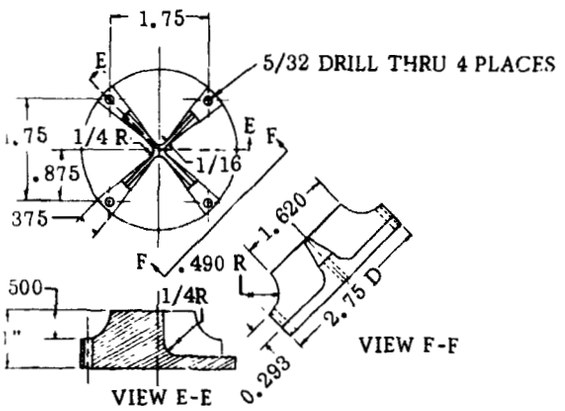

⑥ FLOW DEFLECTOR DETAIL

DESCRIPTION	PART NUMBER	STOCK SIZE
CHANGER, GEOSCIENCE LTD., SOLANA BEACH	P/N 02B1-1	
'ESCO PROD.DIV., BEDFORD, OHIO	P/N 189019-030	
OR W. O. LEONARD, PASADENA	P/N 187250-2	
) VALVE, W. O. LEONARD, PASADENA	P/N 201200-2	
WINTEC, INGLEWOOD, CALIFORNIA	P/N 14275-508	
FLECTOR		2.7" x 1.5
NG BRACKET BASE		1/16 x 9 1/2 x 3
NG BRACKET END		1/16 x 2 3/4 x 3/4
NG BRACKET TOP		1/16 x 9 1/2 x 2 3/4
IG BRACKET STRAP		1/16 x 1 x 18 1/4
NG BRACKET STRAP GUSSET		1/16 x 5/8 x 5/8

The entire test package as shown in Figure 3-6, minus the liquid detector assembly weighs 11 lb. In this system, heavy wall stainless steel tubing and instrumentation bosses were used in order to minimize expansion and contraction relative to existing CRES temperature probe fixtures. Fittings used for temperature probes are described further in Paragraph 5.1.

The relief valve shown in Figure 3-6, but not shown in the original design drawing (Figure 3-8), was added as a safety measure to protect the line between the shut-off valve and the throttling regulator. During certain periods of facility operation, both regulator and shut-off valve could be closed, with the possibility of trapping liquid in this portion of the system. Subsequent heating of this line could then cause an over-pressure condition.

In an actual flight application with the system shown (shut-off upstream of regulator), such trapping of liquid could not occur because the regulator would never be closed-off when the upstream valve was closed, (except on the ground) and only gas would exist at the system inlet. With the system shut off upstream of the regulator, the regulator will sense essentially a 0-psia outlet pressure while in space. At pressures below 4 psia, the bellows and spring assembly within the regulator will hold the regulator seat open.

With the shut-off valve located downstream, a safety feature would be required to prevent overpressure due to trapped fluid. This could be incorporated in the regulator design, or a separate check valve preventing pressure downstream of the regulator from significantly exceeding the upstream pressure could be employed.

The flow deflector shown in Figure 3-8 is designed to provide a radial flow from the heat exchanger. With this piece removed, a direct outlet flow results. In either case the exit area (2.09 in^2) of the exchanger is maintained, resulting in a jet velocity of 5.15 fps for a flow of 4.5 cfm.

The weight of the system as shown in Figure 3-8, except for using aluminum fittings, tubing, and mounting bracketry, would be approximately 8.25 pounds.

SECTION 4

SYSTEM VENT DOWN CHARACTERISTICS

As a result of project THERMO requirements, analyses were performed to evaluate the applicability of using the heat exchanger vent system at tank pressures up to 50 psia and at higher vent flows than for which the system was designed. The data show the limitations imposed by the various components and, therefore, what can reasonably be done to increase the vent capacity of the system.

The analysis was performed for the system configuration shown in Figure 3-8. Basic performance capabilities of individual components are obtained from the data of Tables 2-2 through 2-7. The two basic limitations on maximum vent flow are system flow capacity with saturated GH_2 at the inlet and heat transfer capacity to vaporize a LH_2 inlet.

Figure 4-1 represents an estimate of the maximum system vent flow obtainable as a function of tank pressure when the system inlet is saturated GH_2. For the presently procured heat exchanger design, a flow limitation of 9.15 lb/hr is estimated, regardless of tank pressure. This is illustrated in Figure 4-1. Such restriction could be reduced by increasing the heat exchanger passage sizing.

The vent flow limitations of the system with a liquid inlet are represented by the ability of the heat exchanger to vaporize all the liquid in the vent stream. As the tank pressure increases, the temperature difference between hot and cold sides increases. This allows an increase in vent flow for a fixed exchanger heat transfer area. The maximum flow rate as a function of tank pressure with a 100 percent liquid inlet is plotted in Figure 4-2 for the existing heat exchanger. A superheat requirement of 36°R at the exchanger vent outlet is assumed. Subsequent testing, Section 5.0, has shown this to be a reasonably conservative value for preventing liquid droplets at the exchanger outlet.

In order to vent down from 50 psia in a minimum of time, the data of Figures 4-1 and 4-2 show that a reasonable procedure would be to vent down from 50 psia to 26 psia at 9.15 lb/hr and from 26 psia to 16 psia at 3.5 lb/hr. This pressure and flow schedule is only one of the many possible and assumes the use of a two-step flow adjustment. This could be accomplished by using two different valve sizes or restrictions at the system outlet with the capability of switching from one to the other. Figure 4-1 shows that the limitation on maximum vent flow down to a tank pressure of 26 psia is choking in the heat exchanger. The maximum flow of 3.5 lb/hr at 16 psia tank pressure is due to heat transfer limitations of the exchanger with saturated LH_2 at the inlet (Figure 4-2).

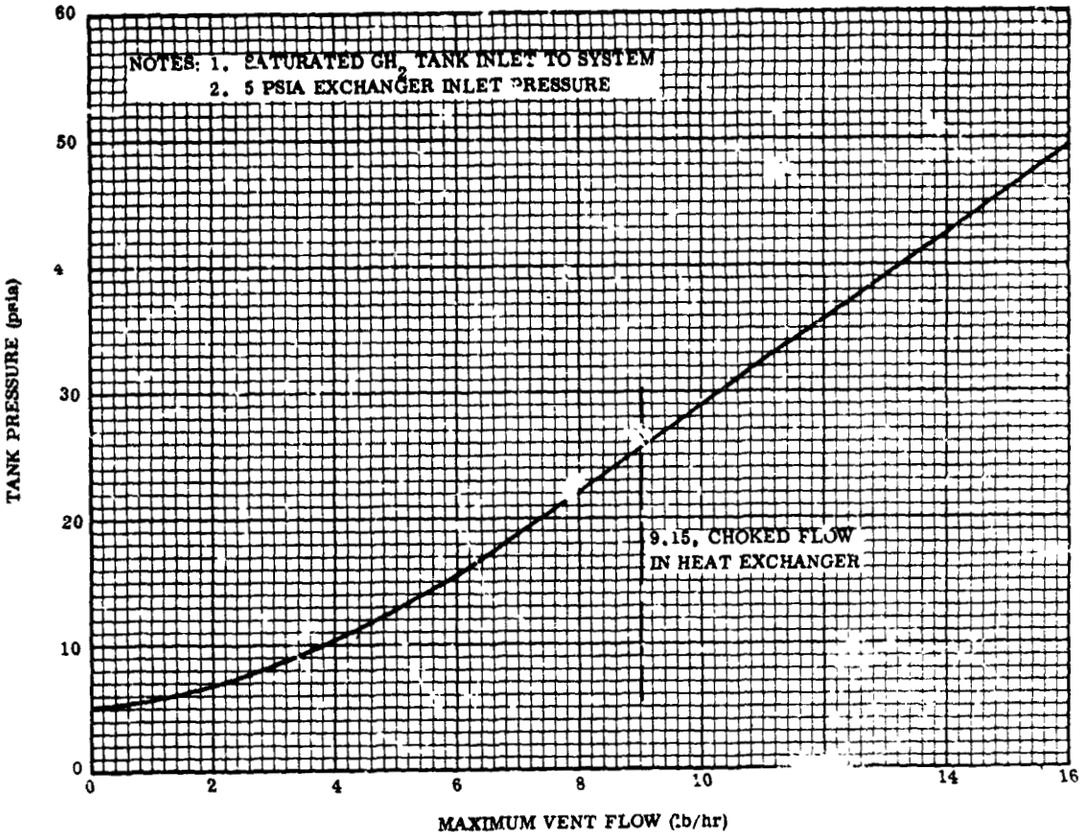

Figure 4-1. System Flow Limitation With GH_2 Inlet

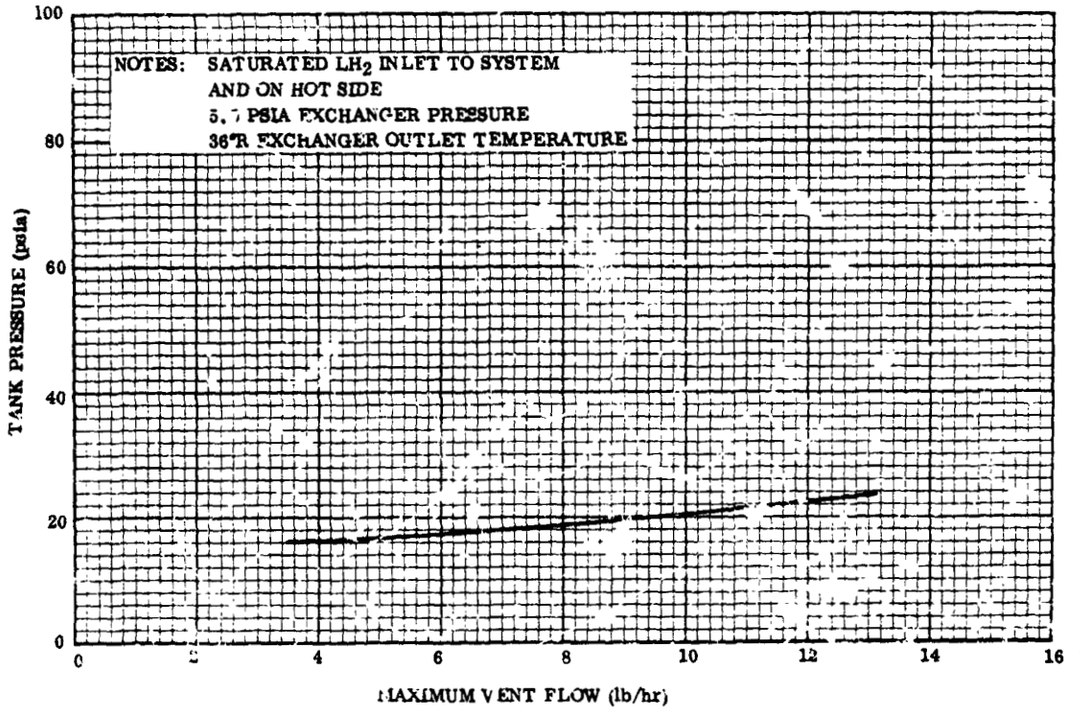

Figure 4-2. System Flow Limitation With LH_2 Inlet

SECTION 5

TESTING PROGRAM

The primary objective of the test program was to demonstrate the feasibility of the heat exchanger vent system to vent superheated gas and efficiently control tank pressure to 17 ± 1 psia when operating in both gaseous and liquid hydrogen. In addition to steady state operation, the transient characteristics of the system were measured when the system was initially actuated and when the vent inlet was cycled from gas to liquid and from liquid to gas. The performance of each component was monitored to ensure that each portion of the system was operating correctly. The test system, testing performed, and test results are described in the following paragraphs.

5.1 TEST SYSTEM

The test package schematic is shown in Figure 5-1. The three way valve upstream of the shutoff valve was used to cycle between gas and liquid at the vent side inlet. The liquid inlet to the three-way valve is at the 5.5-in. level in the tank while the gas inlet is at the 75-in. level. A photograph of the three-way valve is presented in Figure 5-2.

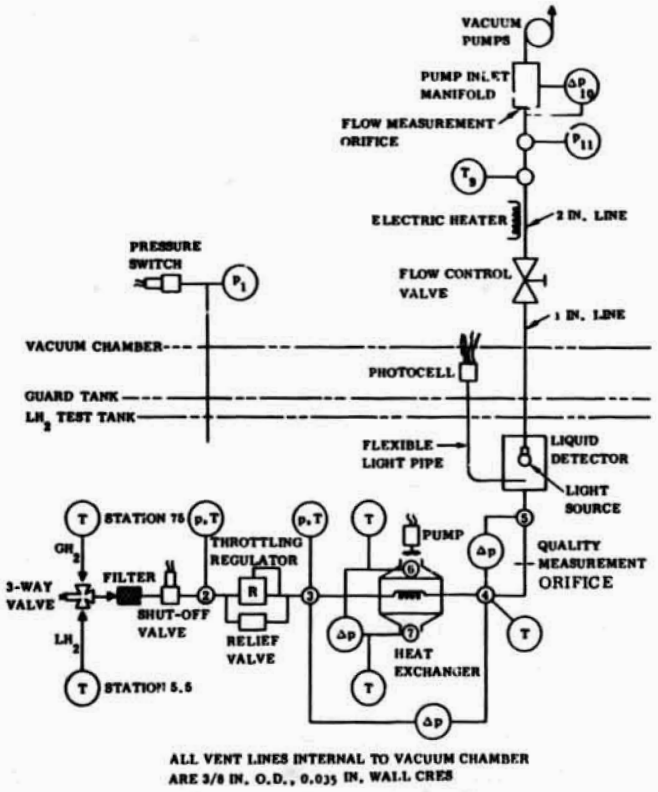

Figure 5-1. Basic Vent System Test Schematic

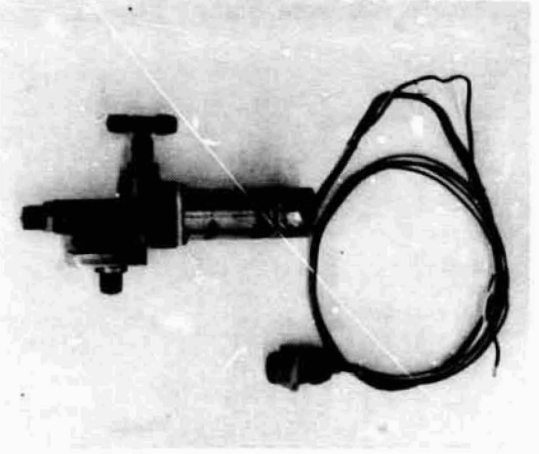

Figure 5-2. Three-Way Valve

The flow control valve upstream of the flow measurement orifice is used to vary the vent-flow rate from 2 to 4 lb/hr. The vent system is evacuated with a bank of Kinney vacuum pumps. The pump inlet manifold (Figure 5-1) is maintained at an absolute pressure of 5-10 mm of Hg during venting and approximately 100 microns of Hg when the vent shut-off valve is closed (non-venting).

The test package instrumentation consists of five 1181 Rosemont platinum resistance probes, one thermocouple (upstream of the flow measurement orifice), six pressure transducers, and one Kolsman gage.

The platinum resistance sensors consist of a coil of platinum wire embedded in a matrix of nonconductive material. Each sensor is 0.15-in. square and 0.05-in. thick and has a response time of 0.15 seconds in liquid. Platinum resistance sensors were chosen over thermistors because of the stability of the platinum probe when subjected to cycling between ambient and cryogenic temperatures. The platinum sensors have the added advantage of being usable in both an LH_2 and LN_2 environment.

The circuit used for readout of the temperature signal was developed under the 1966 Convair IRAD program (Reference 5-1). This circuit was chosen to stabilize the resistance of the lead lines between the sensor and the recording galvanometer. Each sensor is individually calibrated by Rosemont and Convair. The temperature uncertainty is $\pm 0.2°R$, while the reproducibility of data within a set of readings should be $\pm 0.1°R$. The temperature sensors were installed in fittings as shown in Figure 5-3 for use in the test package. The temperature sensor circuit is shown in Figure 5-4.

The thermocouple used was copper-constantan. The pressure transducers were of several different types. Pressures downstream of the regulator and upstream of the flow measurement orifice were measured by two transdeuco P-51A 8-57 transducers. The pressure upstream of the regulator was monitored with a Wiancko P2-1402. Two Edcliff 4-514-30 transducers were used to record the pressure drop across the quality orifice and the pressure drop across the flow measurement orifice. A Wiancko P2-4106-5 was used to meter the pressure drop across the heat exchanger. A Kolsman gage was used to read the pressure drop across the hot side of the heat exchanger. The transducers and thermocouples were fed directly into the Dymec (digital voltmeter) and the Sanborn recorder. The Sanborn recorder, which gives continuous readings of each temperature and pressure measurement, was used to monitor the transient

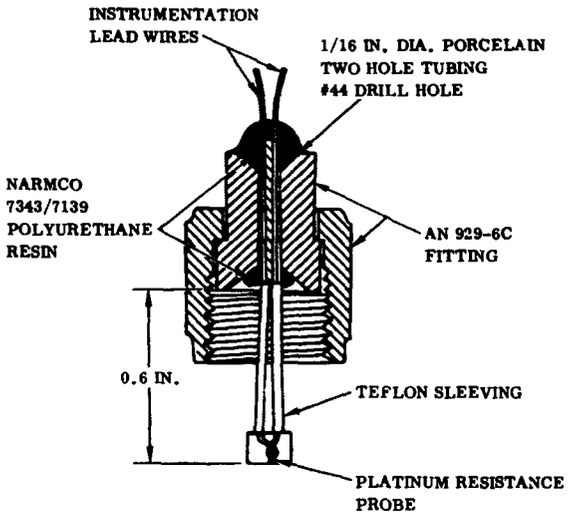

Figure 5-3. Temperature Probe Vacuum Pass-Through

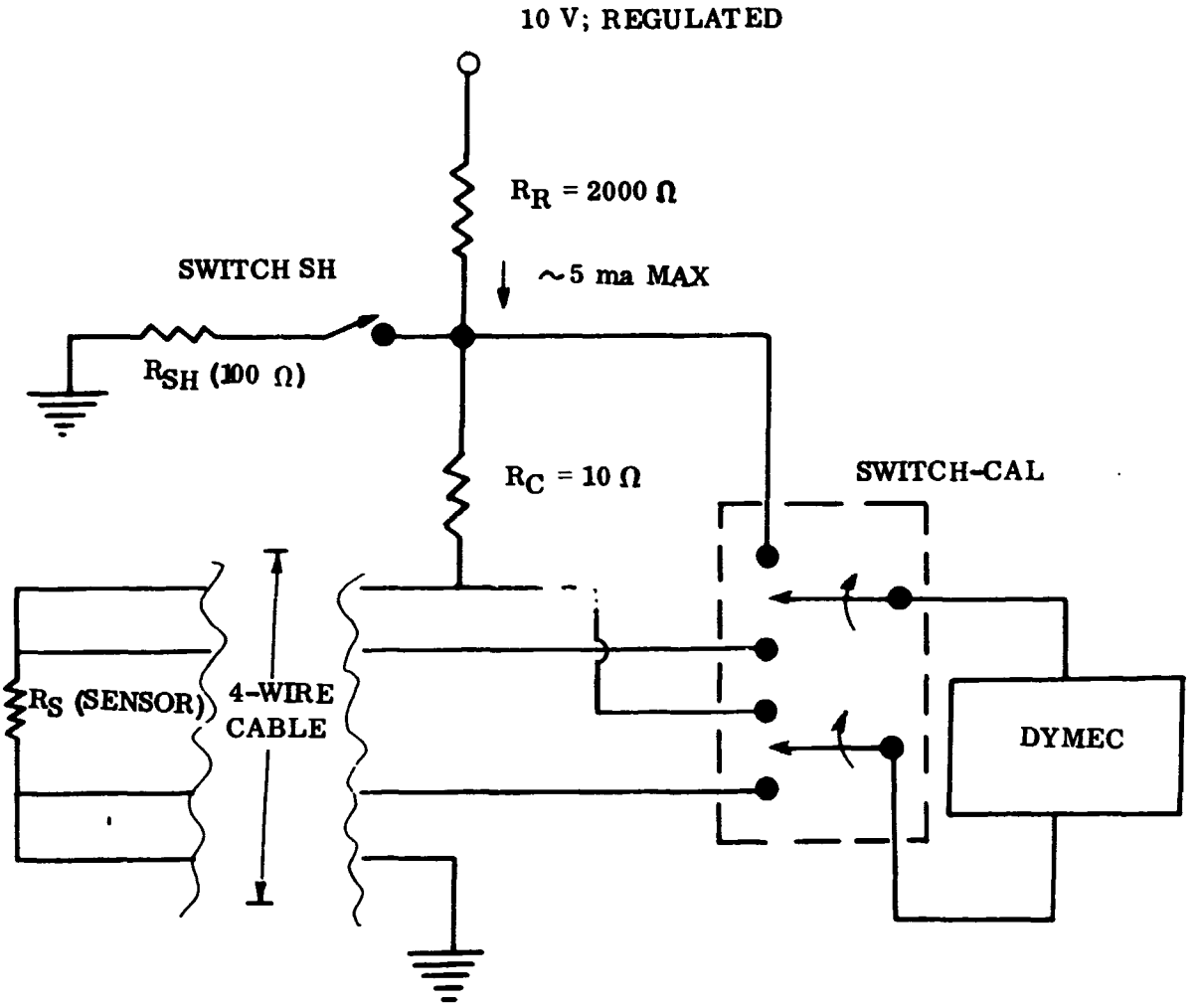

RESISTORS:

R_C - CALIBRATION (10 Ω) R_{SH} - SHUNT (100 Ω)
R_S - SENSOR (3 to 6 Ω)
R_R - CURRENT - LIMITING (2000 Ω)
SENSOR CURRENT: ~5 ma MAX
SENSOR RESISTANCE: 3 to 6 Ω ± 1 Ω
SENSOR ΔV: 15 to 30 mv ± 5 mv
ΔV/ΔT (SENSOR): 1.5 to 3.0 mv/°R
HEATING (SENSOR): ~0.1 MILLIWATT

Figure 5-4. Temperature Sensor Circuit

characteristics of the thermodynamic liquid vapor separator. The steady-state characteristics of the system were recorded on the dymec. The dymec tapes were machine reduced and plotted using the IBM 1040 plotter.

A Beckman wave form generator was used to control frequency and provide a pure sine wave into a McIntosh amplifier so that frequency and voltage at the pump input could be varied. Voltage was measured with a Fluke null-balance voltmeter. Pump speed was recorded on a Mosley strip chart recorder and read from a meter. A schematic of the vent system control circuit is shown in Figure 5-5. The system can be switched between automatic and manual modes. In the manual mode, independent switching of the pump, shut-off valve, and three-way valve can be exercised. In the automatic mode, the pressure switch controls both the shut-off valve and pump, while the three-way valve can be switched between gas and liquid separately.

An Optical Discontinuity Detector (ODD) is provided to determine the qualitative existence or nonexistence of liquid at the exchanger outlet. The principle of this device is to illuminate the fluid stream for observation with a photocell. The illumination is arranged so that the photocell is illuminated only by light reflected from optical discontinuities in the fluid stream. The electrical output from the photocell is recorded on the Sanborn. The illumination in the viewing area is provided by a small light bulb. The optical signal is brought out by a flexible light pipe, contained within a one-fourth-in. metallic tubing. The pipe-to-tubing gas seal is made outside the tank at the light/photocell housing which is in the vacuum chamber near room temperature.

This unit was designed and built under the Convair 1966 IRAD program, and devices very similar to this have been used at Convair to detect water, LN_2 and LH_2 droplets, and other optical discontinuities in slow and fast gas streams. When set up as described above, the ODD was always at least as sensitive as the best visual observation.

A quantitative indication of quality is obtained by use of the double orifice system shown in Figure 5-1. This system is based on the fact that an orifice meter is essentially a head meter measuring volume flow, i.e.;

$$Q = A_o \sqrt{2 g \Delta H}$$

Mass flow is determined from a knowledge of the fluid density. In the present application, the volume flow through the quality orifice is assumed to be due to the gas only. The gas mass flow rate at the quality orifice is thus determined, using values for gas density at the orifice. This method of determining the gas flow in a two-phase mixture is considered reasonably accurate down to qualities of 0.5. As an example, 10-percent liquid by mass at 5 psia saturation represents less than 0.1 percent liquid by volume.

A heater is located downstream of the quality orifice to ensure the vaporization of any liquid present in the vent stream. The total mass flow rate is then measured at the

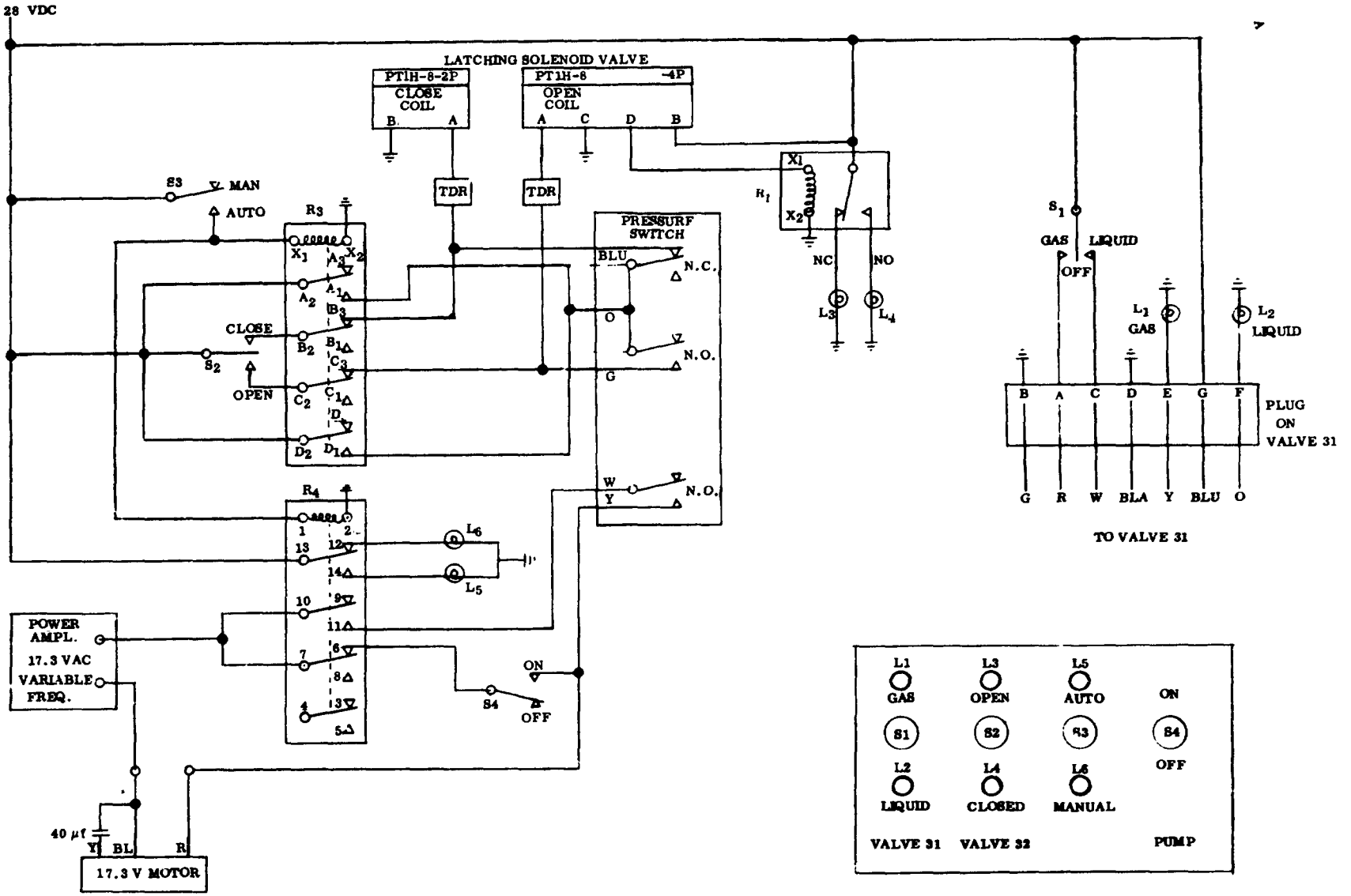

Figure 5-5. Vent System Control Circuit

flow measurement orifice shown in Figure 5-1. Based on the assumption of steady flow, the total mass flow rate at the quality orifice will equal that measured at the downstream flow orifice. Since only the gas flow was measured at the quality orifice, any difference in flow, as measured, would be due to liquid present in the flow at the quality orifice. The use of this method for determining quality is further discussed in Reference 5-2.

The double orifice meter was used as a steady-state quality detector while the optical detector was used to detect small droplets of liquid during transient conditions and for a qualitative check on the double-orifice system.

An illustration of the test tank used along with the location of the test package and test instrumentation is shown in Figure 5-6. A schematic of the overall test facility is presented in Figure 5-7.

Photographs of the test and guard tanks are shown in Figure 5-8 and 5-9.

The test and guard tanks installed in the vacuum chamber are shown in Figure 5-10. A portion of the instrumentation tree is shown in Figure 5-11.

The test tank, guard tank, and instrumentation tree were fabricated under the 1967 IRAD program for use in Convair funded stratification and stratification reduction testing. The test tank is 40 inches in diameter and approximately 85 inches high. The tank walls are 3/16-in. CRES and the elliptical domes are 1/8-in. CRES. The top access cover is 8 and 1/8-in. in diameter and the bottom cover is 21-in. in diameter. Both bottom and top flanges are sealed with 1/16-in. soft copper wire gaskets.

The vent system test package is located approximately 21 inches from the bottom of the tank. Also, in the tank are a series of platinum resistance probes and carbon resistors used to measure the tank temperature profiles and liquid level, respectively. Instrumentation is fed through the top of the test tank through the guard tank to the millivolt recording device used to monitor all the instrumentation . Vacuum pass throughs, Physical Sciences P/N ES-1079, were used for all wiring leaving the test tank. The guard tank, filled with test fluid, was used to reduce the heat leak to the main tank through instrumentation penetrations. The tank was superinsulated with 25 layers of NRC-2 around the entire periphery to reduce the heat leak to 28 Btu/hr to simulate the orbital heating conditions that the test system was designed for. In order to reduce the time between vent system cycles, a heater blanket was attached to the outside of the tank under the superinsulation. The heater blanket was also used to maintain tank pressure at a reasonably constant level while operating manually under various flow-rate conditions. This is necessary because the thermodynamic separator under normal heat flux conditions, removes heat from the tank at approximately 30 times the rate at which it is being added.

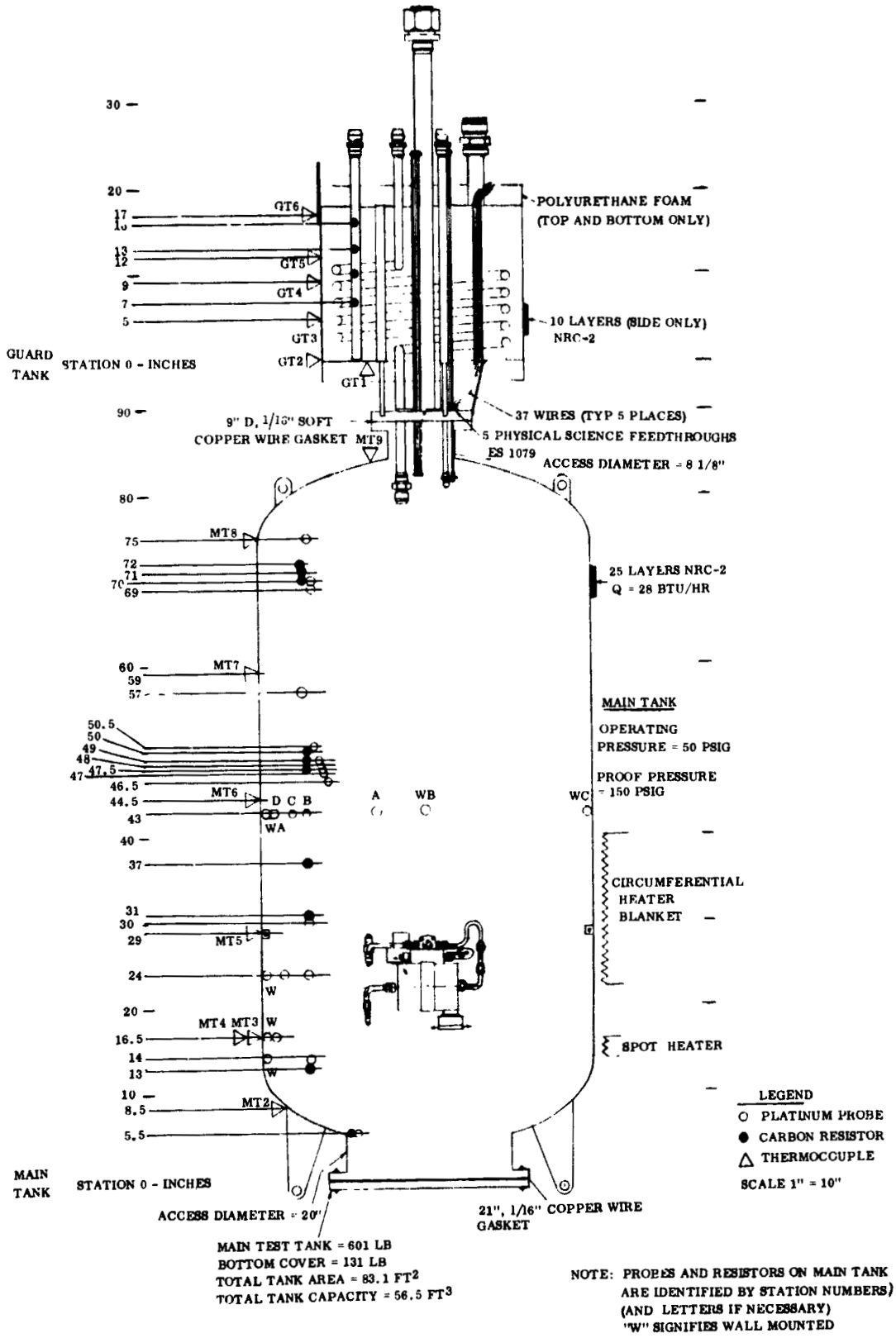

Figure 5-6. Test Tank System Installation Schematic

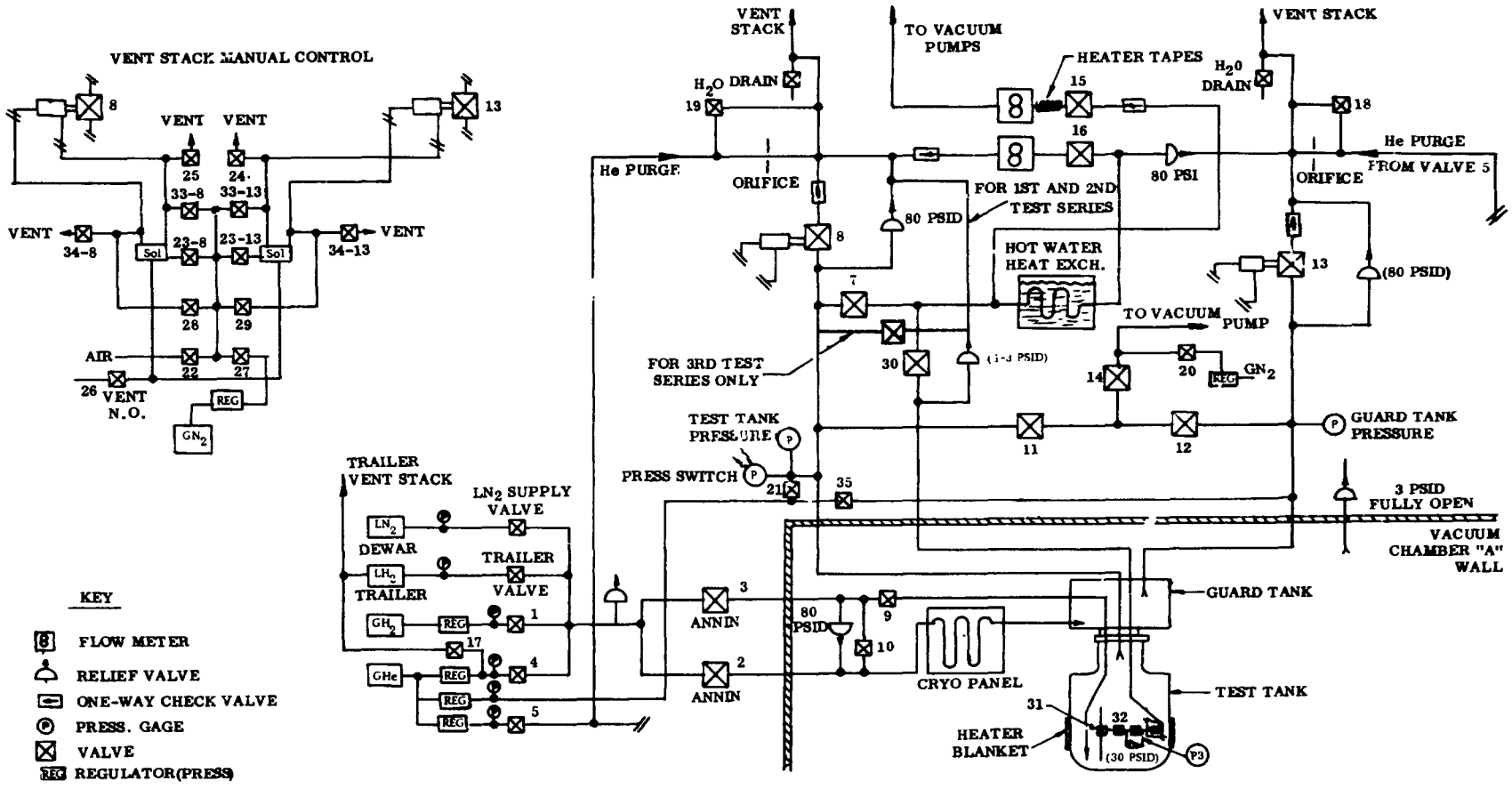

Figure 5-7. Facility Flow Diagram

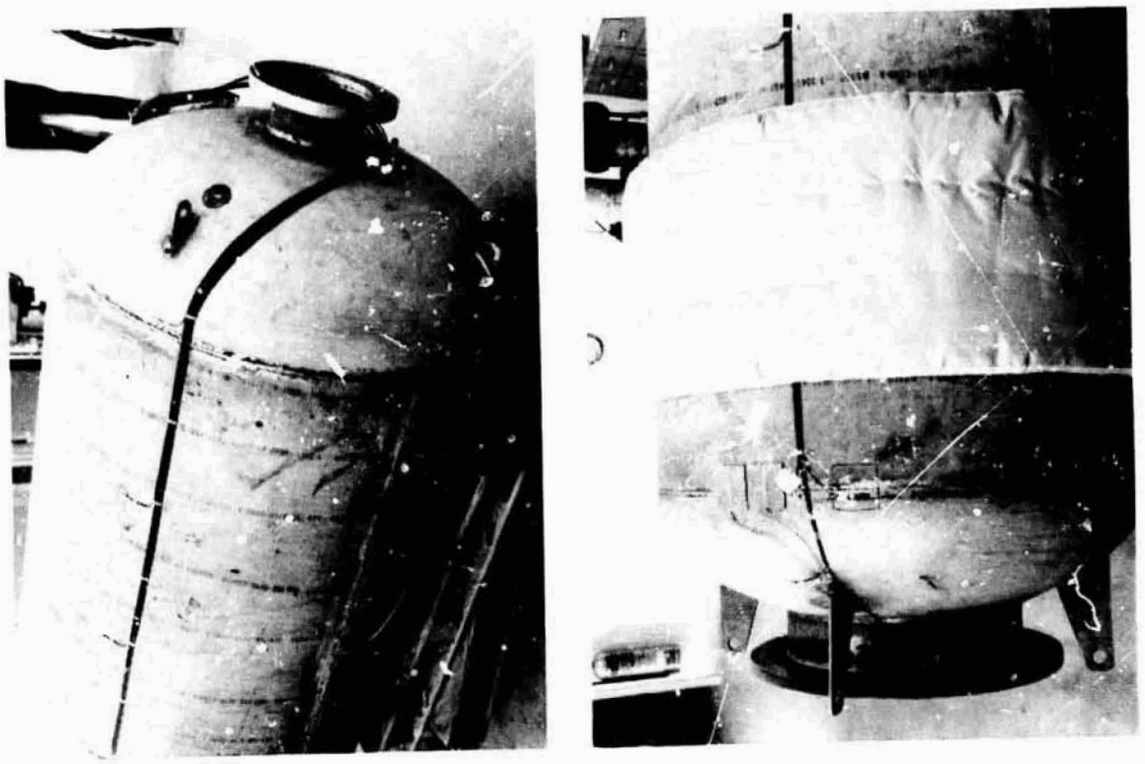

Top End

Bottom End

Figure 5-8. Test Tank

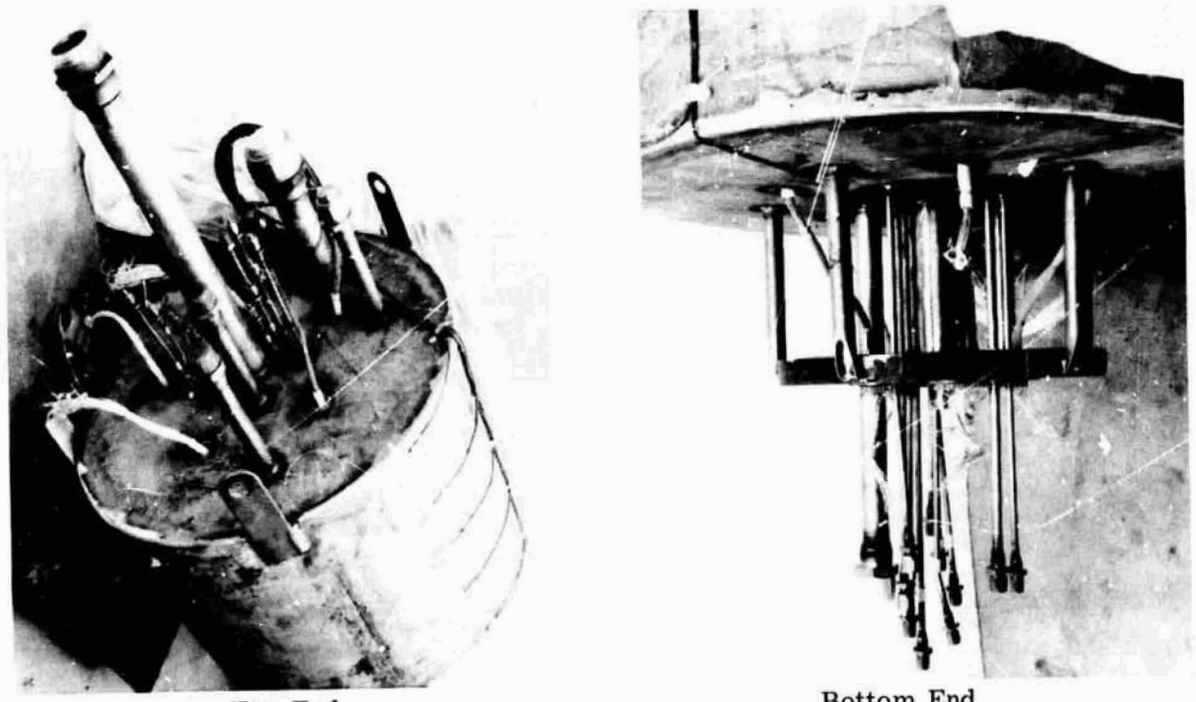

Top End

Bottom End

Figure 5-9. Guard Tank

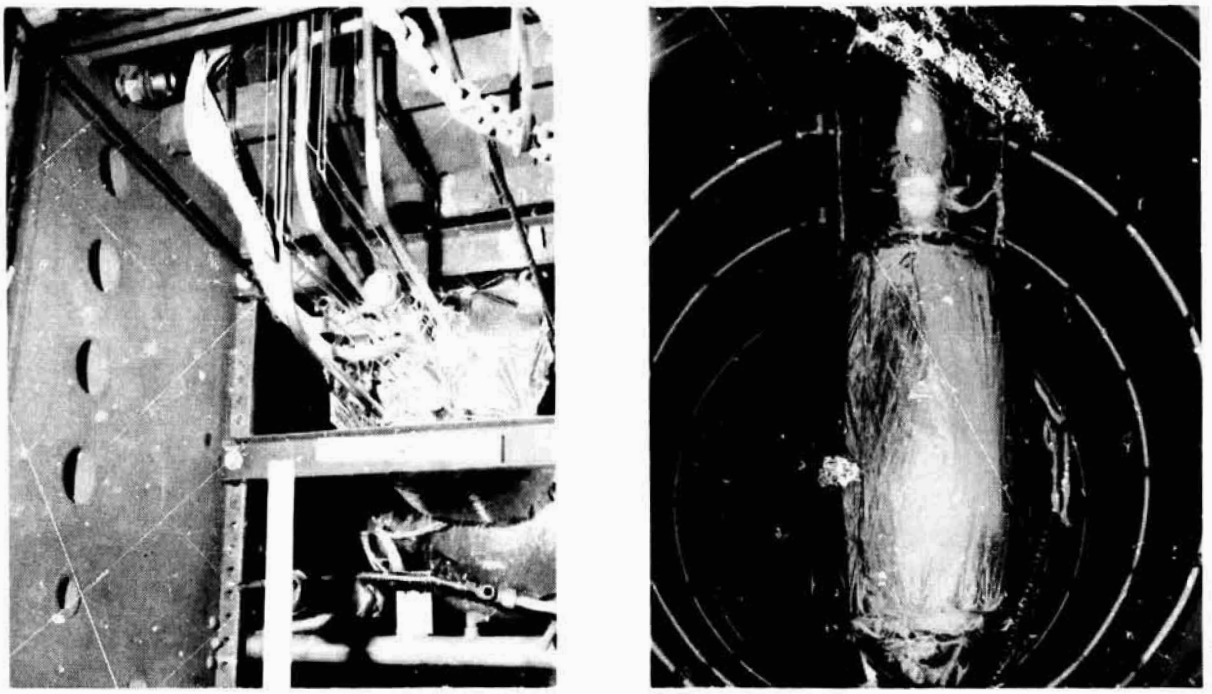

Top View

Side View

Figure 5-10. Test and Guard Tank Installed

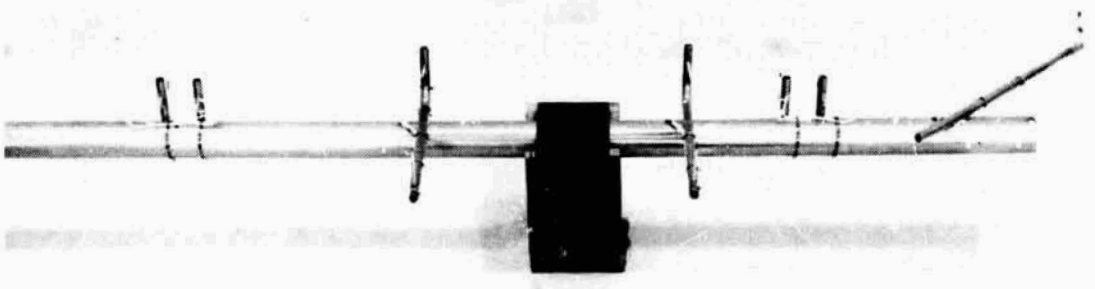

Figure 5-11. Instrumentation Tree (Bottom End)

5.2 TESTING PERFORMED

Testing of the heat exchanger vent system was accomplished in both gaseous and liquid hydrogen under a variety of flow conditions. The pump flow was varied by changing the input voltage and frequency to the motor. The vent side flow rate was varied by adjusting the flow control valve shown in Figure 5-1 (valve 15 of Figure 5-7). Cycling between gas and liquid vent inlets was accomplished with a three-way valve as illustrated in Figure 5-1.

Three major series of tests were performed. In the first series of tests the vent system was installed as shown in Figure 5-6. The pump flow was down through the heat exchanger with the outlet flow from the exchanger directed radially as indicated in Figure 5-6. The flow direction from the exchanger was produced by the flow deflector shown in Figure 3-6. The exit area from the exchanger was such that at nominal flow conditions of 4.5 cfm the exit velocity was approximately 5 fps. Initially, the vacuum chamber was pumped down to approximately 10^{-5} torrs. The test tank was filled with liquid nitrogen and the vent system operation was checked qualitatively. All components appeared to be operating satisfactorily. The instrumentation checked out successfully with the major exception of the optical quality detector which did not function. The first two series of tests were run with this unit not operating. After draining the liquid nitrogen, the test tank was purged with helium several times, then filled with liquid hydrogen. With the liquid initially below the test package (5.5 to 13-in. level) the system was checked out and operated manually at vent-flow rates from 2 to 4 lb/hr, with the vent side inlet in both gas and liquid. Transient data were obtained while cycling the vent inlet from gas to liquid and vice-versa and during system actuation and deactuation. The tank was then filled to the 48-in. liquid level and a series of runs were made, varying vent side flow rate while operating manually and recording transient data. Several automatic cycles (pressure switch controlling) were run with both gas and liquid at the inlet during actuation and switching between gas and liquid during the venting. After a temperature stratification test, the vent system was operated again, but the regulator stuck in the open position and would not regulate. This was after approximately 22 hours of testing. The LH_2 was then vented from the tank and the tank and test system purged with gaseous helium. The vacuum chamber was vented to atmosphere and the regulator tested with ambient helium resulting in satisfactory performance of the unit. The regulator was then separated from the test package and tested in liquid hydrogen at Sycamore Canyon Test Site B. The regulator operated successfully indicating that the cause of failure was either contamination or freezing of hydrogen in the regulator.

The regulator was re-installed in the test package, and a second series of testing was initiated. In this second series of testing, the system position was reversed from that shown in Figure 5-6. The pump was underneath the heat exchanger and the exchanger outlet flow was directed upward (radial flow deflector removed). The axis of the flow was approximately 3 inches off the centerline of the tank.

Automatic cycling (pressure switch controlling) of the unit was accomplished at 13-inch (system in gas), 49-inch (system in liquid), and 70-inch liquid levels. During automatic cycling, the vent flow rate was adjusted to a nominal value of 3 lb/hr, and the pump was operated at design conditions. The vent inlet was cycled between gas and liquid.

Manual operation of the unit was accomplished while controlling tank pressure to 17 ± 1 psia using the heater blanket. Heat exchanger performance was determined over a range of flows from 2 to 4 lb/hr while operating the pump at design conditions (60 cps and 17.3 volts input). This testing was done at liquid levels of 13 and 49 inches. Determination of transient performance was included.

Heat exchanger performance was further evaluated at pump speeds of 3130 rpm to 1100 rpm while maintaining a nominal vent flow of 3 lb/hr. In this case the liquid level was at 49 inches, and both the vent inlet and the system were in liquid.

Following stratification testing and during automatic cycling at the 70-inch liquid level, the regulator again failed to regulate properly. This second series of tests was terminated 7 May 1967, after approximately 35 hours of continuous testing. Again the unit was tested at ambient conditions, following detanking and purging operations; regulation was normal.

On 6 July 1967, a third series of tests was begun with the pump flow down through the heat exchanger. This set of tests was designed to fill in some data not obtained in test one. The quality orifice was more precisely instrumented, and the optical liquid detector was thoroughly repaired and checked out prior to starting the test. A modification was made to the vent system to eliminate freezing of hydrogen as a possible cause of regulator failure. Valve 30, shown in the test facility flow schematic, Figure 5-7, was used as the shut-off valve downstream of the regulator to ensure a pressure downstream of the regulator greater than the triple point pressure. Also, the regulator seals were tightened to reduce regulator leakage flow. The testing was performed with the unit and vent inlet in both gas and liquid. Pump flow was varied over the operating range of the pump, while vent flow was held at approximately 3 lb/hr. Vent flow was varied from 2 to 4 lb/hr while the pump flow was held at the design value. Automatic cycling was accomplished at 13-, 49-, and 70-inch liquid levels.

In this third series of tests, the pump flow was down and the system orientation was as shown in Figure 5-6, except that the heat exchanger outlet flow was directly down with the radial flow deflector removed. This series of tests lasted 42 hours, and all system components performed satisfactorily throughout. Detail tests results and data are presented in the following section.

5.3 TEST RESULTS AND DATA

5.3.1 AUTOMATIC TANK PRESSURE CONTROL. The basic requirement of the system, as mentioned in Paragraph 2.1, is to control LH_2 tank pressure to 17 ± 1 psia when the

external heating rate to the tank is 20-30 Btu/hr. This control must be maintained with the system operating in any orientation and with either gas or liquid at the pump and/or at the vent inlet. Testing was performed at three liquid levels, as discussed in Paragraph 5.2.

During the actual testing, the external heat leakage to the tank was determined to be about 60 Btu/hr. This value was obtained from an equilibrium boiloff test performed at the 49-inch liquid level. A wet test, positive displacement flow meter was used to determine the equilibrium boiloff rate. Demonstration of system performance should not be affected by this higher heating rate, since the vent system is designed to take care of approximately 10 times this amount.

Samples of the test data obtained with the system in the automatic mode and with the pressure switch controlling tank pressure are shown in Figures 5-12 through 5-31. All data are shown plotted as a function of time in hours, measured from midnight on the day of the start of testing. It is noted that heat exchanger hot side outlet temperatures read 0.48°R low during all Series 1 and 2 testing. This is due to the use of the wrong calibration in the data reduction computer program for this particular temperature probe.

In all cases, hydrogen testing was started when the test tank had been filled to the 13-inch liquid level. This occurred for the first series of tests at 01:00:00 hours on 28 April 1967, for the second series of tests at 04:13:00 on 5 May 1967, and for the third series of tests at 04:03:00 on 6 July 1967.

The first set of data shown, Figures 5-12 through 5-17, illustrates automatic operation of the system during the first test series. The liquid level in the tank is at 47 inches. From time 14.0 to 14.25 hours, the vent system was on manual operation in order to adjust the flow control valve 15 to a flow rate of approximately 3 lb/hr. Previous testing had been concerned with determining heat exchanger steady state and transient performance. At time 14.25, the vent system was closed and set in the automatic mode. The heater blanket was set at 200 watts. At time 14.71, the system cycled open. The tank pressure was 18.25 psia, and the vent inlet was in liquid. The heater was then turned off. Figure 5-12 shows that a pressure overshoot occurred to 18.35 psia, at which time the tank pressure started to level off. It was felt that this overshoot was primarily due to a lag in the time to mix the bulk fluid to allow energy transfer between the ullage and the vented fluid. Also, there was residual heating caused by not turning off the heater soon enough to allow equilibrium conditions to be reached prior to the start of venting. In subsequent cycles the heater was turned off prior to anticipated pressure switch actuation in order to minimize residual heat leak into the tank when venting. At time 14.75, the vent inlet was switched to gas, and the tank pressure decayed quite rapidly, and, as shown by Figure 5-13, the ullage gas began to destratify. At time 14.79, the inlet was again switched to liquid and the tank pressure rose before continuing to decay (Figures 5-12 and 5-14). As seen from Figure 5-13, a slight jump in ullage temperature also occurred at this time. This lag in rate of decay with the

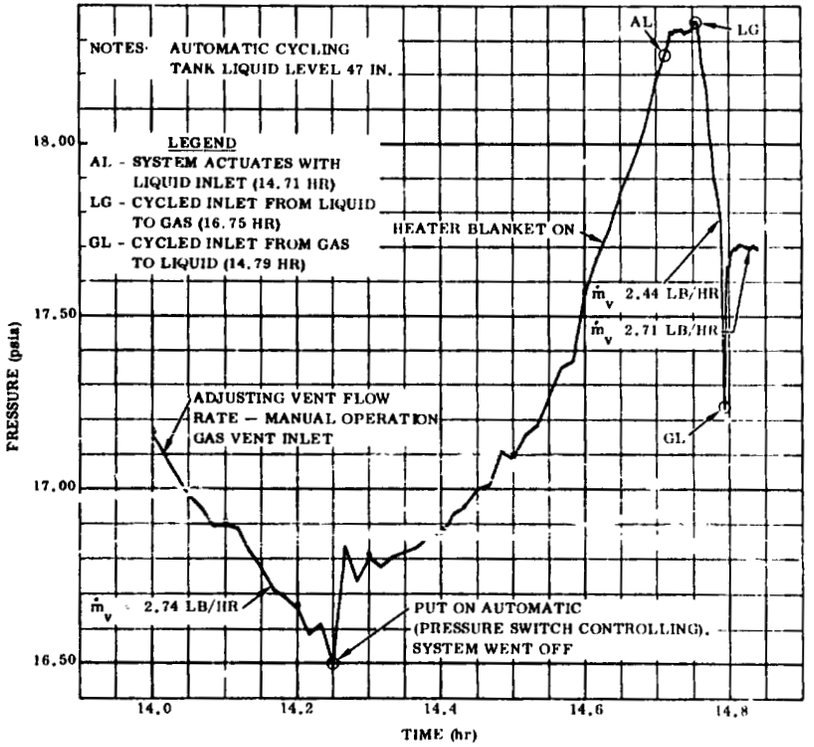

Figure 5-12. Tank Pressure, (First Test Series, 14 to 14.85 hrs)

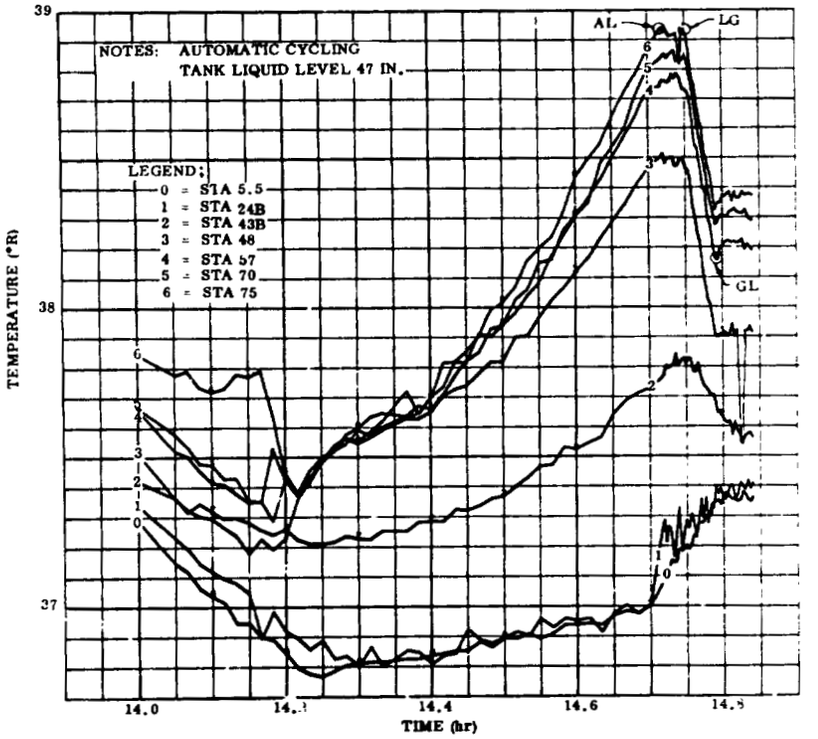

Figure 5-13. Temperature Profile (First Test Series, 14 to 14.85 hrs)

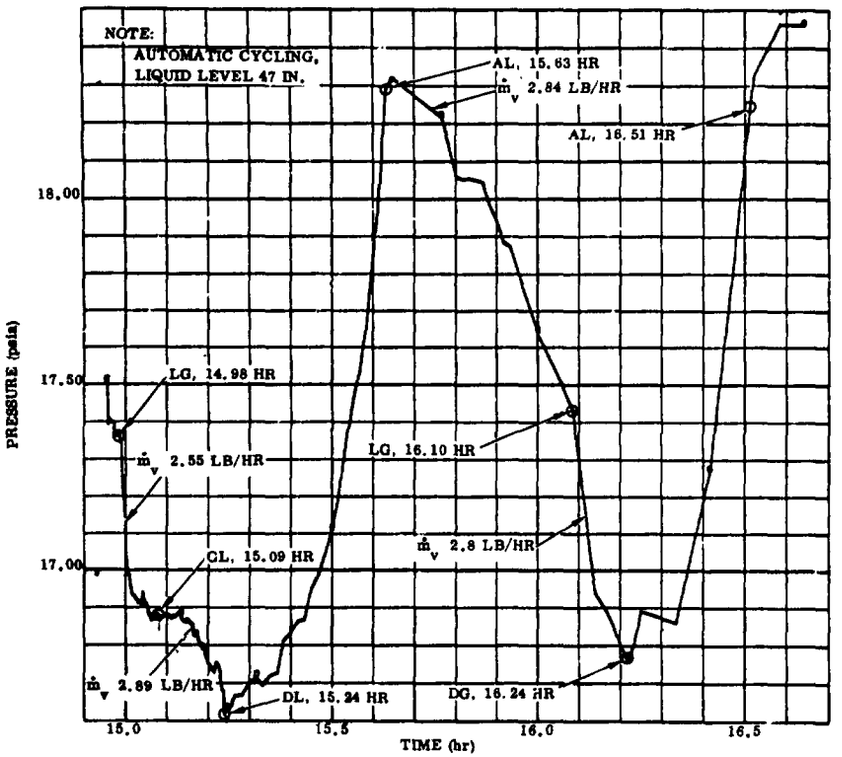

Figure 5-14. Tank Pressure (First Test Series, 14.9 to 16.7 hrs)

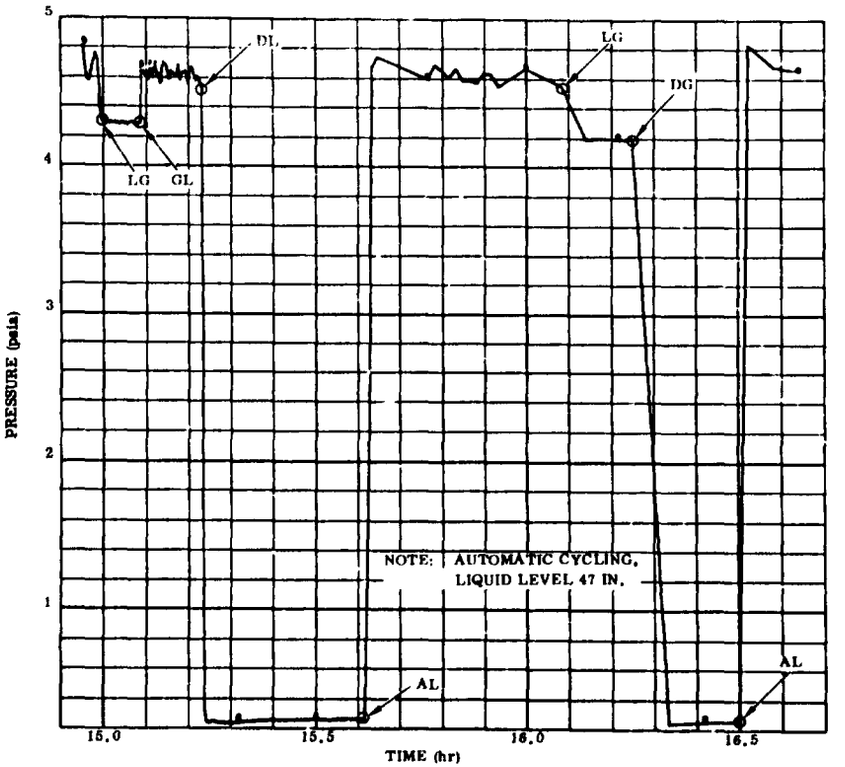

Figure 5-15. Regulator Pressure (First Test Series, 14.9 to 16.7 hrs)

LEGEND

0 REGULATOR UPSTREAM
1 REGULATOR DOWNSTREAM (EXCHANGER COLD SIDE INLET)
2 EXCHANGER COLD SIDE OUTLET
3 EXCHANGER HOT SIDE OUTLET (READS 0.48" R LOW)

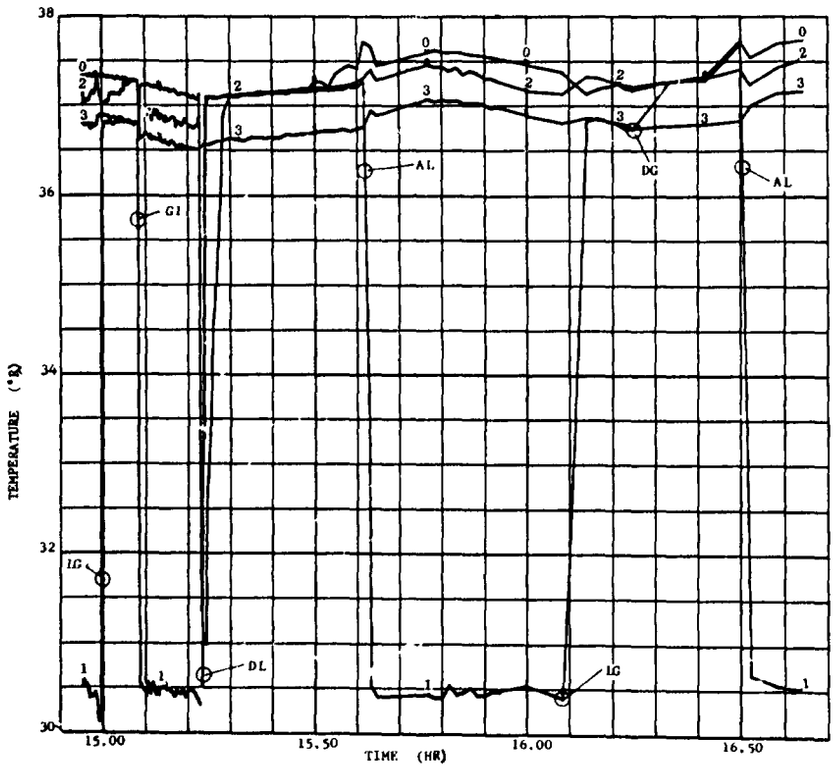

Figure 5-16. Heat Exchanger Temperatures (First Test Series, 14.9 to 16.7 hrs)

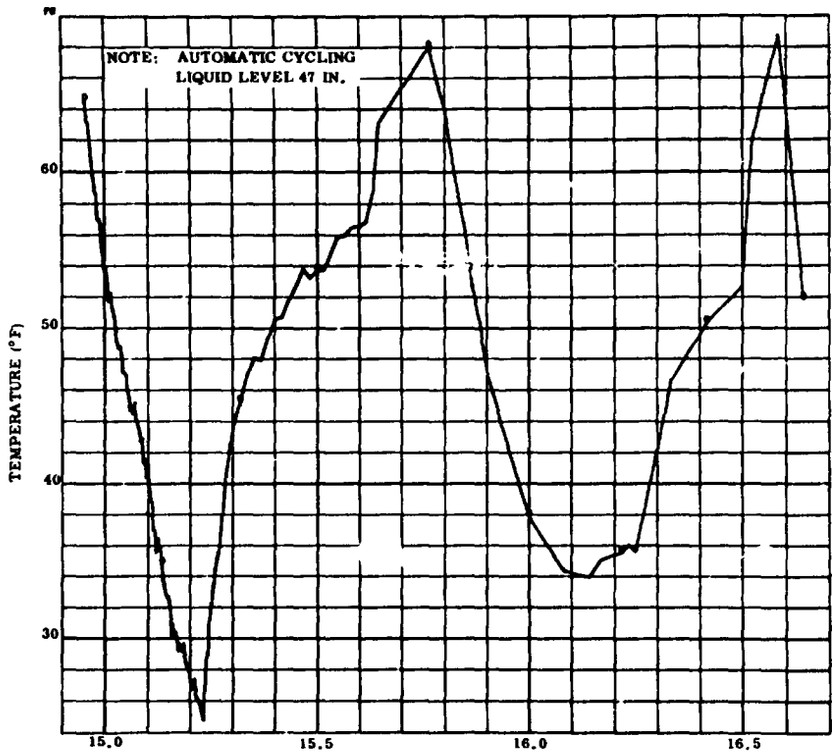

Figure 5-17. Flow Orifice Inlet Temperature (First Test Series, 14.9 to 16.7 hrs)

liquid inlet is also shown in Figure 5-14 at 15.08 and 15.63 and was attributed to a lag in mixing the fluid to obtain energy transfer between ullage and liquid. Figures 5-12 and 5-14 indicate that as the testing progresses this lag between pressure decay when switching from gas to liquid diminishes as the tank fluid is further mixed. Figures 5-12 and 5-14 also show that the pressure switch was operating in a band which was slightly above the design range; however, this band shifted to within design limits after several operating cycles.

Vent flow rates with a gas inlet were determined to be nominally about 10-percent less than when the inlet was in liquid. This was due primarily to a change in regulator outlet pressure when switching between gas and liquid. As shown in Figure 5-15, the regulator outlet pressure was typically 4.6 psia when operating with a liquid inlet and 4.2 psia with a gas inlet (8.8 percent reduction). Regulator performance is discussed further in Paragraph 5.3.7. A minor change in flow rate was also caused by small changes in the heat exchanger outlet temperature when switching between gas and liquid as illustrated in Figure 5-16. Some slight variation in flow during a run also occurred because of a change in the temperature at the inlet to the flow measurement orifice illustrated in Figure 5-17. It was difficult to maintain an exactly constant temperature upstream of this orifice since the onset of flow would reduce the temperature, which would then need to be compensated for by a change in the variac power level used to heat the line upstream of this orifice. The influence of the vent fluid in cooling the line temperature near the heater was seen by the reduction in temperature (Figure 5-17) when the shutoff valve was open and hydrogen was flowing through the vent line.

This first series of tests proved that a thermodynamic liquid vapor separator was an efficient system for venting vapor only from a hydrogen tank subjected to orbital heating rates. It also showed the importance of tank fluid mixing and liquid ullage coupling in controlling tank pressure. It is noted that during this first series of testing, the pressure transducer at the flow measurement orifice did not operate, so a Kolsman gage was read periodically in order to determine the vent side flow rate. Also, the Kolsman gage measuring the heat exchanger hot side pressure drop and the liquid detector did not function. All other instrumentation read consistently well.

Even though the liquid detector did not operate satisfactorily, the temperature and flow data obtained for the heat exchanger indicated a high efficiency and no liquid loss. This is illustrated in Figure 5-16. The regulator downstream temperature was the heat exchanger inlet temperature. When this temperature was between 30 and 31°R, the regulator was operating with a liquid inlet to the three-way valve upstream. The temperature between the shutoff valve and regulator was quite close to the fluid temperature in the tank at that location. The heat exchanger cold side outlet closely approached the hot side temperature, indicating the high efficiency of the heat exchanger unit. Heat exchanger performance is discussed further in Paragraph 5.3.4.

The second series of tests was conducted with the system rotated 180°, with the pump underneath the heat exchanger, and with a vertical hot side jet issuing from the top of the exchanger. This type of flow pattern proved to be more effective in mixing the tank contents than that induced by the radial jet of the first test series. Checkout of the instrumentation resulted in repair of the transducer circuit used for measuring the pressure drop across the flow measurement orifice. Fixes on the optical liquid detector and replacement of the pressure differential gage or the pump did not prove successful when the system was tested again. Additional instrumentation was added in the form of a transducer upstream of the flow measurement orifice.

Samples of automatic cycling during the second series of tests are presented in Figures 5-18 through 5-26. Figures 5-18 through 5-20 show tank pressure, tank fluid temperature distribution, and temperatures within the test package as the system operates through two complete cycles with the test package located in the hydrogen vapor and gas and liquid vent inlet conditions as noted on the figures.

The heater blanket shown in Figure 5-6 was used to increase the pressure rise rate and reduce the time between vent cycles. Adjustment and actuation of the heater blanket was probably responsible for the variations in pressure rise rate indicated by Figure 5-18. Between 6 and 6.22 hours, the heater blanket was adjusted to a value of 200 watts. At time 6.25 hours, the heater blanket was turned off. Figure 5-18 shows that the pressure decay rate was approximately constant with either gas or liquid at the vent inlet.

Figure 5-20 indicates that a significant amount of superheat existed at the heat exchanger exit, even though the liquid taken from the bottom of the tank was quite cold. Regulator downstream temperature was the same as the heat exchanger inlet temperature. Station 5.5 represents the liquid inlet location and Station 75 the gas inlet. These temperatures are shown in Figure 5-19 along with other temperatures illustrating stratification of the tank fluid and the effect of mixing on this temperature stratification.

The second set of data, Figures 5-21 through 5-23, shows system operation in liquid at the 49-inch level with the pump flow up. Two automatic cycles are represented, with actuation occurring at 18 psia and deactuation at 16.4 psia (Figure 5-21). Tank fluid temperature profiles are presented in Figure 5-22 and heat exchanger temperatures in Figure 5-23.

When liquid was at the inlet to the system, a slight delay in tank pressure decay was present due to the time required to mix the fluid and translate the energy removed from the liquid to a reduction in ullage pressure. This phenomena was more pronounced when the exchanger outlet flow was radial, as shown previously in Figures 5-12 and 5-14, indicating better mixing with the upward flow configuration.

With respect to heat exchanger performance, the same general comments made for Test Series No. 1 are true for this test, the main difference in changing the pump flow

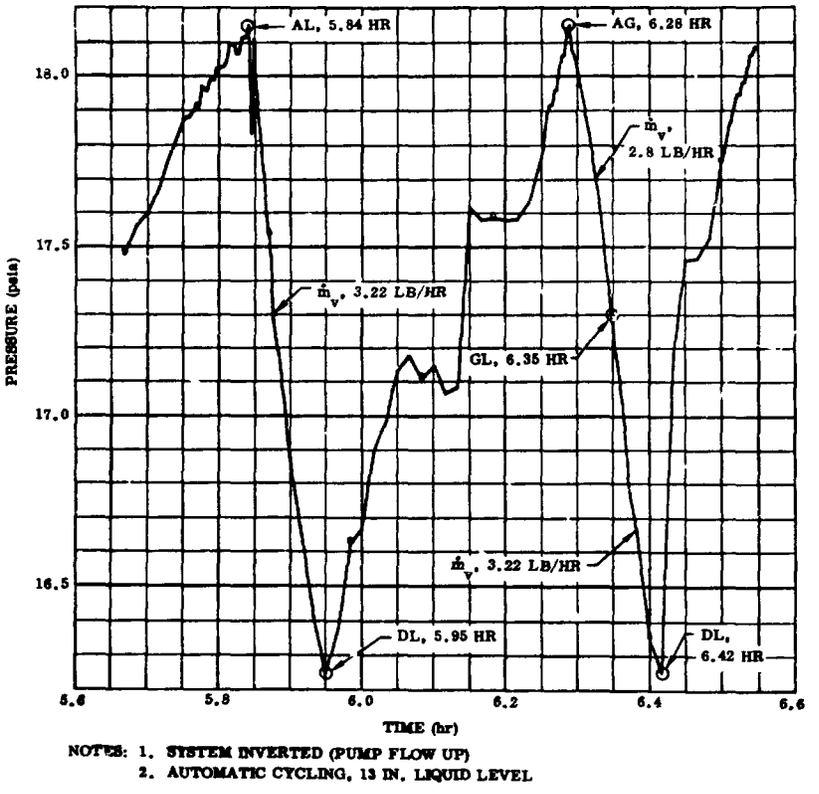

Figure 5-18. Tank Pressure (Second Test Series, 5.65 to 6.55 hrs)

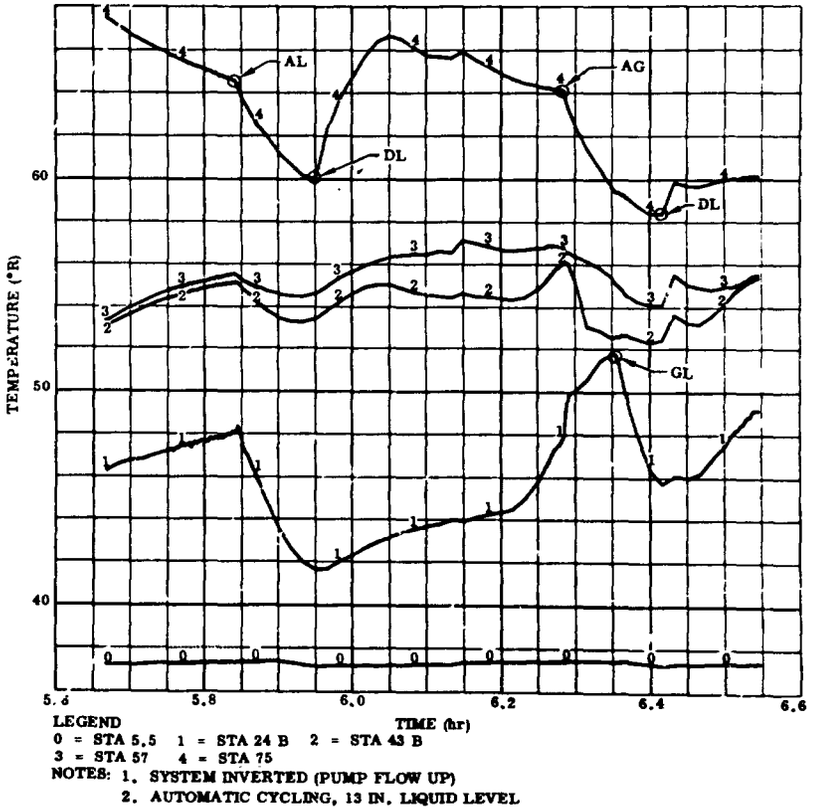

Figure 5-19. Temperature Profile (Second Test Series, 5.65 to 6.55 hrs)

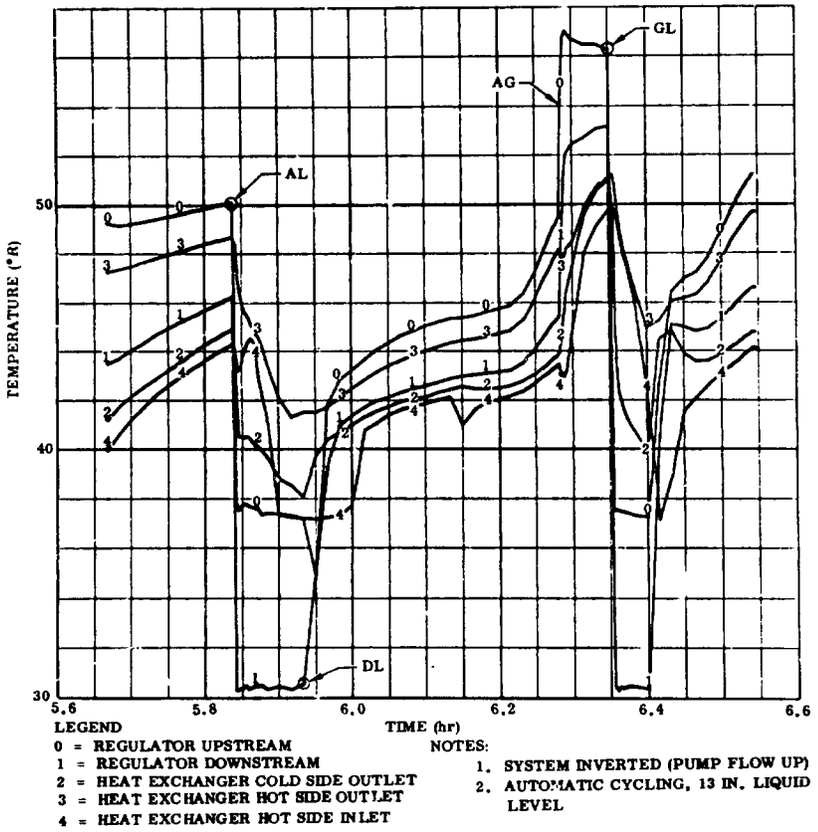

Figure 5-20. Heat Exchanger Temperature (Second Test Series, 5.65 to 6.55 hrs)

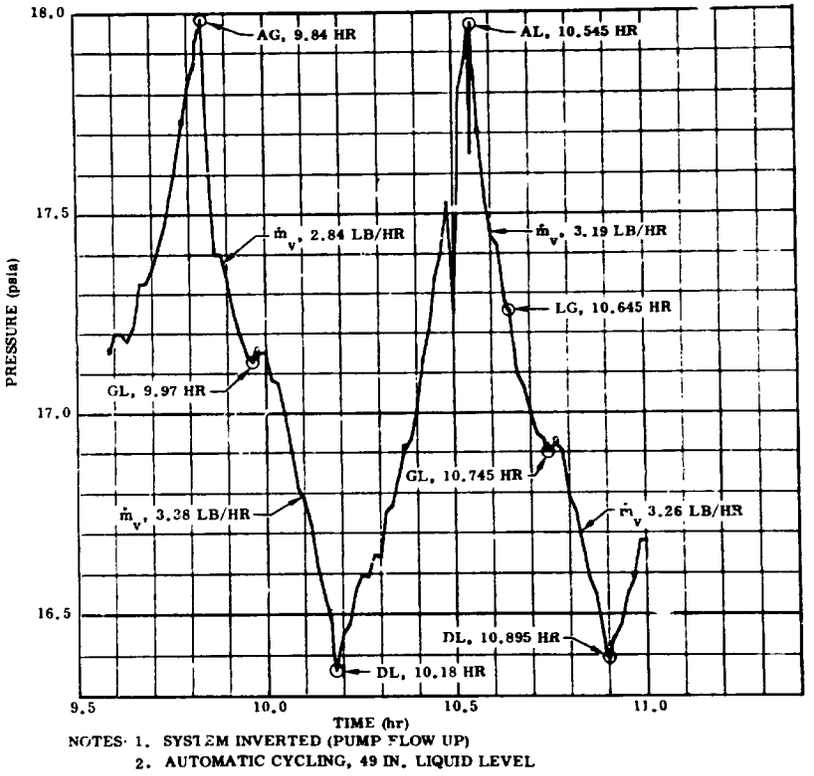

Figure 5-21. Tank Pressure (Second Test Series, 9.6 to 11.0 hrs)

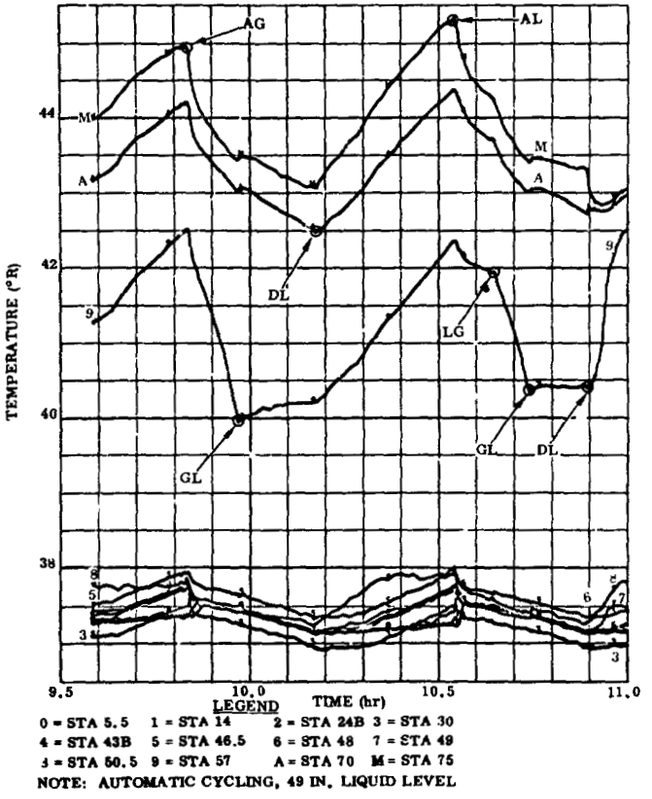

Figure 5-22. Temperature Profile (Second Test Series, 9.6 to 11.0 hrs)

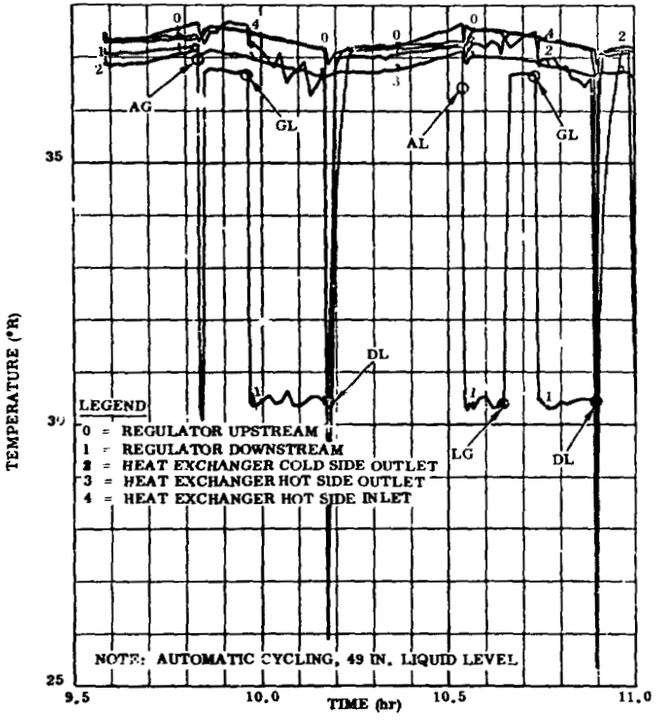

Figure 5-23. Heat Exchanger Temperature (Second Test Series, 9.6 to 11.0 hrs)

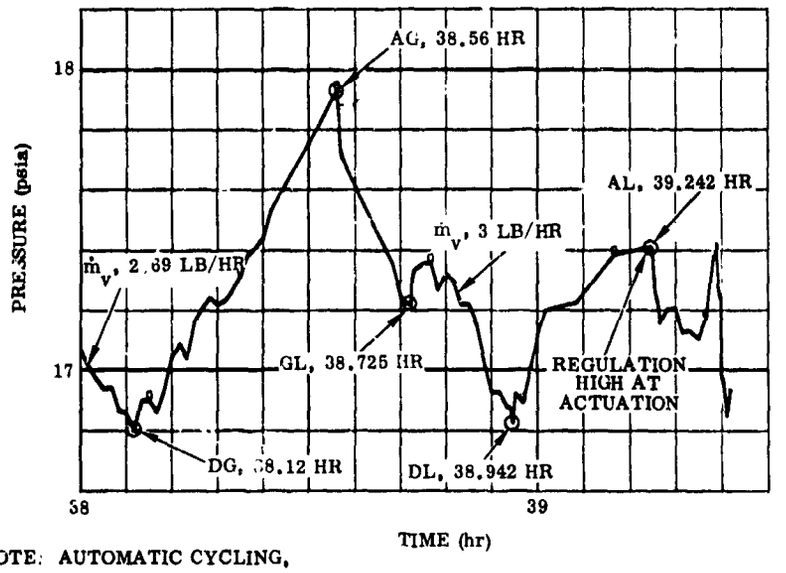

NOTE: AUTOMATIC CYCLING, 70 IN. LIQUID LEVEL

Figure 5-24. Tank Pressure (Second Test Series 38.0 to 39.5 Hours)

NOTE: AUTOMATIC CYCLING, 70 IN. LIQUID LEVEL

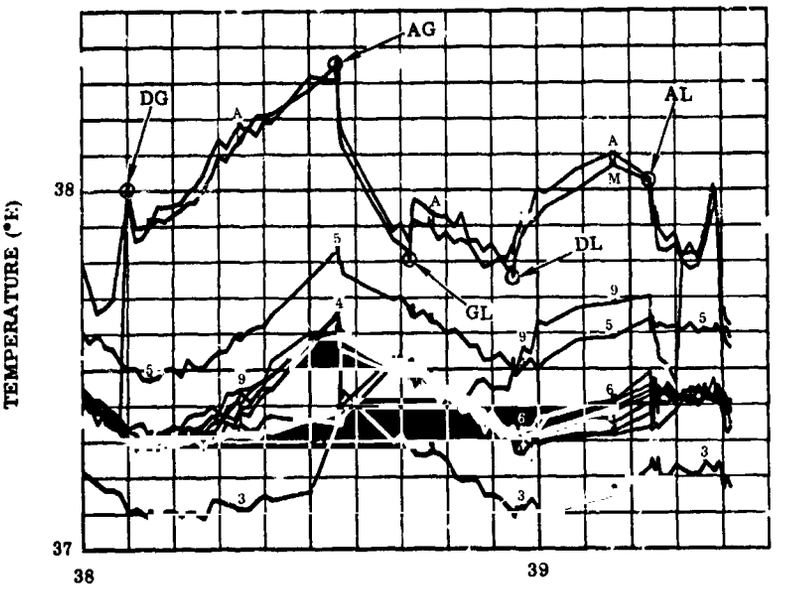

LEGEND

0 = STA 5.5 1 = STA 14 2 = STA 24B 3 = STA 30
4 = STA 43B 5 = STA 46.5 6 = STA 48 7 = STA 49
8 = STA 57 9 = STA 70 A = STA 71 M = STA 75

Figure 5-25. Temperature Profile (Second Test Series 38.0 to 39.5 Hours)

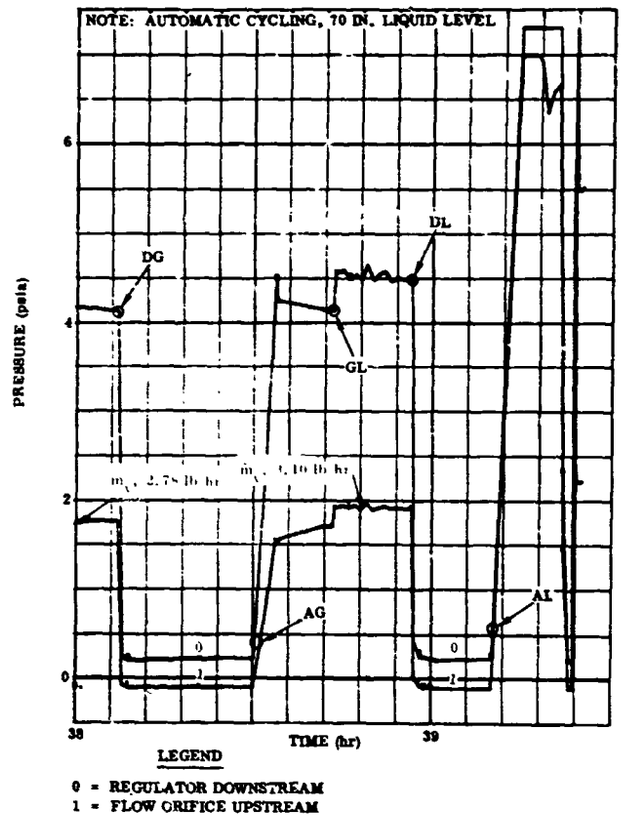

Figure 5-26. Regulator and Flow Orifice Pressures (Second Test Series 38.0 to 39.5 Hours)

pattern was the shorter stratification reduction time with the flow up.

Figures 5-24 through 5-26 present tank pressure, fluid temperature profile, and regulator pressure data obtained during automatic cycling at the 70-inch liquid level. Between this testing and testing at the 49-inch level, stratification and stratification reduction testing was accomplished under the Convair 1967 IRAD (Independent Research and Development) program. During destratification testing, only the pump was operated, even though the entire system remained immersed in LH_2. Reduction and detailed analysis of the data obtained are presently being completed and will be available to NASA in January 1968. The Convair IRAD program under which this is being accomplished is titled "Propellant Management" IRAD No. 111-1283-911.

During venting at the 70-inch liquid level, the unit operated through only one complete cycle and then the regulator failed to regulate properly as discussed in Paragraph 5.2. Referring to Figures 5-24 and 5-26, automatic deactuation occurred at 16.8 psia and 38.1 hours, actuation at 17.9 psia and 38.56 hours, and another deactuation at 16.8 psia and 38.95 hours. When the next actuation occurred at 17.4 psia and 39.242 hours, the regulator failed to regulate, as shown in Figure 5-26. The actual pressure at the outlet of the regulator at this time was approximately 0 psig or 14.7 psia. The value of 7.5 psia shown in Figure 5-26 represents the upper limit of the transducer.

During the third test series a modification was made to the system, as shown in Figure 5-7. The shutoff valve used in Test Series 1 and 2 was maintained in the open position, while a facility valve (Valve 30) downstream of the test package, external to the vacuum chamber, was used as the vent system shutoff valve. This modification was made to maintain a pressure above the triple point in the vent system test package to ensure that any leakage through seals, when the system is off, would not produce freezing of hydrogen within any valves or lines of the system.

During the third test series, the orientation of the test package was the same as for Test Series No. 1, except that the outlet flow from the heat exchanger was directed downward rather than radially. Samples of the data obtained during automatic cycling are presented in Figures 5-27 through 5-31.

Figure 5-27 presents data obtained with the system in gas and the liquid level at 13 inches. As in the second test series, no significant effect on tank pressure decay was seen when switching between gas and liquid at the vent inlet.

Figures 5-28 and 5-29 show results at a liquid level of 49 inches. The significant fact shown by these curves is that tank pressure decay with liquid at the vent inlet is very slow and a long lag in pressure reduction occurs when switching from gas to liquid.

Heat exchanger performance was similar to that obtained in Test Series 1 and 2. Furthermore, for this third test series the liquid detector was operating satisfactorily and no liquid was observed at the exchanger outlet during automatic cycling. The very

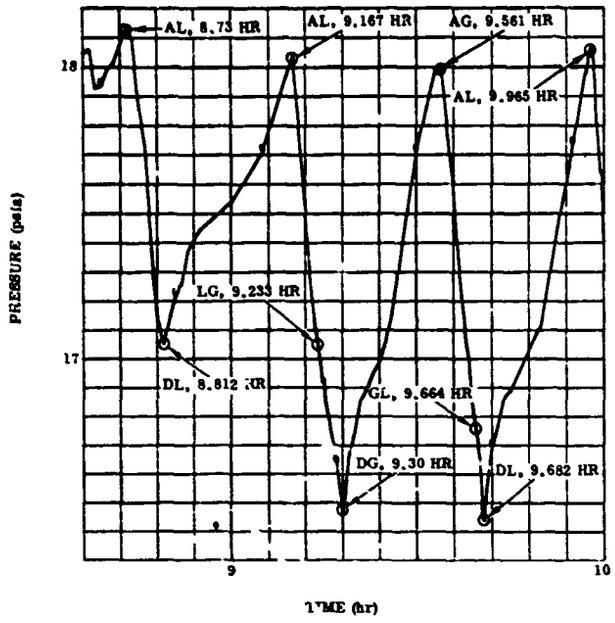

NOTES: 1. AUTOMATIC CYCLING, 13 IN. LIQUID LEVEL
2. PUMP FLOW DOWN WITH DOWNSTREAM SHUTOFF

Figure 5-27. Tank Pressure (Third Test Series 8.6 to 10 Hours)

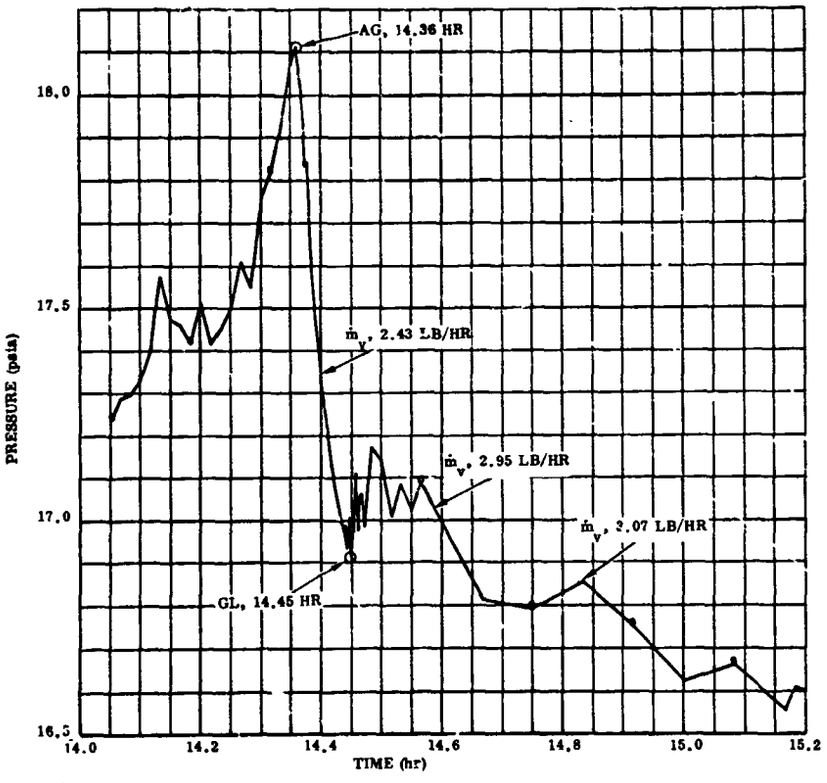

NOTES: 1. AUTOMATIC CYCLING, 47 IN. LIQUID LEVEL
2. PUMP FLOW DOWN WITH DOWNSTREAM SHUTOFF

Figure 5-28. Tank Pressure (Third Test Series 14 to 15.2 Hours)

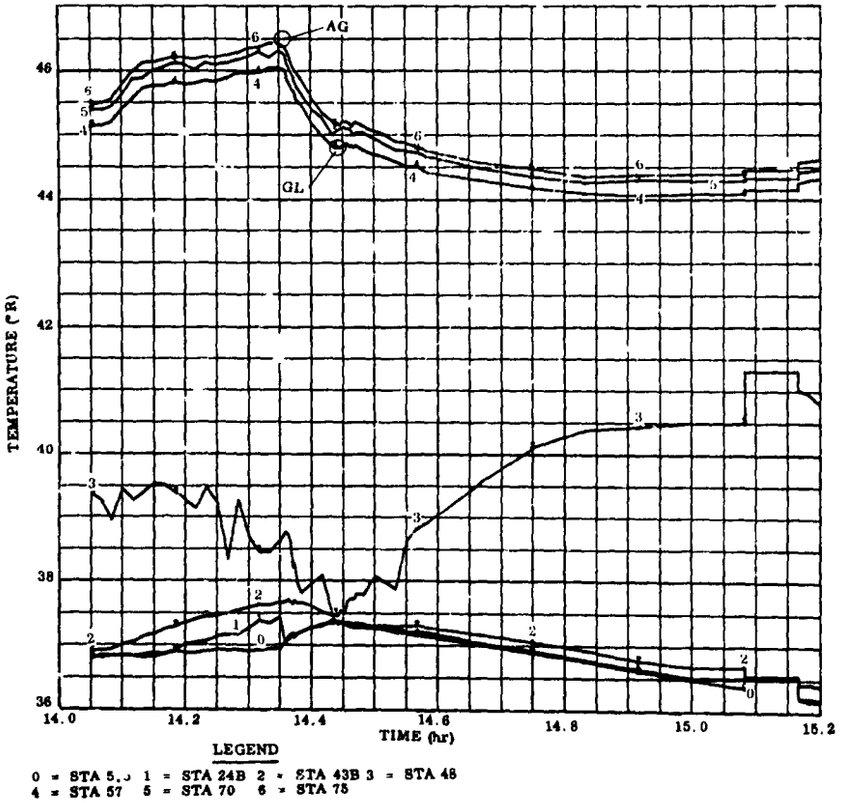

Figure 5-29. Temperature Profile (Third Test Series 14 to 15.2 Hours)

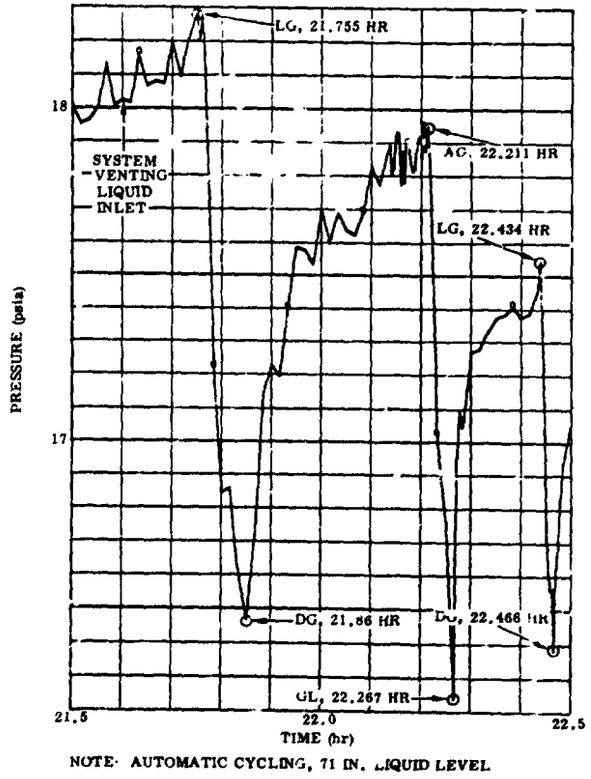

NOTE· AUTOMATIC CYCLING, 71 IN. LIQUID LEVEL

Figure 5-30. Tank Pressure (Third Test Series 21.5 to 22.5 Hours)

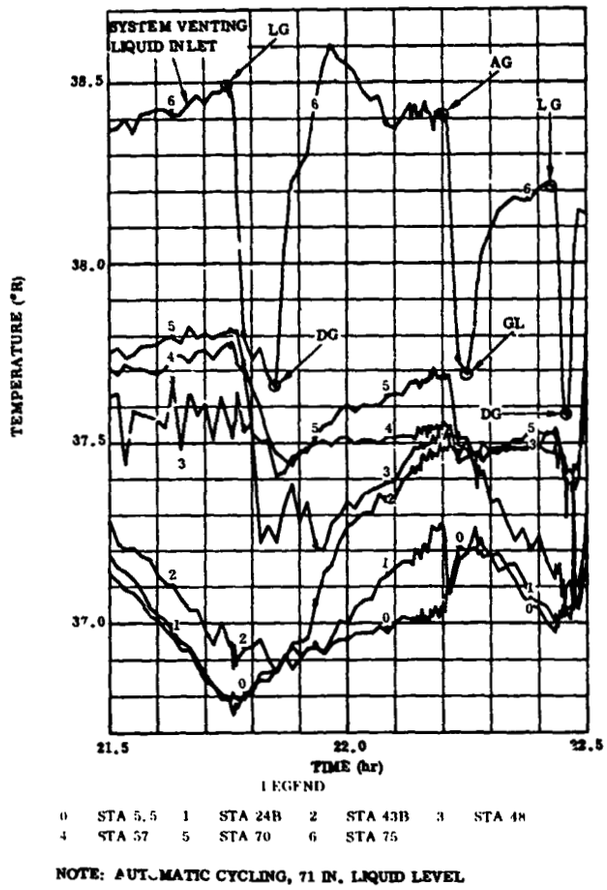

Figure 5-31. Temperature Profile (Third Test Series 21.5 to 22.5 Hours)

slow pressure decay was because fluid mixing was insufficient to accomplish significant energy transfer between the bulk fluid and the ullage. This is illustrated in Figure 5-29 where the bulk fluid was seen to subcool with respect to the ullage during system venting with a liquid inlet.

Figures 5-30 and 5-31 present data obtained at the 70-inch liquid level showing that, in this case, tank pressure decay with a liquid vent inlet was nonexistent. In fact, the tank pressure rose when the vent inlet was in liquid. In this case, it appeared that the energy transfer from the ullage to the vented fluid was less than the energy input to the ullage from the wall and penetrations. This was due to the poor fluid mixing characteristics of the system when the heat exchanger outlet flow was directed downward. This was somewhat to be expected from the poor results of testing at the 49-inch liquid level, since complete fluid mixing between liquid and ullage would be even more difficult at the higher liquid level.

At the present time no quantitative correlation has been developed to determine the time between tank pressure decay and start of venting with a liquid inlet. Such a correlation would be a function of liquid level in relation to pump and heat exchanger location, tank size, pump power, vehicle acceleration, and direction and velocity of flow from the exchanger. Qualitative data obtained to date show that at one g the higher the liquid level the longer the time lag and that the higher the induced liquid velocity at the liquid/vapor interface, such as due to orientation of exchanger hot side outlet flow, the shorter the time lag.

5.3.2 ANALYSIS OF TANK PRESSURE DECAY RATES. The theoretical tank pressure decay rate while venting can be calculated when the vent fluid properties are known and the tank pressure decay model is assumed. Since very little temperature stratification occurred in the tank during the second series of tests, a homogeneous decay model was assumed for analyzing these data. The pressure change in a tank under equilibrium can be expressed as,

$$\frac{\Delta p}{\Delta t}, \frac{\text{psia}}{\text{hr}} = 1.15 \left(\frac{\dot{Q}, \text{Btu/hr}}{m_T, \text{lb}_m} \right)$$

Where $\dot{Q}$ is the heat removed from the tank and m is the total mass of fluid within the tank.

The net heat removed from the tank is the sum of the heat removed in the vent fluid and the heat added to the tank by normal heat leak and by input pump power. The heat removed from the tank is given by

$$\dot{Q}_{out} = \left(\frac{e\lambda}{1-e} + h_v - h_L \right) \dot{m}_v$$

where h_L is the enthalpy of the saturated liquid, h_v is the enthalpy of the fluid leaving the tank, e is the vapor to liquid density ratio, λ is the heat of vaporization at saturated conditions, and $\dot{m}_v$ is the vent flow rate.

Thus:

$$\frac{\Delta p}{\Delta t} = \frac{1.15\left[\left(\frac{e\lambda}{1-e} + h_v - h_L\right)\dot{m}_v - \dot{Q}_{in} - P_{in}\right]}{m_T}$$

The fluid vented is essentially at uniform conditions at or near the design flow rate. The nominal heat leak into the tank as measured by boiloff readings is approximately 60 Btu/hr. The pump input power at the design speed is nominally 5 watts or 17 Btu/hr. Thus:

$$\frac{\Delta p}{\Delta t} = \frac{(214\,\dot{m}_v - 77)\,1.15}{m_T}$$

This equation is plotted in Figure 5-32 for liquid levels of 13-, 49-, and 70-inches over a range of flow rates. The data from the second test series, also shown in Figure 5-32, for the three levels agrees fairly well with the calculated results. The boiloff readings were taken at the 49-inch level. The 13-inch liquid level data fall below the theoretical line. This difference was not due to incomplete mixing, since the decay rates for both liquid and gas inlets are similar. It is possible that additional heat leak into the tank occurred when the level was at 13 inches because these runs occurred in the early part of testing when the heat flux to the tank may have been above the steady state equilibrium heat flux. In order to make the calculated and experimental results agree, the heat flux to the tank would have been approximately 215 Btu/hr.

5.3.3 SYSTEM TRANSIENT CHARACTERISTICS. Transient operation of the vent system when actuated and deactuated and when the vent inlet was cycled from gas to liquid and liquid to gas is illustrated in Figures 5-33 through 5-38.

The first Sanborn strip chart, Figure 5-33, shows the deactuation and actuation of the system with liquid at the vent inlet and with system shutoff occurring upstream of the regulator. Figure 5-33 shows that when the shut-off valve was closed and the pump was turned off, the temperature at the outlet of the exchanger immediately dropped to saturation temperature corresponding to p_3 and T_3. Boiloff of liquid trapped in the heat exchanger maintained p_3 fairly constant for approximately 7 seconds, at which time both pressures and temperatures began to drop as liquid boiloff continued. It is assumed that the 7 second delay in further temperature and pressure reduction was a result of the time it took to cool the heat exchanger and system masses which were at tank fluid temperature (approximately 38.5°R) at the time of system shut-off. Further boiloff as the system evacuated, resulted in an additional drop in exchanger temperature. Following complete boiloff of the trapped liquid, the system temperature increased

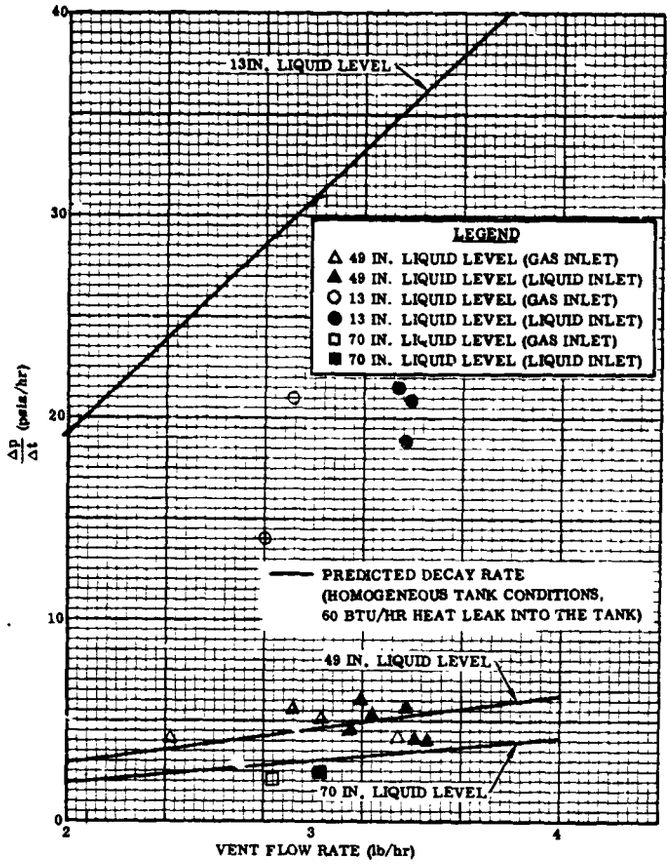

Figure 5-32. Pressure Decay Rates During Venting

to that of the tank fluid. The recorders were turned off between transients so the jog in the temperature curves appeared when it was turned on. The system was then actuated with a resultant sharp increase in the flow to a steady state value as indicated by Δp_{10}. The heat exchanger vent side outlet temperature shows a slight perturbation about the steady state operating point before settling out to its steady state value. These data indicate that the heat capacity of the exchanger is sufficient to vaporize any liquid initially present in the vent stream and that liquid is not vented during system start up.

Figure 5-34 shows the system transient when switching from gas to liquid. The system was initially operating at steady state in gas. Switching from gas to liquid inlet caused an increase in flow, as evidenced by Δp_{10}, and a reduction in heat exchanger inlet temperature (T_3). Cycling liquid to gas produces the reverse effect. During all cycling, the heat exchanger outlet temperature (T_4) did not change appreciably.

The data obtained from the Sanborn recorders, Figures 5-33 and 5-34, indicate that no liquid was present at the heat exchanger outlet at actuation or when cycling from gas to liquid. This can be deduced by the uniformly high heat exchanger outlet temperatures. This was also confirmed by the results of the third test series, where the liquid detector was in operation, and was true for all vent flows tested (up to 4 lb/hr).

System transients during the third test series, with the system vent shutoff located downstream of the heat exchanger, are shown in Figures 5-35 through 5-38. Results are similar to those with the shutoff upstream, except that, during deactuation, temperatures in the heat exchanger did not drop. The liquid detector channel shows that no liquid was present at the exchanger outlet during transient operation, except for that trapped in the exchanger at deactuation as shown in Figure 5-35.

As shown by p_3 readings taken from a pressure gage, the pressure in the exchanger eventually equalizes with the tank pressure, as would be expected, due to vaporization of liquid trapped in the exchanger. On the Sanborn, p_3 went off scale when the downstream shut-off valve was closed.

5.3.4 HEAT EXCHANGER PERFORMANCE. During the first and second series of tests, the liquid detector was not working and initial calculations were made on both sets of test data to determine if liquid was present at the heat exchanger outlet. The flow measurement orifice was calibrated in helium and in air as shown in Figure 5-39. This calibration curve was used to determine all system flow rates. During hydrogen testing with the vent inlet in gas, pressures and temperatures at the quality orifice were determined and the quality orifice was calibrated using the flow orifice as a base. The average $C_D M$ for the quality orifice was determined to be 0.965.

Using this average $C_D M$, flow rates were calculated for the quality orifice when liquid was at the vent inlet. Flow measurement orifice and quality orifice flow readings are compared in Figure 5-40 when the vent inlet was in liquid. The deviation from the 45° line is not statistically significant according to the Chi-squared test for

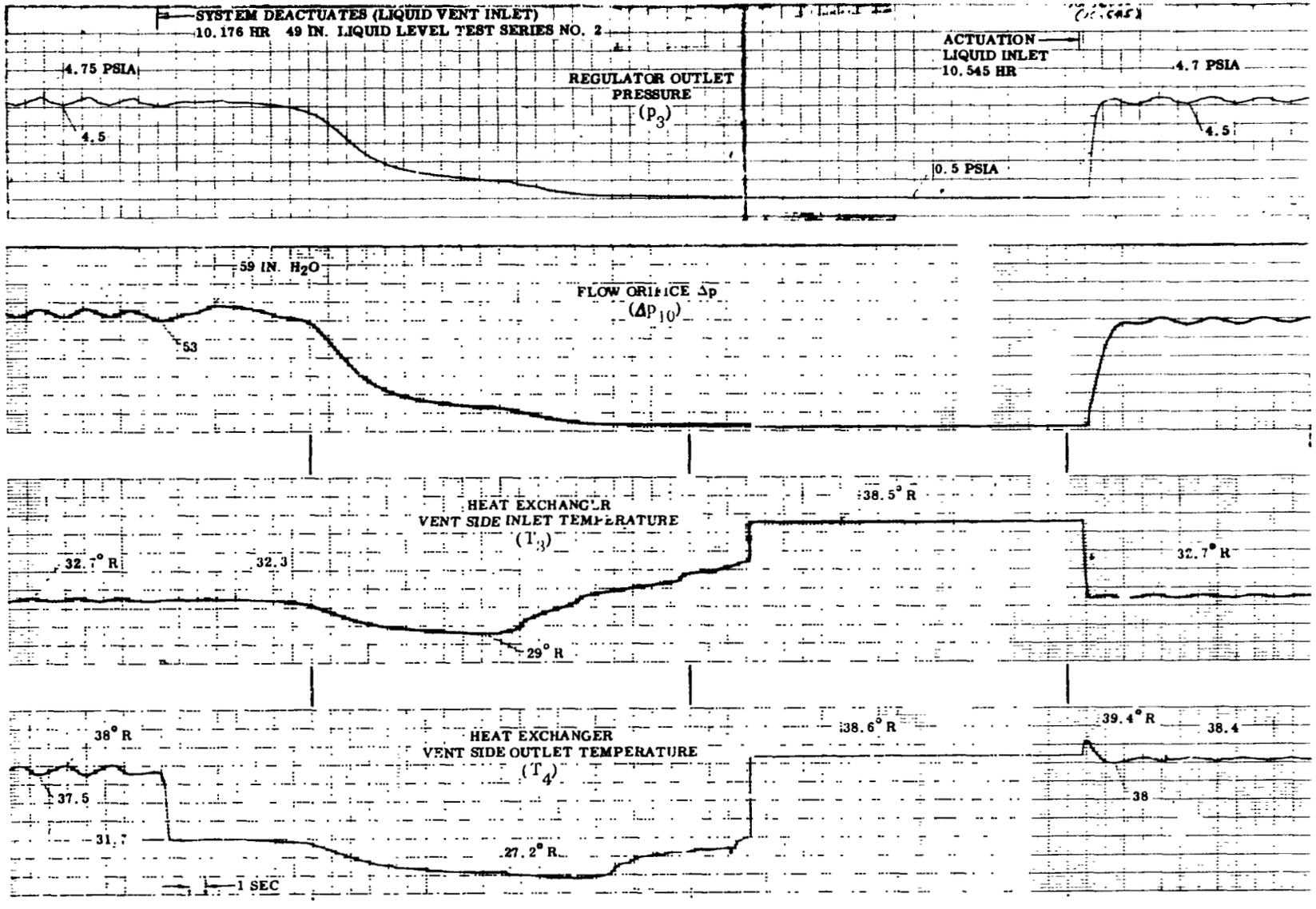

Figure 5-33. System Actuation and Deactuation - Shutoff Upstream

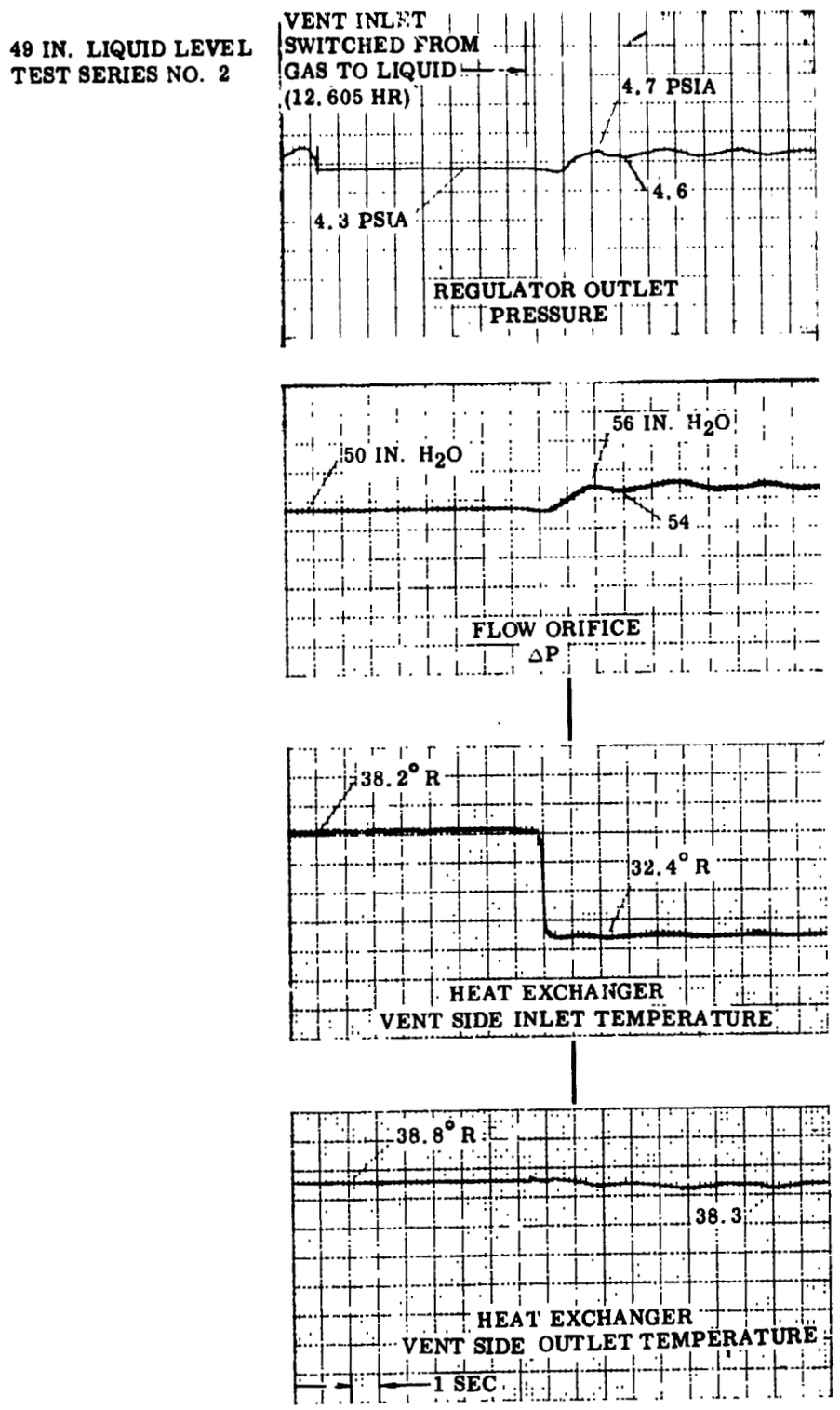

Figure 5-34. Gas to Liquid Transient - Shutoff Upstream

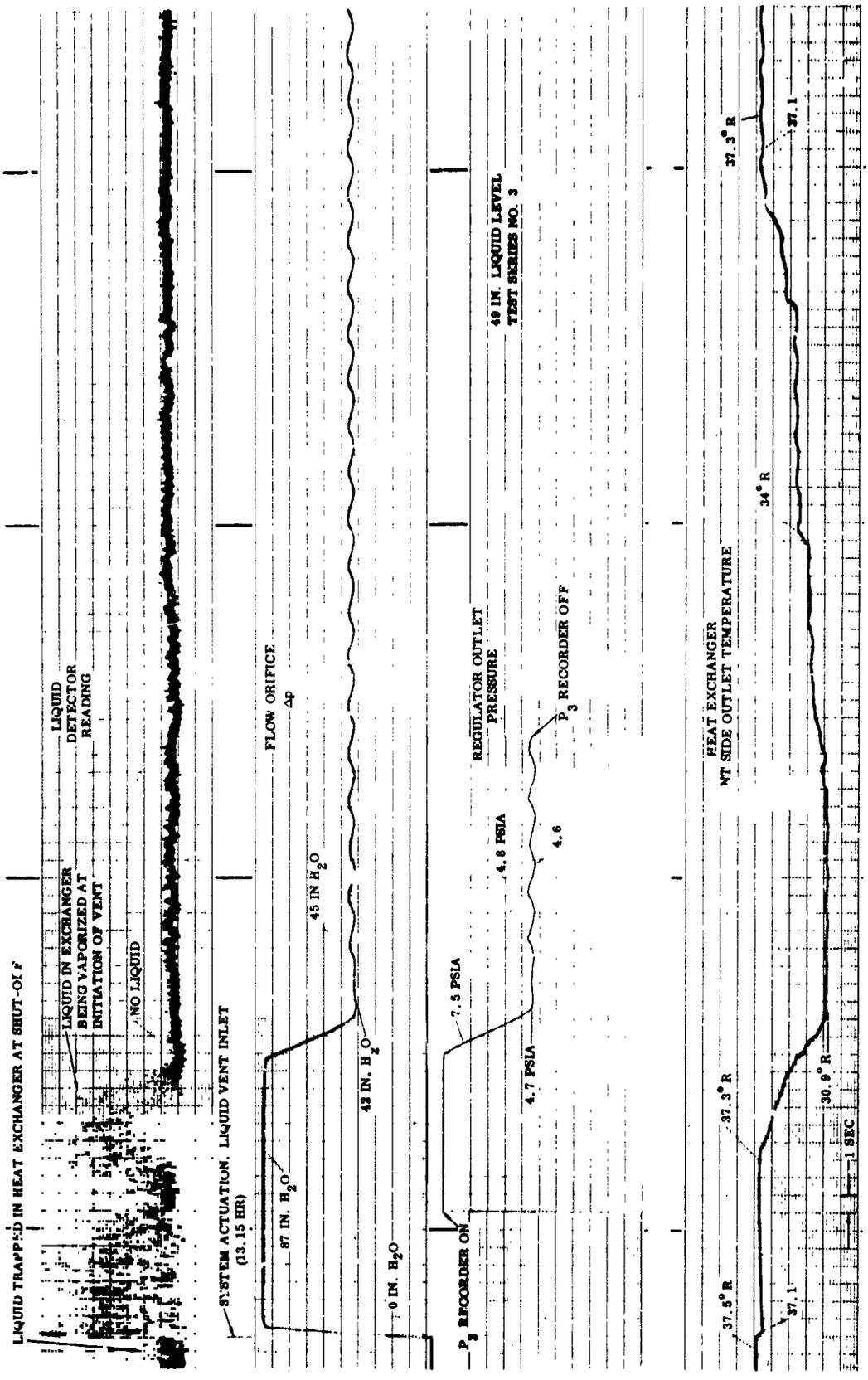

Figure 5-35. System Actuation - Shutoff Downstream

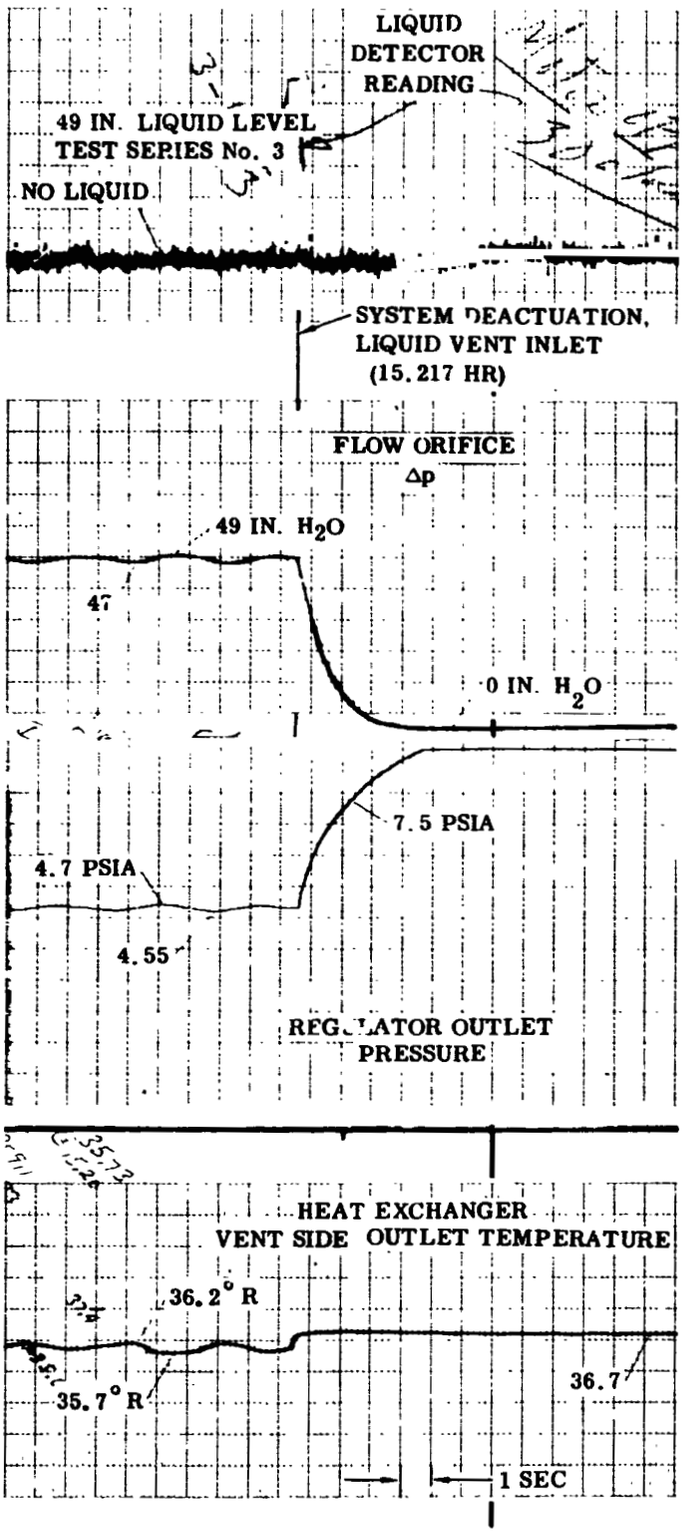

Figure 5-36. System Deactuation - Shutoff Downstream

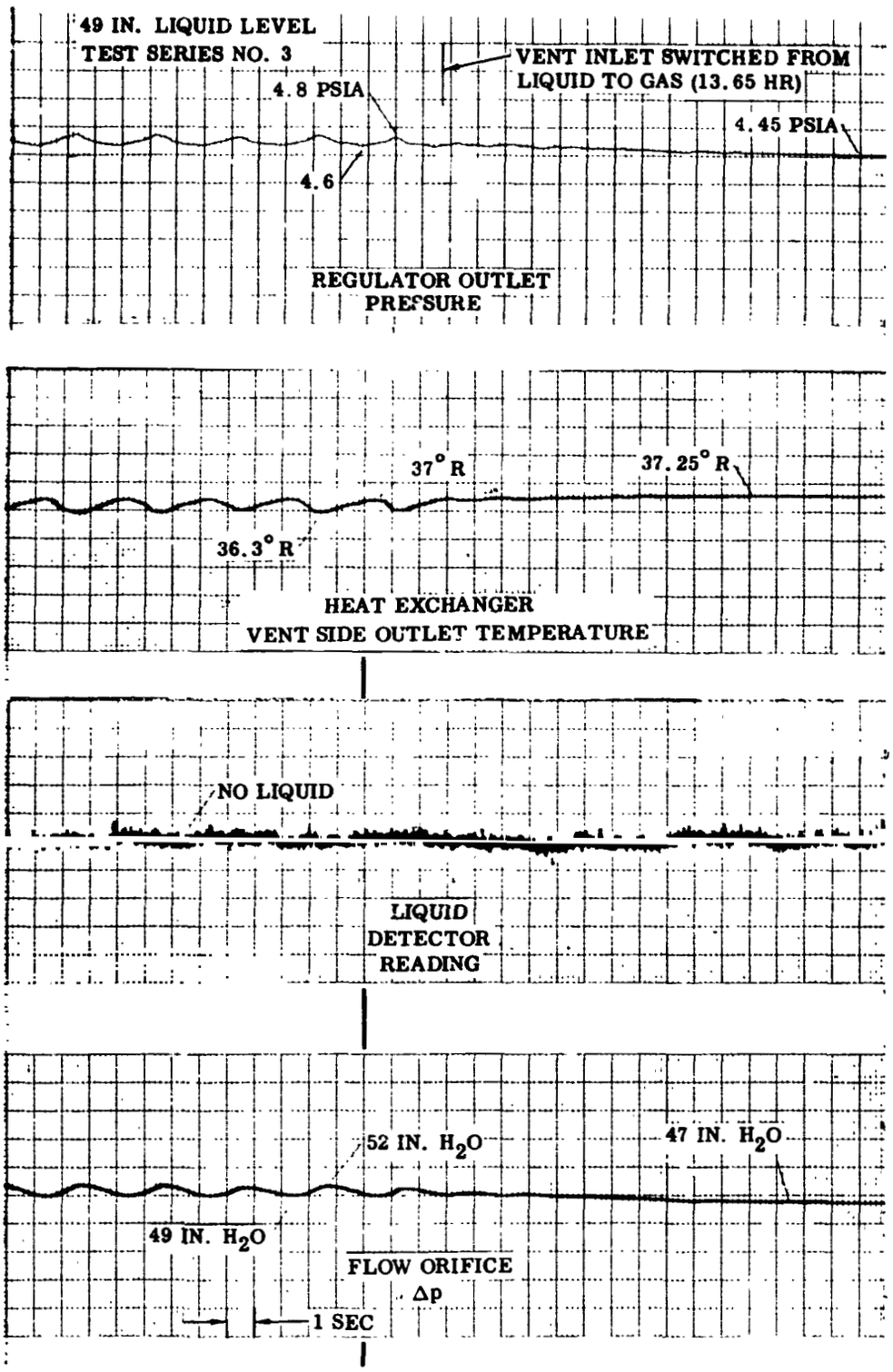

Figure 5-37. Liquid to Gas Transient - Shutoff Downstream

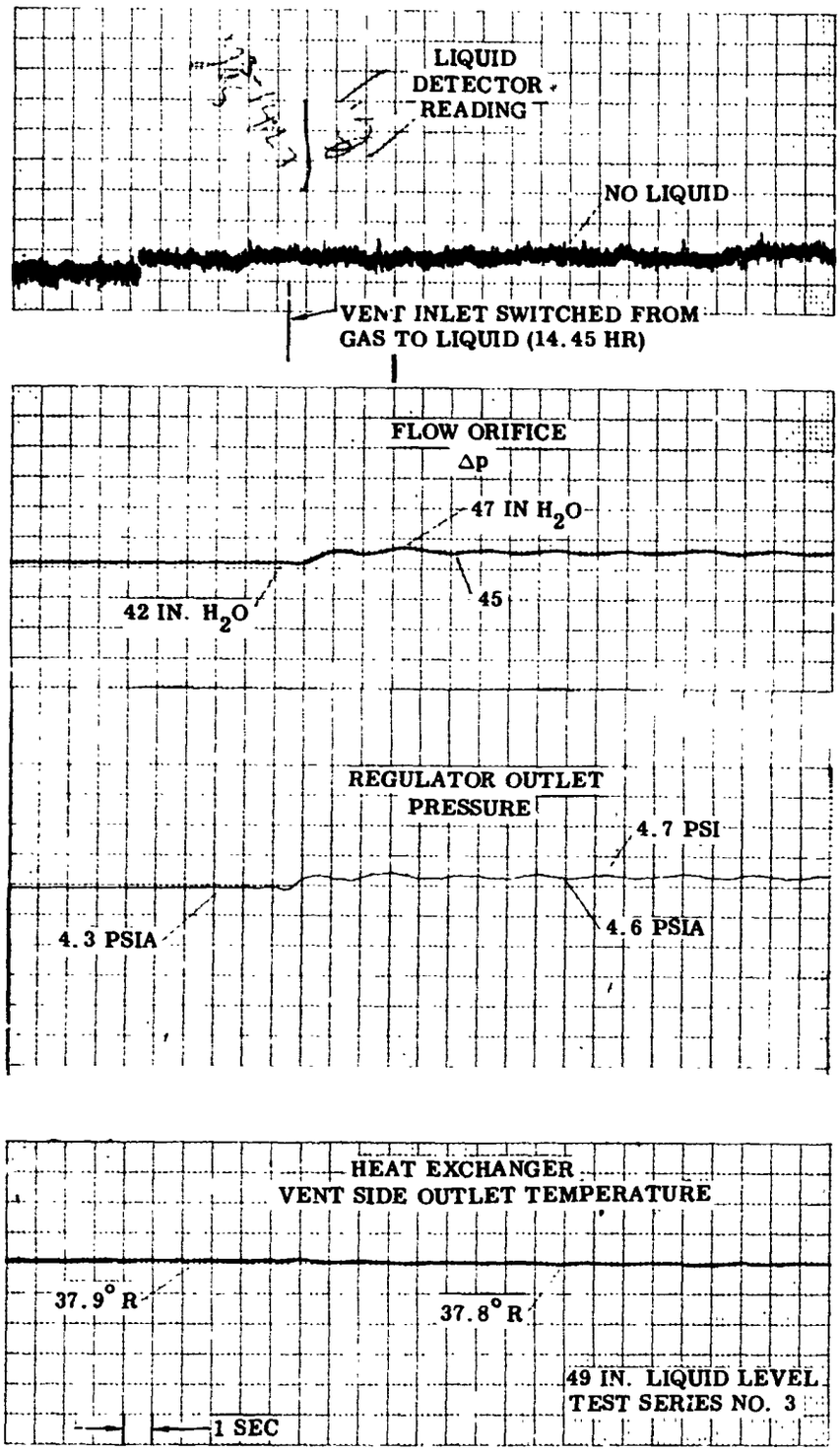

Figure 5-38. Gas to Liquid - Shutoff Downstream

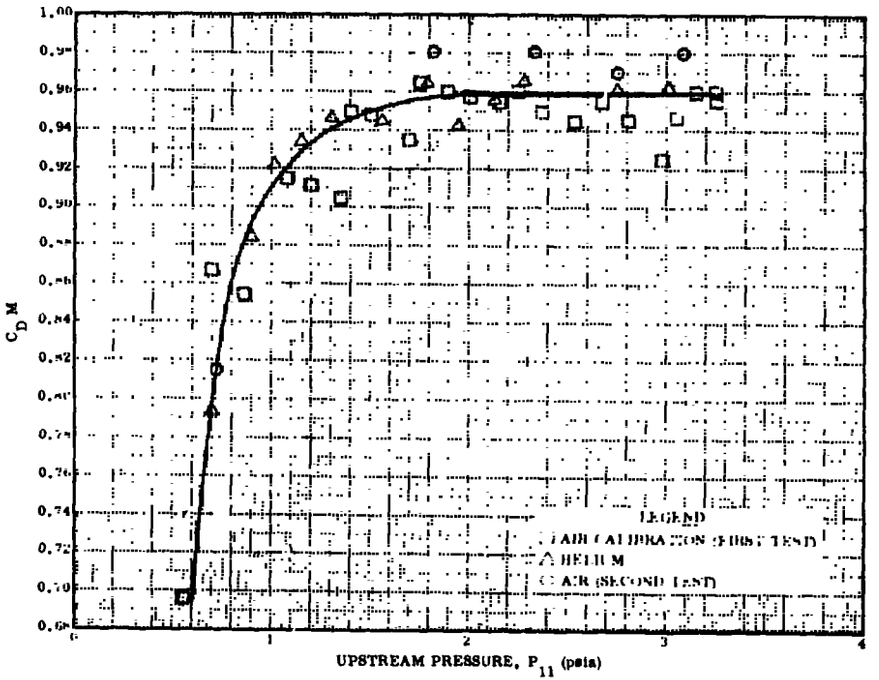

Figure 5-39. Flow Orifice Calibration Curve

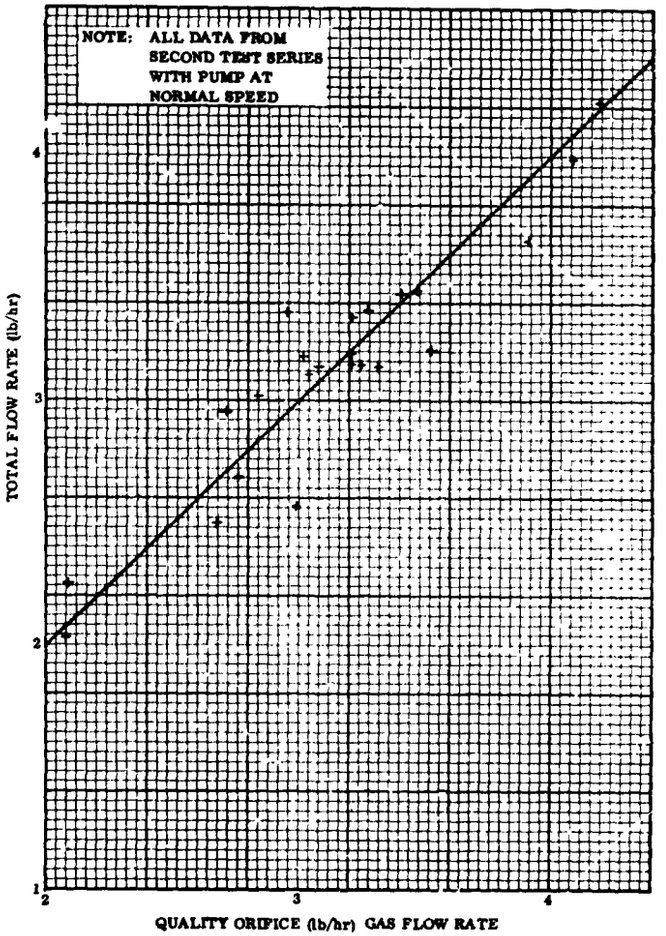

Figure 5-40. Quality Orifice Gas Flow Versus Total System Flow

goodness of fit. This indicates that no liquid was present at the heat exchanger outlet when liquid was at the inlet to the three-way valve. This was corroborated by the consistently superheated gas present at the heat exchanger outlet under design conditions with liquid or gas at the inlet to the vent system and, also, from results of the third test series when the liquid detector was operating. Data showed that the cold side outlet temperature was at least 6°R superheated under all vent flow rates tested with full pump power.

In order to obtain a quantitative indication of heat exchanger thermal performance as a function of flow rate, heat exchanger effectiveness, $T_{co}-T_{ci}/T_{Hi}-T_{ci}$ is used. Heat exchanger effectiveness is plotted against vent side flow rate in Figure 5-41 for liquid hydrogen on the hot side and in Figure 5-42 for gaseous hydrogen on the hot side. In both cases, the vent side inlet was liquid hydrogen. As shown in Figure 5-41, the actual effectiveness exceeded the effectiveness calculated from the design performance values of Table 2-5.

The exchanger effectiveness values when operating with gaseous hydrogen on the hot side, as shown by Figure 5-42, were lower than those presented in Figure 5-41 for liquid hydrogen on the hot side. This was due to the lower hot side heat transfer coefficients when operating with a superheated gas. It was expected that, with saturated gas on the hot side, condensation would occur and heat transfer coefficients would be as high as with the liquid. The high hot side temperatures when the unit was in gas (liquid level at 13 inches) were due to a significant amount of temperature stratification existing in the ullage. These hot side temperatures were such that the actual vent side exchanger outlet temperature was at least as high when the system was in gas as when it was immersed in liquid, even though the exchanger effectiveness was lower. The definition of effectiveness as used here is not an absolute measure of the exchanger performance when operating with a boiling fluid. For a given exchanger vent side outlet pressure, vent side outlet temperature is the primary measure of efficient system operation. This effectiveness is, however, a good measure of the performance of the exchanger in the superheat region, giving an indication of the system's ability to vent pure vapor. A zero effectiveness value would mean that saturated vapor was being vented, with a good chance that liquid could also be present in the vent stream.

The effect on overall heat transfer coefficient of changing the regulator outlet pressure from 5.5 psia to 4.5 psia was investigated. As the regulator outlet or heat exchanger pressure is changed, a corresponding change in saturation or cold side temperature will result. The heat transfer coefficients on the hot side and on the cold side in the superheat or gas flow regions are insensitive to such changes in temperature and pressure. The boiling coefficients are, however, fairly sensitive to temperature difference. Based on vendor data, the overall UA product is 190 Btu/hr °F in the boiling region with an inside boiling value ($h_{fC}A$) of 530 Btu/hr °F. This results in a hot side ($h_{fH}A$) of 296 Btu/hr °F where;

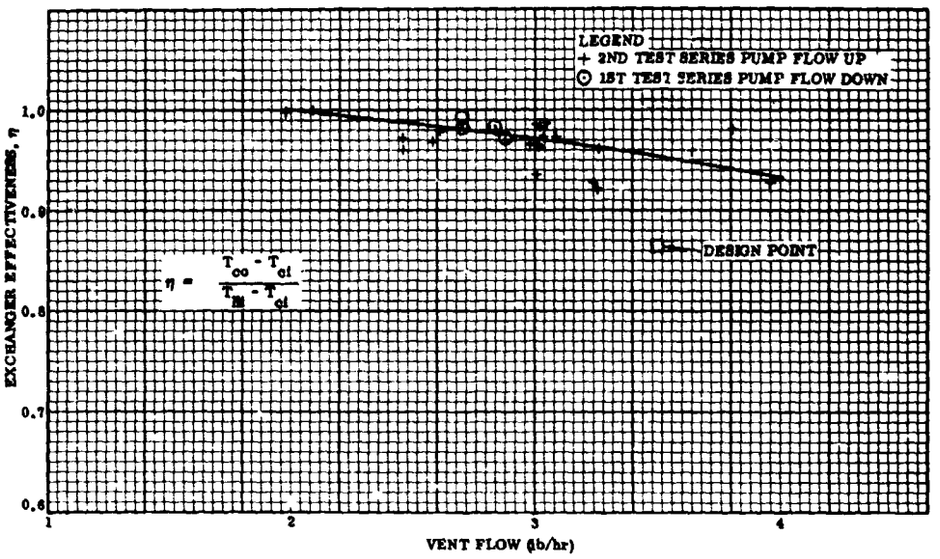

Figure 5-41. Heat Exchanger Effectiveness in Liquid Hydrogen

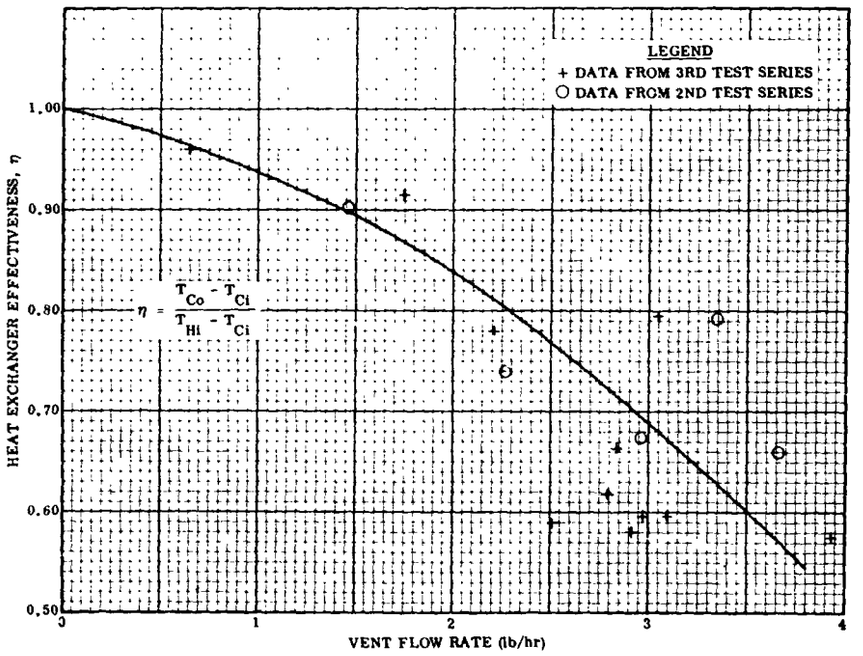

Figure 5-42. Heat Exchanger Effectiveness in Gaseous Hydrogen

$$UA = \frac{1}{\frac{1}{h_{fH}A} + \frac{1}{h_{fc}A}}$$

The data are for a hot side temperature of 37.5°R corresponding to 17 psia saturation pressure and a cold side temperature of 31°R corresponding to 5.5 psia.

Assuming that the hot side coefficient is constant, calculations were made to determine the cold side coefficient for a pressure of 4.5 psia (temperature of 30.1°R). Data from Reference 1-1 and heat balance methods described in Paragraph 2.2.3 were used.

The cold side coefficient ($h_{fc}A$) was determined to be 545 Btu/hr °F and the overall UA value 192 Btu/hr °F. This represents a change in the overall coefficient between 5.5 psia and 4.5 psia of only 1 percent.

Heat transfer coefficients on both hot and cold sides of the exchanger are calculated to be forced-convection dominated and not affected by natural convection or g-level. The primary purpose of running tests with the vent system in two orientations; pump flow down through the exchanger opposing any natural convection effects and pump flow up, augmenting natural convection, was to verify that natural convection or gravity effects are not present. This is further discussed in Section 13 of Reference 1-1. The data of Figures 5-41 and 5-42 indicate no significant difference between exchanger performance in the two orientations. This verifies the conclusion that the heat transfer is indeed forced-convection dominated and not affected by gravity level.

Heat exchanger performance was further determined as a function of hot side flow rate by varying the pump speed. Both the vent and hot sides were in liquid, and the vent flow rate was maintained constant at approximately 3 lb/hr. The results of these tests are presented in Figures 5-43 and 5-44. Figure 5-43 shows exchanger effectiveness versus pump speed which is proportional to hot side flow rate. It is seen that the effectiveness is zero (saturated outlet fluid) at pump speeds below 80 percent of the design value (966 lb/hr flow). This is also illustrated in Figure 5-44 where heat exchanger outlet temperature and liquid detector readings are shown as a function of pump speed. With the outlet temperature at saturated conditions, liquid was observed at the system outlet. This occurred at a pump speed of 2131 rpm, corresponding to flow rate of 838 lb/hr. Dymec readings of exchanger outlet temperature, showed that saturated outlet conditions occurred at hot side flow rates slightly above this value.

From the foregoing data it was shown that liquid was not present at the exchanger outlet until completely saturated conditions were reached. Therefore, any superheating of the vent gas with the present exchanger design results in a pure gas vent.

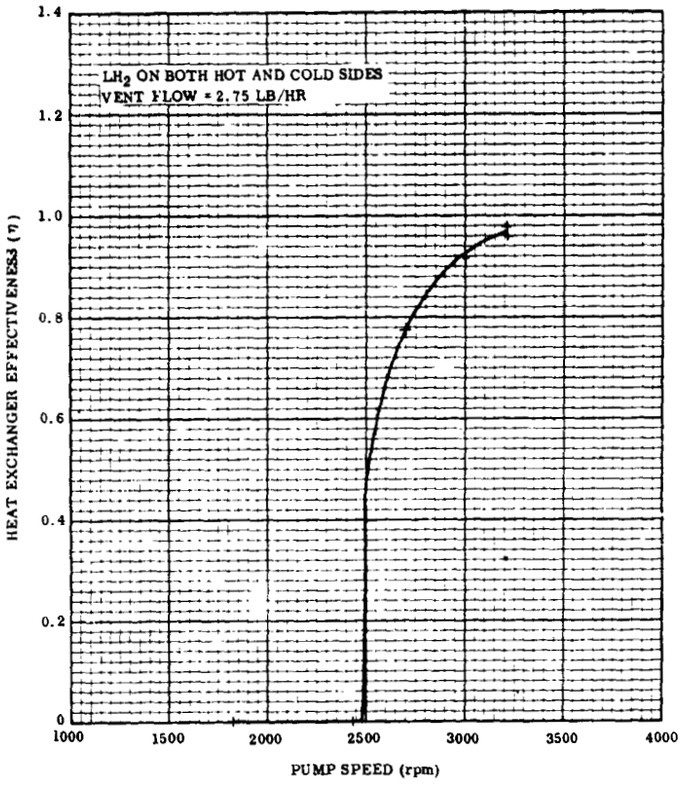

Figure 5-43. Heat Exchanger Effectiveness Versus Hot Side Flow

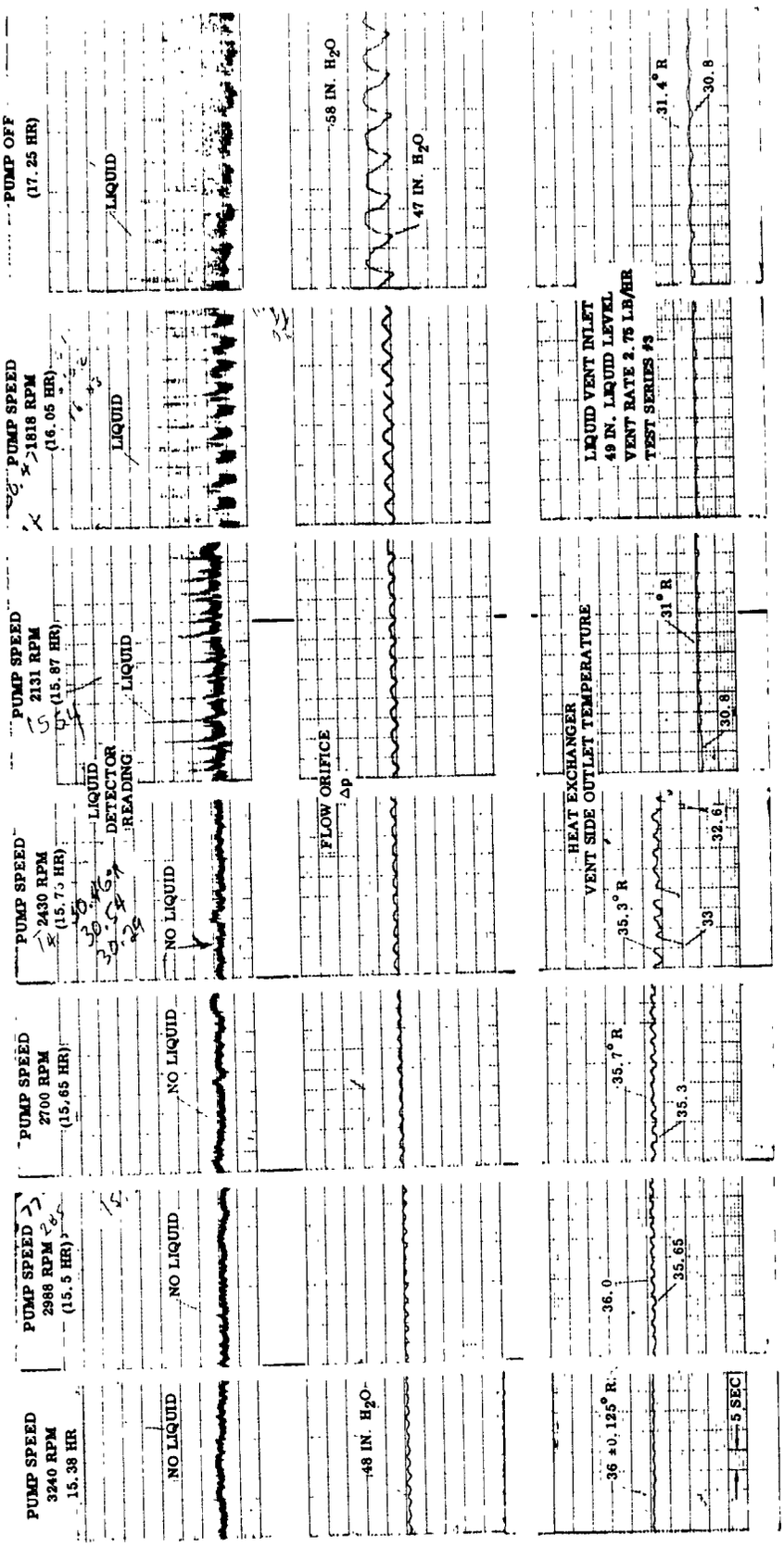

Figure 5-44. Heat Exchanger Outlet Conditions Versus Hot Side Flow

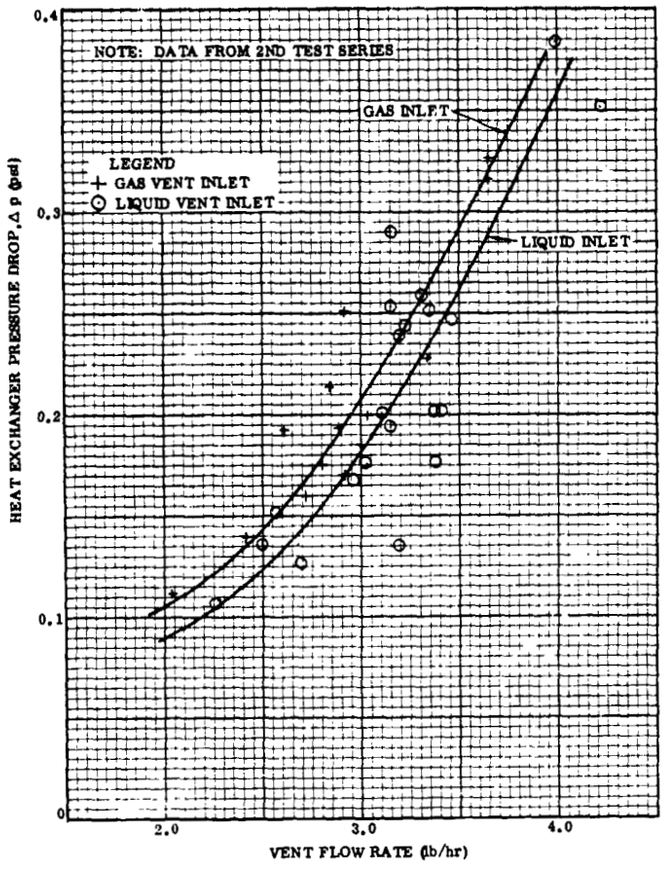

Figure 5-45. Heat Exchanger Pressure Drop Versus Flow Rate

Heat exchanger vent side pressure drop was also measured during testing. These data are plotted in Figure 5-45 as a function of vent flow rate, for both gas and liquid inlets. The actual pressure drop was well below the design point presented in Table 2-5.

5.3.5 PUMP PERFORMANCE. This section contains a summary of the data obtained on the pump operating characteristics.

During liquid hydrogen testing, the pump speed and power were changed by varying the frequency and voltage in the same proportions. That is, when lowering frequency from 60 to 30 cycles the input voltage was lowered from 17.3 to 8.65 volts.

The circuit of Figure 5-46 was used to measure the input power to the pump motor. The power to a single phase induction motor is $P = C\ I \cos \phi$, where ϕ is the phase angle between the voltage C and the current I. The voltage vector diagram of Figure 5-46 shows how the voltage measurements A, B, and C are used to obtain the motor power. The derivation is presented below:

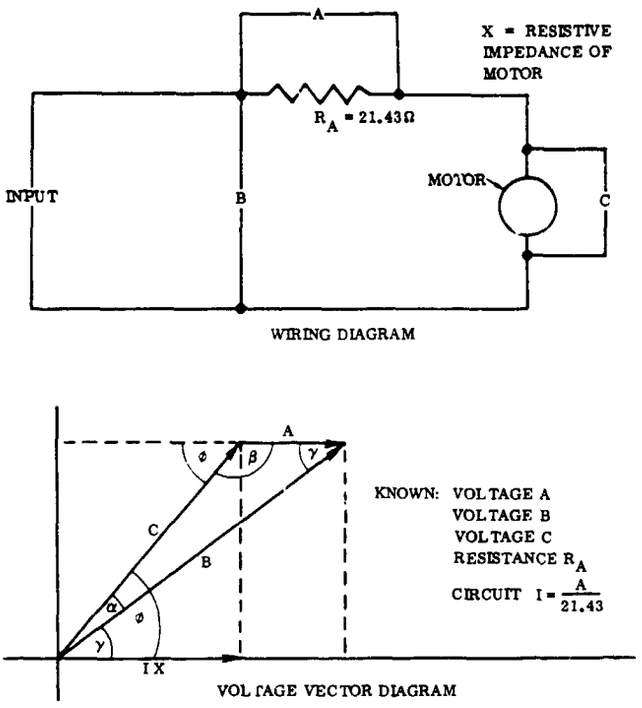

Figure 5-46. Pump Motor Power Measurement

From the law of cosines; and referring to Figure 5-46

$$\cos \beta = \frac{A^2+C^2-B^2}{2AC}$$

$$= \cos (180° - \phi) = - \cos \phi$$

The circuit current $I = \frac{A}{R_A} = \frac{A}{21.43}$

and

$$P = CI \cos \phi = \frac{B^2-A^2-C^2}{42.86}$$

Data obtained during testing at Convair with the pump flow through the Geoscience heat exchanger are presented in Figures 5-47 and 5-48. Pump performance curves obtained from Pesco (Reference 3-4) are presented in Figure 5-49. System resistance curves for the Pesco tests and for the Convair tests are also shown. Pressure drop data, to obtain the Convair curve, were taken from results of testing done on the heat exchanger at Geoscience (Reference 3-3). The hot side flow coefficient (C_f) was determined to be 3.6, based on a flow diameter of 1.63 inches.

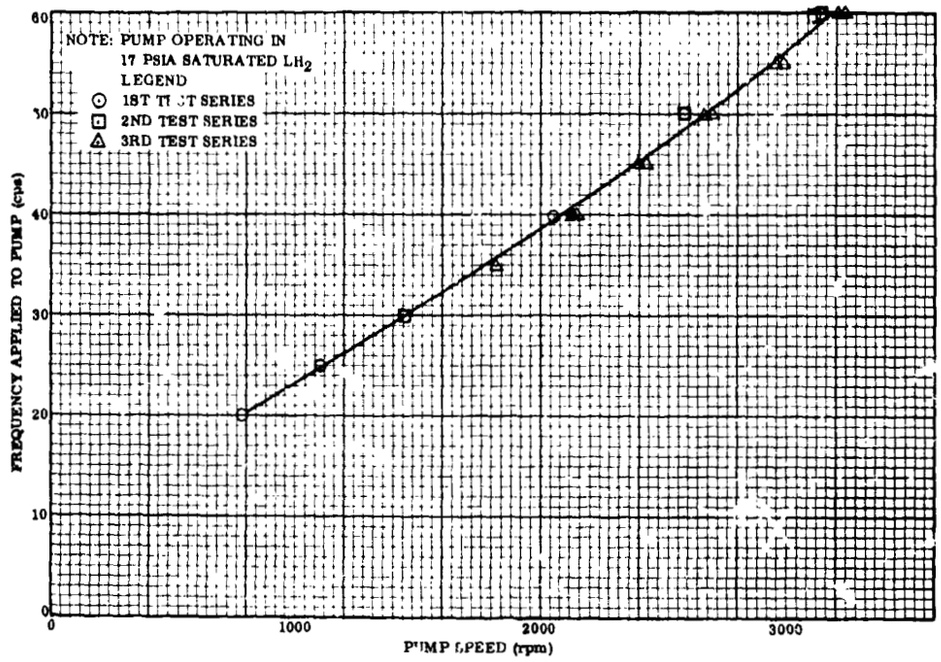

Figure 5-47. Pump Speed Versus Applied Frequency

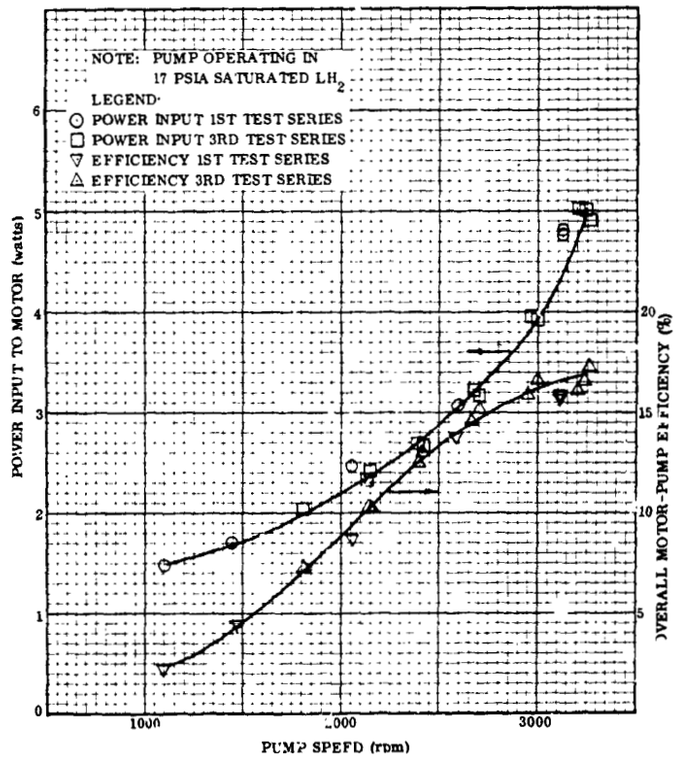

Figure 5-48. Pump Performance Versus Speed

NOTES: 1. 17.5 VOLT 60 CPS, SINGLE PHASE INPUT AND 40 μF EXTERNAL CONDENSER
2. CALCULATED PERFORMANCES ARE BASED ON TESTED PERFORMANCE IN AIR WITH 400 CPS INPUT AT APPROX. 22,600 RPM AND THE ACTUAL RPM AND WATTS FROM TESTS WITH 60 CPS INPUT IN SATURATED LH_2

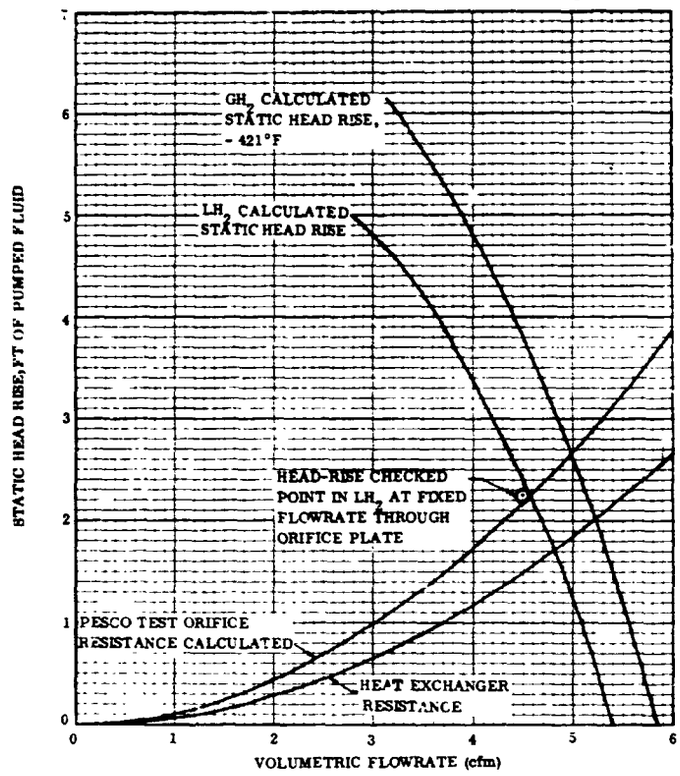

Figure 5-49. Pesco Pump Performance Curves

Then

$$H_{ex} = \frac{C_f V^2}{2g}$$

where

H_{ex} = head loss through the exchanger

V = flow velocity

From the Figure 5-49, the pump flow rate and static head rise would be 4.8 cfm and 1.7 ft, respectively, when flowing LH_2 through the exchanger and operating at a speed of 3200 rpm.

In order to determine flow rates, head rise, and pump fluid power the pump affinity laws are used. In the present case, where the flow resistance is assumed constant;

$$Q \approx N$$

$$H \approx N^2$$

$$P_h \approx N^3$$

Where P_h is the hydraulic output power of the pump ($P_h = Q\, H\rho$).

From the above data, the pump flow rate in LH_2 as a function of rpm was determined to be;

$$Q,\ \text{cfm} = 4.8 \left(\frac{\text{rpm}}{3200}\right) = 1.5 \times 10^{-3}\ (N,\ \text{rpm})$$

or for a LH_2 density of 4.36 lb/ft^3

$$\dot{m},\ \text{lb/hr} = 0.393\ (N,\ \text{rpm})$$

The static head rise is similarly determined to be

$$H,\ \text{ft} = 0.0738\ (Q,\ \text{cfm})^2$$

In determining pump operating characteristics a number of assumptions were made. To obtain a completely accurate performance map for the pump operating in hydrogen at various speeds, a special flow set-up should be made and the unit operated over a range of speeds and static head conditions while accurately measuring speed, head and flow rate. This would require instrumentation capable of accurately measuring very low pressure drops.

The transient speed characteristics of the pump were also measured during start-up and shut-down. Start-up time in gaseous hydrogen; i.e., to go from zero rpm to 3310 rpm (97 percent of steady state) was typically 1.7 seconds. The time required to reach steady state (3410 rpm) was 4 seconds. Total shut-down time from full speed was approximately 12 seconds. For operation in LH_2 the time to go from 0 rpm to 3060 rpm (97 percent of steady state) was 1.8 seconds and the time to go to full speed (3150 rpm) was 4 seconds. Time from full speed to 0 rpm was 5 seconds for the LH_2 case.

Pesco data showed a coast-down or shut-down time of 14 seconds from 3440 rpm in GH_2 and 3 seconds from 3100 rpm in LH_2. The coast-down times are an indication of freedom of rotation, and the above values indicate a freely rotating unit.

5.3.6 PRESSURE SWITCH PERFORMANCE. The pressure switch is required to sense tank pressure and actuate the pump and shut-off valve at a maximum pressure of 18 psia. Deactuation should occur at a minimum pressure of 16 psia. The minimum deadband of the unit should be 0.5 psi. Actuation and deactuation data obtained by the vendor are presented in Paragraph 3.1. A summary of the data obtained at Convair division during hydrogen testing is presented in Table 5-1.

During the Convair testing, the actuation point was sometimes slightly out of tolerance on the high side. The total band was, however, in tolerance and discussions with the vendor, Frebank, indicate that, with a slight adjustment to the switch setting, control of the pressure within 16 to 18 psia could be easily accomplished.

5.3.7 REGULATOR PERFORMANCE. The regulator performed satisfactorily throughout testing except for the problem encountered after 22 hours of the first test series and 35 hours of the second test series when the unit regulated high and appeared to be stuck open. Subsequent testing indicated that the cause of failure was probably the formation of solid hydrogen in the regulator.

The unit performed satisfactorily throughout the third test series with the shut-off located downstream to prevent expansion of LH_2 to a vacuum within the regulator. Location of the shut-off valve downstream is recommended in order to eliminate the possibility of such freezing.

Regulator outlet pressure during normal operation is presented in Figure 5-50 as a function of vent-flow rate for both liquid and gaseous hydrogen inlets. The regulated pressure was slightly lower with the gas inlet than with the liquid inlet, as would be expected. Also, regulation was approximately 0.5 psi lower than the original requirements of 5 ± 0.5 psia when operating with gas. Control of the pressure with a liquid hydrogen inlet was, however, the most critical for heat transfer purposes and was generally within the requirements. In any case, the pressure regulation obtained resulted in satisfactory overall system performance.

Table 5-1. Summary of Automatic Cycling Actuation and Deactuation

Test Series	Liquid Level	Actuation Time, Hours	Actuation Tank Pressure, PSIA	Deactuation Time, Hours	Deactuation Tank Pressure, PSIA	Δ p, PSI
1	47"	14.71	18.25	15.24	16.62	1.63
1	47"	15.63	18.29	16.24	16.76	1.53
1	47"	16.51	18.24			
2	13"	5.84	18.15	5.95	16.25	1.9
2	13"	6.28	18.15	6.42	16.25	1.9
2	13"	6.55	18.15	6.65	16.25	1.9
2	13"	6.82	18.1	6.943	16.28	1.82
2	49"			8.72	16.35	
2	49"	8.97	18.0	9.28	16.41	1.59
2	49"	9.84	17.99	10.18	16.36	1.63
2	49"	10.545	17.98	10.895	16.4	1.58
2	70"			38.12	16.8	
2	70"	38.56	17.95	38.942	16.81	1.14
2	70"	39.242	17.41			
Special Ambient Helium Check, 5/19/67			18.15		16.4	1.75
3	13"	8.73	18.12	8.812	17.05	1.07
3	13"	9.167	18.04	9.3	16.46	1.58
3	13"	9.561	18.0	9.682	16.44	1.56
3	13"	9.965	18.05			
3	47"	13.15	18.05	13.73	16.5	1.55
3	47"	14.36	18.11			
3	71"	21.3	17.9	21.86	16.46	1.44
3	71"	22.211	17.95	22.466	16.38	1.57

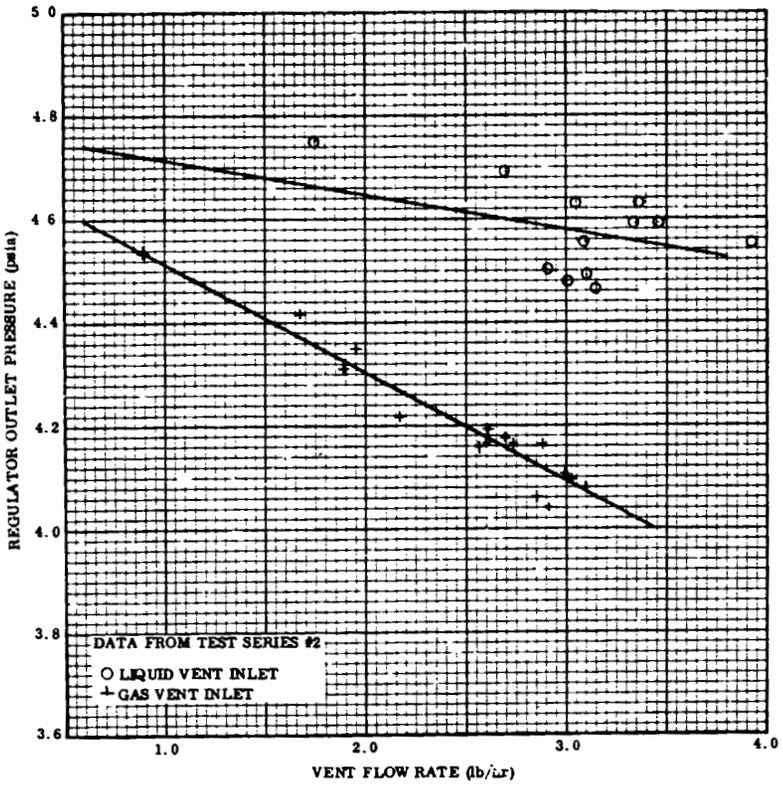

Figure 5-50. Regulator Outlet Pressure Versus Flow Rate

A test was performed, during the third series, to determine the minimum flow rate at which the regulator could still control downstream pressure with a liquid inlet. The pressure was controlled to 5.5 psia with a liquid flow rate of approximately 0.07 lb/hr. This indicated that operation at very low vent flows, as would be required for a continuous vent system, would be feasible with this type of regulator.

Test data were also obtained on regulator performance during vent down from tank pressures up to 29 psia. These data showed that the regulated outlet pressure was not effected by changes in tank pressure of this magnitude.

5.3.8 VENT DOWN FROM HIGHER TANK PRESSURES. In order to obtain data applicable to the project THERMO orbital experiment, venting through the heat exchanger was accomplished following stratification testing at pressures up to 29 psia. Results of such a vent-down are presented in Figures 5-51 through 5-53, showing tank pressure, heat exchanger temperatures, and flow-rate, respectively.

The significant factor is that the exchanger outlet temperature remains very near the hot side temperature throughout venting, even at flow rates up to 4 lb/hr with a liquid inlet. Higher vent flow rates were not achieved due to limitations on the facility vent system. The data show that vent-down at significantly higher flow rates, as discussed in Section 4.0, can be accomplished by providing the means to increase the down-stream system capacity.

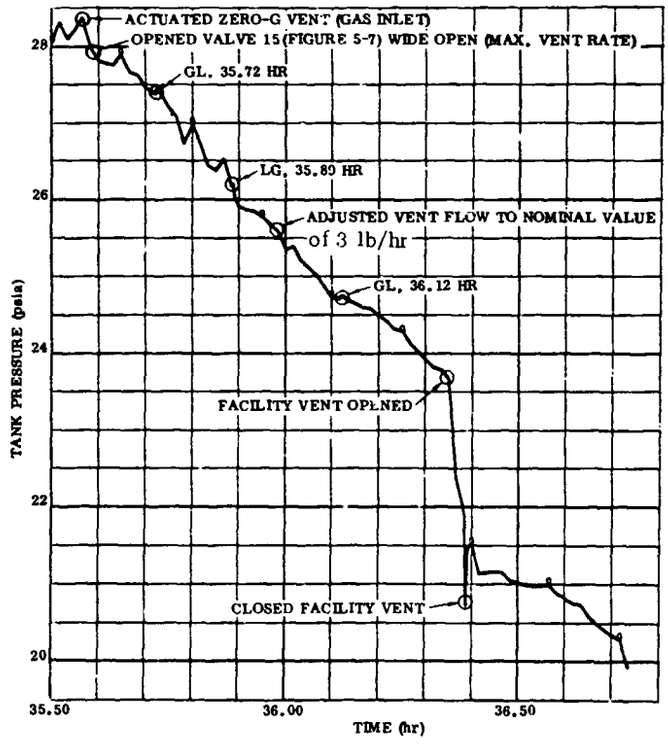

Figure 5-51. Tank Pressure During Vent Down From 29 psia

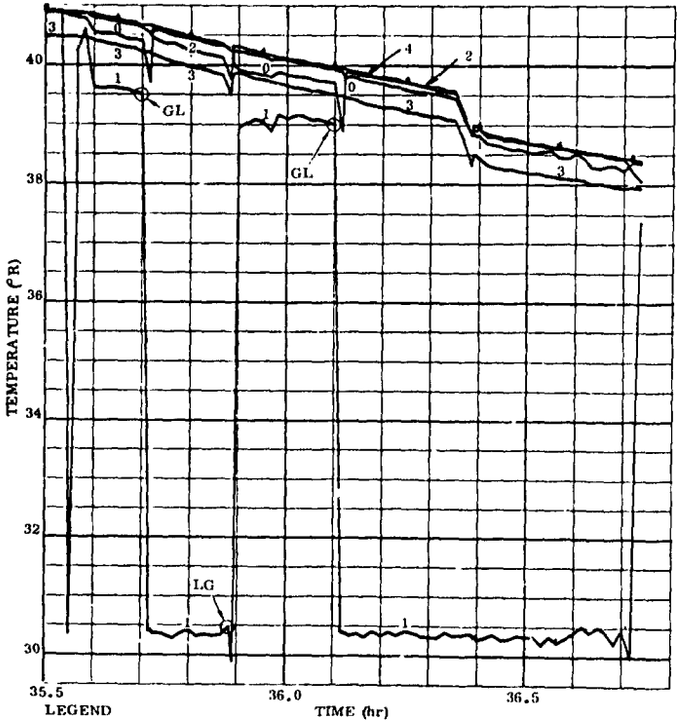

Figure 5-52. Heat Exchanger Temperatures During Vent Down From 29 psia

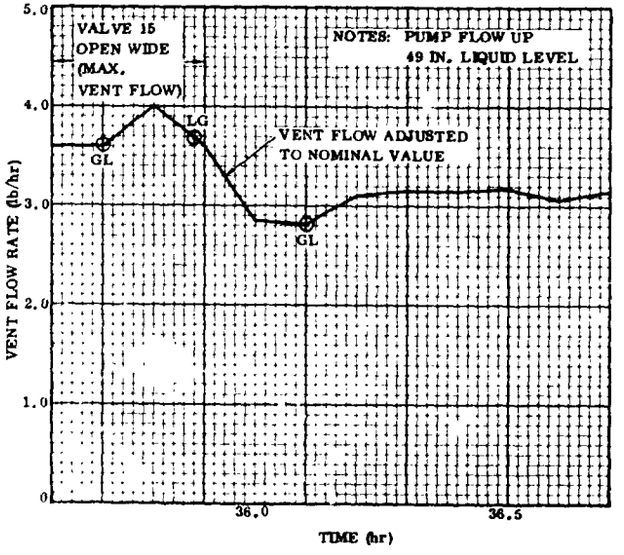

Figure 5-53. Vent Flow Rate During Vent Down From 29 psia

SECTION 6.0

FLIGHT QUALIFICATION TEST PROGRAM

The testing recommended to qualify the zero-g vent system for use in a manned orbital propellant storage and vent experiment is discussed in this section.

Two systems should be tested; however, only one system would need to be operated through the complete life test. This system could also be used as the one burst test specimen.

To minimize costs without degrading the effectiveness of the qualification program, it is recommended that the existing hardware used in the feasibility demonstration tests be put into flight configuration and used as the life and burst test specimen. Only minor modification and refurbishment of the existing components would be required. A second system would be fabricated and qualification testing performed, except for the full life and burst tests. A third specimen would be used in the flight system following complete inspection testing. The inspection testing sequence would consist of component acceptance testing, a proof cycle, vibration in the most critical axes as determined during qualification testing, and two more proof cycles.

The order of qualification testing would be as follows:

a. Initial Acceptance Testing of Individual Components

b. Proof Cycle (of complete test specimen)

c. High Temperature Soak Test

d. Proof Cycle

e. X-Axis Vibration

f. Proof Cycle

g. Y-Axis Vibration

h. Proof Cycle

i. Z-Axis Vibration

j. Proof Cycle

k. Acceleration

1. X-Axis

2. Y-Axis

3. Z-Axis

l. Proof Cycle

m. Life Test

n. Proof Cycle

o. Burst Test

Details of the foregoing tests are presented in the following paragraphs.

6.1 COMPONENT ACCEPTANCE TESTING

Initial acceptance testing of individual components will be accomplished prior to assembly of the basic test package. The basic test package is defined as the vent system heat exchanger, pump, throttling regulator, filter, temperature probes, and other instrumentation as shown in Figure 6-1. The test specimen shut-off valve is considered a part of the overall test specimen but is separate from the basic test package. This is also the case with the pressure switch.

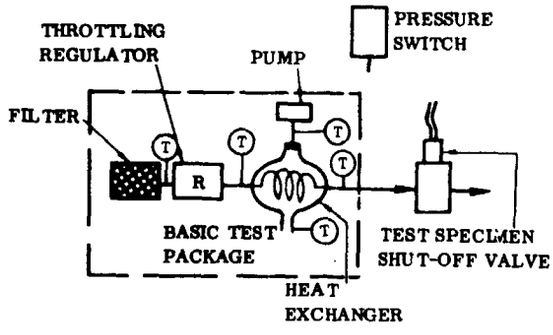

Figure 6-1. Qualification Test Package

A brief summary of testing to be accomplished on the above components follows:

Heat Exchanger. Flow tests, using Freon and water will be performed to check conformance to pressure drop and heat transfer requirements.

Throttling Regulator. Hydrogen flow testing will be accomplished with the unit immersed in LH_2 to verify operation at its required set-point.

Pump. The pump will be operated for a short time in air and for a longer time in both GH_2 and LH_2. The speed of the unit will be monitored and the coast down times measured to determine that the unit is freely rotating.

Shut-Off Valve. Flow testing will be accomplished with cold hydrogen gas in the same set-up used for the regulator acceptance test. Unit pressure drop will be measured and checked against specification requirements. Minimum actuation voltages will also be checked during this cold flow test, as well as at temperatures up to 160° F.

Pressure Switch. Actuation and deactuation will be checked at temperatures from -80° F to +160° F to verify consistency of operation and conformance with the specifications. Actuation and deactuation will also be measured while performing a 5 g vibration scan.

In conjunction with the above tests, the components will be subjected to internal and external leakage tests to verify conformance to specification requirements. The foregoing testing is designed only to determine that no major flaws exist in workmanship or assembly and that the unit is likely to operate satisfactorily when installed in the overall test package. Extensive testing and qualification will be accomplished when assembled as a complete vent system, as described in the following paragraphs.

6.2 PROOF CYCLE

The following operations shall constitute a proof cycle, the results of which shall form the basis for indicating satisfactory performance of the Test Specimen.

6.2.1 AMBIENT LEAKAGE CHECK.

a. With the test specimen installed in the test system of Figure 6-2, and with valves V1, V2, and V3 closed, and the test specimen shut-off valve open, pull a vacuum and check the helium background level with the helium leak detector. Then, using a helium spray, check each component and fitting for leakage.

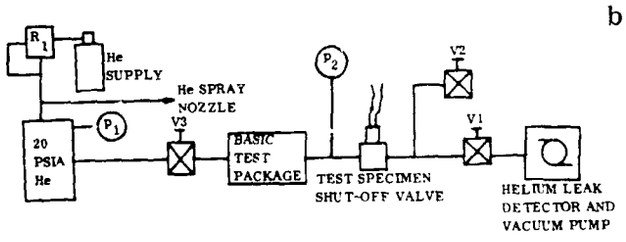

Figure 6-2. Ambient Leakage Test Set-Up

b. Close the test specimen shut-off valve and open valve V3. Measure the pressure rise rate within the test package at p_2. When the pressure p_2 reaches 16 to 20 psia, measure the leakage rate through the test specimen shut-off valve using the helium leak detector and vacuum pump.

6.2.2 CRYOGENIC LEAKAGE CHECK. With the test specimen installed as shown in Figure 6-3, and with valve V1 open and the vacuum pumps running, open the specimen shut-off valve. Allow the flow to reach steady-state conditions, and then close the specimen shut-off valve and measure the pressure rise rate within the test package at p_2. When the pressure p_2 reaches 16 to 20 psia, measure the leakage rate through

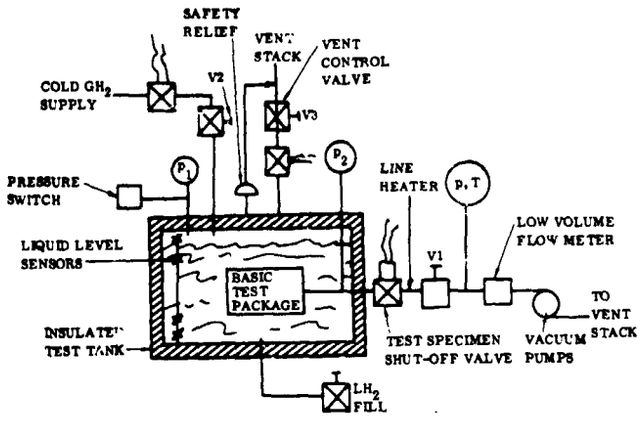

Figure 6-3. Cryogenic Leakage and Flow Cycle Test Set-Up

the test specimen shut-off valve using a low volume flow meter.

6.2.3 AUTOMATIC CYCLING AND FLOW CHECK. Install the test specimen as shown in Figure 6-3. With valve V1 open, the vacuum pumps running, and the system on automatic (pressure switch controlling operation of pump and shut-off valve), slowly pressurize the LH_2 dewar to the pressure switch actuation point. Gaseous hydrogen may be used as a pressurant. When actuation occurs, shut off the GH_2 pressurization. If heat leak into the dewar is such that the pressure does not decay at $0.15 \pm .05$ psi/min, slowly open valve V3 such that the tank pressure does decay at this rate. Record pressure at which system actuates. Following system actuation and while venting through the test specimen, record temperatures and pressures upstream and downstream of the regulator, temperature and pressure at the cold side outlet of the exchanger, exchanger hot side inlet and outlet temperatures, system vent rate, and pump speed. When the pressure switch actuates the system closed, the pressure in the dewar should begin to rise. Record this deactuation point. Close vent valve V3 and allow the dewar pressure to rise to the pressure switch actuation point. Record this pressure.

Perform the above testing through a minimum of 4 complete cycles; two cycles with the liquid level above and two cycles with the liquid level below the basic test package. Repeat the cryogenic leakage test of Paragraph 6.2.2 and then the ambient leakage test of Paragraph 6.2.1.

6.3 HIGH TEMPERATURE SOAK TEST

Install the test specimen in a controlled temperature environment at 160° F. Allow the entire system to reach temperature equilibrium. Maintain the test specimen at this temperature for four hours. Operate the solenoid and determine its minimum actuation voltage in both opening and closing modes. Then, turn on the pump momentarily to check that it does start and operate. Apply pressure to the pressure switch, and record actuation and deactuation points.

6.4 VIBRATION TESTING

Install the test specimen as shown in Figure 6-4. With the pressure in the test dewar controlled to 17 ± 1.0 psia, and valve V3 open, perform a 20 g vibration scan. Dewar pressure is maintained at 17 ± 1.0 psia by proper regulation of valves V1 and V2.

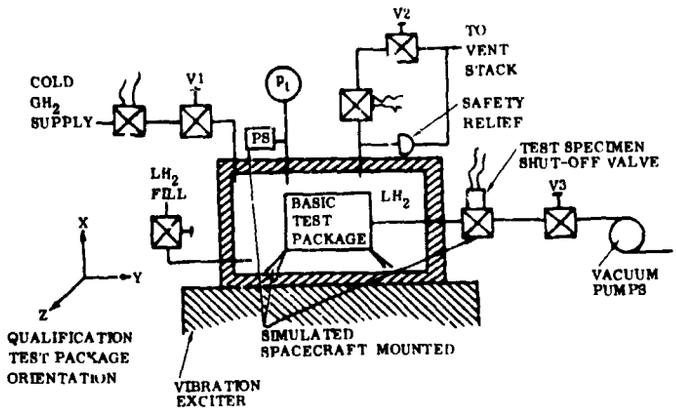

Figure 6-4. Vibration Test Set-Up

Record vibration levels at critical points on the test specimen. Following the 20 g scan, and with the vacuum pumps running, open the test specimen shut-off valve. Allow the vent flow to stabilize, and with the system on automatic, allow the dewar pressure to rise to the pressure switch actuation point. Pressurization with GH_2 through valve V1 may be used to increase the pressure rise rate. When actuation occurs, close valve V1 and allow the pressure to decay. The rate of decay may be increased by opening valve V2. Control the cycling of the test specimen to approximately one complete cycle every eight minutes by proper adjusting and sequencing of valves V1 and V2. With the system operating in this manner, slowly perform a 5 g vibration scan such that venting is occurring at each of the critical frequencies. Record vibration levels at critical points, temperatures, and pressures upstream and downstream of the regulator, temperature and pressure at the cold side outlet of the exchanger, exchanger hot side inlet and outlet temperatures, system vent rate, and pump speed.

The above testing will be accomplished with the test specimen in X-Axis, Y-Axis, and Z-Axis orientations as shown in Figure 6-4.

6.5 ACCELERATION TESTING

The test specimen is installed on a centrifuge as shown in Figure 6-5. During acceleration, helium flow at LN_2 temperature is maintained through valve V1 with valves V3 and the test specimen shut-off open and the vacuum pump running. Pressure (p_2) at the regulator outlet is recorded. Pressure is also applied to the pressure switch sensing port, and actuation and deactuation values are determined during acceleration. This testing is accomplished with the test specimen in X-Axis, Y-Axis, and Z-Axis orientations.

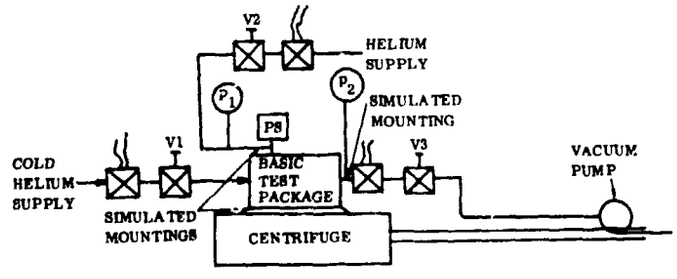

Figure 6-5. Acceleration Test Set-Up

6.6 LIFE TEST

With the shut-off valve located downstream of the system, formation of solid hydrogen within the system would not be a problem. It is felt that the primary life requirement of the unit is the actual duration of venting and the number of actuation and deactuation cycles. Based on a vent flow of 3 lb/hr, from Figure 2-9, the vent time fraction is 0.036. For a 14-day mission, this results in 12.1 hours of actual venting. From Paragraph 2.2.4.3 the minimum vent down time for the orbital system is estimated to be 10 minutes resulting in 72.6 cycles of operation over the 14-day mission.

For the life test, the test specimen will be installed in the system shown in Figure 6-3, and operated in the same manner as for the automatic cycling and flow check described in Paragraph 6.2.3. The vent down duration will be approximately 10 minutes. In order to provide a significant safety factor over actual operational requirements, 400 cycles of actuation and deactuation over a 200-hour period are specified. This results in a total vent time of 66.7 hours, assuming 10 minutes per cycle.

After each 100 cycles of operation a cryogenic leakage check as outlined in Paragraph 6.2.2 will be performed. In addition to the foregoing tests, a test will be performed to verify that extended-duration soaking is not detrimental to the system. In this test the vent system, while non-operating, will be submerged in LH_2 for 14 days. A vacuum will be maintained downstream of the test specimen shut-off valve during this period. Proof cycles per Paragraph 6.2.3 will be performed before and after the soak test.

6.7 BURST TEST

The specimen is installed as shown in Figure 6-6. With valve V1 open to the atmosphere and the test specimen shut-off valve closed, slowly pressurize the test tank to the point at which the test specimen fails, as evidenced by a significant increase in leakage at the valve V1 exit, the test specimen shut-off valve, or the pressure switch. Pressurization will be stopped and the tank vented at this point, or upon reaching 200 psig (four times the maximum operating pressure), whichever occurs first. This phase of the burst test will determine the ability of the regulator and heat exchanger to withstand an external pressure, since at atmospheric outlet pressure the throttling regulator will be closed and the only flow through valve V1 will be due to leakage through the regulator and heat exchanger assembly. The test is then repeated with valve V1 now closed,

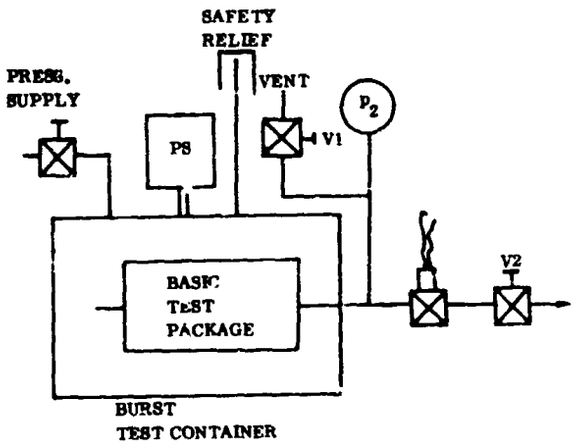

Figure 6-6. Burst Test Set-Up

allowing the pressure p_2 to slowly equalize with the tank pressure due to internal leakage through the regulator. This will determine the ability of the shut-off valve to contain pressure. If any portion of the system has failed during the previous test, that portion of the system will be capped off.

SECTION 7

CONCLUSIONS AND RECOMMENDATIONS

The following conclusions and recommendations are made as a result of this program.

a. The feasibility and efficiency of the system to control tank pressure while venting only vapor when operating in an environment at least as severe as that of the orbital experiment has been demonstrated. The next logical step in preparing for operational use of the system would be to perform complete qualification testing of the system. Such a program is outlined in Section 6.0.

b. Tank fluid mixing and liquid/ullage coupling are extremely important for efficient pressure control. Tank pressure decay with the system and the vent inlet in liquid and with the heat exchanger outlet directed downward was very slow. This is attributed to the fact that liquid mixing and subsequent liquid/ullage coupling were not sufficient enough to reduce the tank pressure. This was verified by temperature measurements which showed the liquid in the tank was progressively subcooled, with the respect to the ullage, as energy was removed via the heat exchanger.

c. The best location for the shut-off valve appears to be downstream of the heat exchanger and external to the propellant tank, in order to minimize the possibility of the formation of solid hydrogen by LH_2 leakage to a vacuum.

d. Results showed that flow directly up the center of the tank was best in promoting fluid mixing. In this case, pressure control was very efficient for both gas and liquid inlets. Radial flow at the exchanger outlet was second best, and flow directly down was significantly worse than either radial or upward flow.

e. It is recommended that for orbital testing the system be located near one end of the tank with the heat exchanger outlet flow directed toward the other end.

f. Since it was verified that tank mixing is an essential criteria for efficient operation of this system and is integral with it, it is recommended that further analyses and testing be accomplished with this system to determine its mixing characteristics in LH_2 at various liquid levels, pump speeds, and power levels.

SECTION 8

REFERENCES

1-1 Mitchell, R. C.; Hudson, V.; Stark, J. A.; and White, R. C.; "Study of Zero-Gravity, Vapor/Liquid Separators," GDC-DDB65-009, NAS8-20146, January 1966.

2-1 Caine, G.; "Estimated Performance In Liquid Hydrogen of Typical Pesco A.C. Motor Driven Vaneaxial Fans as Modified to Operate With 17.3 Volts and 60 CPS Input," 8 July 1966.

2-2 Blatt, M. H.; "Heat Exchanger For Zero-G Vapor/Liquid Separation," GDC-584-4-59, 8 May 1967.

2-3 McAdams, W. H.; Heat Transmission, McGraw-Hill, 1954.

2-4 Strek, F.; "Heat Transfer in Liquid-Mixers — Study of a Turbine Agitator With Six Flat Blades," International Chemical Engineering, October 1963.

2-5 Abdalla, K. L.; Krysinger, T. C.; and Andracchio, C. R.; "Pressure-Rise Characteristics for a Liquid-Hydrogen Dewar for Homogeneous, Normal Gravity Quiescent, and Zero Gravity Tests," NASA TMX 1134, September 1965.

2-6 Personal Communication With Mr. Gordon Smith of the Lewis Research Center; 8 September 1966.

2-7 "Study of Cryogenic Stratification Reduction Techniques," General Dynamics Fort Worth FPR-027-3, 15 August 1966.

2-8 Hyman, D.; "Mixing and Agitation," Advances in Chemical Engineering, Academic Press; New York, 1962.

3-1 Galluci, B.; Nicolai, H.; "Inspection Test Results Regulator Valve," Wallace O. Leonard Report No. 187252, 21 February 1967.

3-2 Ballucci, B.; Nicolai, H.; "Inspection Test Results Solenoid Valve," Wallace O. Leonard Report No. 201202, 21 February 1967.

3-3 Sabin, C. M.; "Test Report of Geoscience Ltd., Heat Exchanger 02B1-1 With Boiling Freon 11 and Water," Geoscience Ltd. Report No. GLM-54, February 1967.

3-4 Caine, G.; "Test Data Sheet and Performance Curves," Pesco Project No. 116124-A, 8 March 1967.

3-5 Friend, A. E.; "Frebank Part Number 8394-1 Pressure Switch Conformance Data," Frebank Report No. 8394-1, 31 January 1967.

5-1 Bradshaw, R. D.; Kneisel, K. M.; Fisher, R. A.; Blatt, M. H.; Stark, J. A.; and Tatro, R. E.; "Propellant Thermodynamic Behavior," GDC-ERR-AN-1039, December 1966.

5-2 "Cryogenic Quality Meter," Industrial Nucleonics Corp. CPB 02-1263-64, Final Report Contract NAS8-11736, 2 November 1964.